

Aus der Klinik und Poliklinik für Hals-, Nasen- und Ohrenheilkunde
Klinikums der Ludwig-Maximilians-Universität München

Direktor: Prof. Dr. med. Martin Canis

**The role of a novel cross-talk between EpCAM and EGFR in
the regulation of epithelial-to-mesenchymal transition (EMT)
in head and neck carcinomas**



Dissertation

zum Erwerb des Doktorgrades der Humanbiologie
an der Medizinischen Fakultät der
Ludwig-Maximilians-Universität zu München

vorgelegt von

Min Pan

aus

Sichuan, China

2019

**Mit Genehmigung der Medizinischen Fakultät
der Universität München**

Berichterstatter: Prof. Dr. rer. nat. Olivier Gires

Mitberichterstatter: PD. Dr. Dorit Di Gioia

Prof. Dr. Axel Kleespies

Prof. Dr. rer. nat. Heiko Hermeking

Dekan: Prof. Dr. med. dent. Reinhard HICKEL

Tag der mündlichen Prüfung: 26.11.2019

CONTENTS

ABSTRACT	1
ABBREVIATIONS:	3
1. INTRODUCTION	5
1.1 Head and neck cancer	5
1.1.1 Heterogeneity of HNSCCs	6
1.1.2 Clinical management of head and neck cancer	8
1.2 Epithelial-to-mesenchymal transition (EMT)	9
1.2.1 EMT transition states	11
1.2.2 Regulatory networks of EMT	13
1.3 Epidermal growth factor receptor (EGFR)	16
1.3.1 Structure of EGFR	16
1.3.2 EGFR ligands and signaling	18
1.3.3 EGFR biology and anti-EGFR treatment in HNSCCs	20
1.4 Epithelial cell adhesion molecule (EpCAM).....	23
1.4.1 Structure of EpCAM	23
1.4.2 Regulated intramembrane proteolysis (RIP) of EpCAM and EpCAM- mediated signalling	26
1.4.3 EpCAM in cancer	28
2. ZUSAMMENFASSUNG	29
3. MATERIALS AND METHODS.....	31
3.1 Human samples	31
3.2 Cell lines and treatments.....	32
3.3 siRNA treatment.....	32
3.4 Immunohistochemistry and immunofluorescence staining.....	33
3.5 Flow cytometry, immunoblotting and immunoprecipitation	34
3.6 Protein expression and cross-linking	36

3.7	Recombinant human EpEX-Fc purification and characterization.....	36
3.8	Migration assay, cell proliferation, and BrdU incorporation.....	37
3.9	Reverse transcriptase polymerase chain reaction analysis.....	38
3.10	Statistical analyses.....	39
3.11	Survival analysis.....	39
4.	RESULTS.....	41
4.1	EpCAM and EGFR define subclasses of HNSCCs with disparate clinical outcome.....	41
4.1.1	EpCAM and EGFR expression in HNSCCs.....	41
4.1.2	EpCAM and EGFR expression predict disparate clinical outcomes of HNSCCs.....	43
4.1.3	Correlation of EGFR and EpCAM expression subtypes with clinical parameters.....	47
4.2	EGF induces EMT in HNSCC cell lines, but induction of EpCAM RIP by EGF is not a common mechanism in HNSCC cells.....	50
4.2.1	Characterization of HNSCC cell lines with a high co-expression of EGFR and EpCAM.....	52
4.2.2	EGF treatment results in disruption of cell-cell contact and EMT in HNSCC cell lines that overexpress EGFR.....	53
4.2.3	EGF stimulation does not promote RIP of EpCAM in HNSCC cell lines...54	
4.3	EGF treatment does not result in reduction of EpCAM in a panel of carcinoma cell lines.....	57
4.3.1	Expression of EpCAM assessed by flow cytometry.....	58
4.3.2	Expression of EpCAM assessed by Western blot analysis.....	59
4.3.3	Expression of EpCAM assessed by IFS-confocal analysis.....	61
4.4	EpEX is an EGFR ligand that induces downstream signaling pathways.....	62
4.4.1	Endogenous EpCAM associates with EGFR.....	63

4.4.2 Naturally shed EpEX molecules are present in supernatant of cancer cells in multimeric form.....	64
4.4.3 Generation of recombinant soluble EpEX-Fc fusion protein	65
4.4.4 Soluble EpEX directly binds to the extracellular domain of EGFR.....	68
4.4.5 EpEX-Fc specifically activates EGFR downstream signaling pathways ...	69
4.4.6 Activation of EGFR downstream signaling by EpEX-Fc is EGFR-dependent, but does not require full length EpCAM	72
4.5 Effects of EpEX-Fc and EGF are dosage-dependent and differ in cellular outcome	73
4.5.1 Proliferation assay	74
4.5.2 Migration assay	77
4.6 EpEX-Fc impedes EGF-induced EMT in HNSCC cell lines.....	79
4.6.1 EGF ^{high} drives mesenchymal characteristics, but EpEX-Fc sustains an epithelial phenotype and impedes EGF-induced EMT in HNSCC cells.....	79
4.6.2 EGF does not induce EMT in Cal27 cells	80
4.6.3 EpEX-Fc impedes EGF-induced EMT via modulation of EMT-TFs levels	81
4.7 MEK-ERK, but not AKT signalling is required for EGF-induced EMT.....	84
4.7.1 Systematic evaluation of cell signaling contributions to EGF/EGFR-mediated EMT.....	85
4.7.2 MEK-ERK signaling is the central mediator in EGF-induced EMT in HNSCC	86
4.8 Strength and duration of ERK1/2 activation integrates differential cellular fates	
88	
4.8.1 Differential responsiveness of HNSCC cell lines to EGF determines disparities in cellular outcome	88
4.8.2 EGF and EpEX shape different ERK activation dynamics, rewiring different cell fates.....	89

4.8.3 EpEX impedes EGF-induced EMT by altering the signal strength of ERK1/2 activation	91
4.9 EGFR and EpCAM expression levels control EMT induction <i>in vitro</i> and mimic the <i>in vivo</i> situation	92
4.9.1 Establishment of an <i>in vitro</i> system to mimic EGFR and EpCAM expression profiles in primary HNSCC.....	93
4.9.2 EGFR and EpCAM levels associated with differential responsiveness to EGF in ERK activity	94
4.9.3 EGFR and EpCAM levels control EMT induction in tumor cells	95
4.10 pERK1/2 and Slug define HNSCC patients with poor outcome.....	98
4.10.1 Concurrent expression pattern of phospho-ERK and Slug in HNSCC samples.....	99
4.10.2 Slug correlates with ERK activation.	99
4.10.3 Phospho-ERK and Slug predict poor survival of HNSCC patients	101
5. DISCUSSION	102
5.1 Duality of EGF/EGFR signaling in HNSCC.....	102
5.2 A novel cross-talk between EpCAM and EGFR.....	107
5.3 Functional consequences of the crosstalk between EGFR and EpCAM.....	110
5.3.1 EpEX induces proliferation and exhibits an inhibitory effect on EGF-induced cell migration	110
5.3.2 EpEX impedes EGF-induced EMT by altering the integrated signal strength of ERK1/2 activation.	111
5.3.3 EGFR and EpCAM define subpopulations of HNSCC with differing clinical outcome	112
5.3.4 EGFR and EpCAM levels control EMT induction <i>in vitro</i> and mimic the <i>in vivo</i> situation	114
5.3.5 pERK1/2 and Slug define HNSCC patients with poor outcome	115
6. BIBLIOGRAPHY	119

7. CONTRIBUTION STATEMENT	136
8. PUBLICATIONS	137
9. AFFIDAVIT/ EIDESSTATTLICHE VERSICHERUNG	138
10. ACKNOWLEDGMENT	139

Abstract

Head and neck squamous cell carcinomas (HNSCCs) are characterized by remarkable molecular heterogeneity that leads to stark therapy resistance and dismal clinical outcome. Intratumoral heterogeneity provides the basis to foster epithelial-mesenchymal-transition (EMT), and thus firmly associates with tumor progression, treatment resistance, and metastasis formation. The present thesis addressed the expression and function of the major determinant of epithelial differentiation, EpCAM, and of the therapeutic target EGFR in clinical samples (n=180) and *in vitro* models of HNSCC. The observation that EGFR^{low}/EpCAM^{high} HNSCC patients possess considerably improved survival raised important questions regarding the molecular mechanism for the observed discrepancies in clinical outcomes, which could be answered in depth in the present study. EGF/EGFR has dual capacity in cellular fate decision regarding proliferation and EMT, through shaping different ERK activation dynamics and, consequently, EGF/EGFR signaling modulates the expression of EMT-transcription factors (EMT-TFs) Slug, Snail, and Zeb1. Moreover, EpEX, the soluble ectodomain of EpCAM, was identified as a novel ligand of EGFR that activates pERK1/2 and pAKT, provokes EGFR-dependent proliferation, but impedes EGF-induced EMT. EpEX competitively rewires EGF/EGFR-ERK signaling and inhibits EMT-TF induction, leading to the inhibition of EGF-mediated EMT. The levels of pERK1/2 and Slug in clinical samples of HNSCC further reflected this mechanism, the high expression of which predicted poor clinical outcome. Therefore, the emerging

crosstalk between EGFR and EpCAM, converging at the level of pERK, represents a promising target to improve patient-specific adjuvant treatment of HNSCCs.

Abbreviations:

AJCC, American Joint Committee on Cancer
BrdU, bromodeoxyuridine
CRISPR-Cas9, clustered regularly interspaced short palindromic repeat
CSC, cancer stem cell
CTF, C-terminal fragment;
DAPT, N-[N-(3,5-Difluorophenacetyl)-L-alanyl]-S-phenylglycine t-butyl ester;
DFS, disease-free survival;
EGF, epidermal growth factor;
EGFR, epidermal growth factor receptor;
EGFR_{ex}, extracellular domain of EGFR;
EMT, epithelial-mesenchymal transition;
EMT-TF, EMT transcription factors;
EpCAM K.O.1, EPCAM-knockout clone 1;
EpCAM, epithelial cell adhesion molecule;
EpCAM-YFP, fusion of EpCAM with yellow fluorescence protein;
EpEX, extracellular domain of EpCAM;
EpICD, intracellular domain of EpCAM;
ERK1/2, extracellular signal-regulated kinase 1/2;
Fc, fragment crystallizable region;
FDA, Food and Drug Administration;
GFP, green fluorescent protein;
HC, heavy chain;
HCT8WT, HCT8 wild type;
HEK293, human embryonic kidney 293;
HNSCC, head and neck squamous cell carcinoma;
HPV, human papillomavirus;
IHC, immunohistochemistry;
Lef-1, lymphoid enhancer-binding factor 1;
LMU, Ludwig-Maximilians-University;
MEK, MAPK-ERK kinase;
MW, molecular mass;
OS, overall survival;
pAKT, phosphorylated AKT;
pEMT, partial EMT;
pERK1/2, phosphorylated extracellular signal-regulated kinase 1/2;
PI3, phosphoinositide-3;
qRT-PCR, quantitative real-time PCR;
Raf, rapidly accelerated fibrosarcoma kinase;
Ras, rat sarcoma gene;
RIP, regulated intramembrane proteolysis;
shRNA, short hairpin RNA;

siRNA, small interfering RNA;
TCGA, The Cancer Genome Atlas;
TGF α , transforming growth factor alpha;
TKI, tyrosine kinase inhibitor;
TNM, tumor, node, metastasis;
YFP, yellow fluorescence protein;
Zeb1, zinc finger E-box-binding homeobox 1
LN, lymph node

1. INTRODUCTION

1.1 Head and neck cancer

Head and neck cancer is a broad term that encompasses malignancies that arise in epithelia of the mucosal linings of the upper aerodigestive tract, the majority of which are squamous cell carcinomas. Head and neck squamous cell carcinomas (HNSCCs) are the sixth most-common carcinomas worldwide, affecting 600,000 patients per year, with mortality rates of 40–50% (Parkin, Bray, Ferlay, & Pisani, 2005). The two most important risk factors to develop a HNSCC are excessive alcohol and tobacco consumption, and high-risk human papillomavirus (HPV) infection, the latter particularly in oropharyngeal tumors. The disease characteristics are defined by phenotypic, biological, and clinical heterogeneity, which are currently undertaking noticeable changes, as our comprehension of the etiologies and the molecular landscape of this disease have progressed (Leemans, Snijders, & Brakenhoff, 2018). Disappointingly, despite the advances of therapeutic strategies on surgery, radiation, chemotherapy, and targeted therapy, survival has not evidently improved in recent years owing to the frequent development of locoregional recurrences, lymph-node metastases, and distant metastases (Leemans, Braakhuis, & Brakenhoff, 2011). Thus, metastatic disease and therapy resistance remain central challenges in the treatment of HNSCCs. Anatomic site, TNM stage, HPV status, and histopathological characteristics of the tumor are determining factors for risk stratification of HNSCCs. Except for the HPV status, molecular risk factors with clinical utility are lacking (Cancer

Genome Atlas, 2015). Therefore, generating an integrated evaluation system of molecular risk factors to prognosticate HNSCCs progression is in great demand.

1.1.1 Heterogeneity of HNSCCs

Recent insight has revealed that HNSCCs are remarkably heterogeneous (Cancer Genome Atlas, 2015; Mroz, Tward, Hammon, Ren, & Rocco, 2015; Puram et al., 2017; Stransky et al., 2011). High intratumoral heterogeneity generates an outstanding cellular diversity, which allows for the development of cellular subpopulations characterized by differential transcriptome signatures (Puram et al., 2017), thus providing the basis to equip cancer cells with tumor-initiating properties, variable degrees of epithelial-to-mesenchymal transition (EMT) and treatment resistance, ultimately hampering an accurate prognostication, therapeutic strategy decision, and determination of the cancer-driving genes. Recent studies have documented the importance of intra-tumor heterogeneity in tumor development, treatment resistance, and metastasis formation (Almendro, Marusyk, & Polyak, 2013; Bedard, Hansen, Ratain, & Siu, 2013; Burrell, McGranahan, Bartek, & Swanton, 2013; Gerashchenko et al., 2013; Hiley, de Bruin, McGranahan, & Swanton, 2014; Murugaesu, Chew, & Swanton, 2013). Accordingly, high intra-tumor heterogeneity also predicts poor overall survival of patients with HNSCC (Mroz et al., 2015; Mroz et al., 2013).

HNSCCs can be divided into various subclasses with different prognoses by utilizing expression profiling based on a study from Chung *et al.* (Chung et al., 2004). Notably, one subgroup with an EGFR-associated expression profile, evidenced by high

expression of phosphorylated form of EGFR (Tyr-1173), TGF α (major ligand of EGFR), MKK6 (an EGFR downstream signaling cascade kinase), and FGF-BP (an angiogenic switch molecule induced by EGF), presented a relatively poor prognosis. Additional subclasses of HNSCCs can be distinguished by making use of genetic analyses. The first and most noticeable distinction is the difference between HPV (+) and HPV (-) tumors. By profiling 279 HNSCCs, the study from The Cancer Genome Atlas represented a comprehensive landscape of somatic genomic alterations (Cancer Genome Atlas, 2015). HPV (+) tumors exhibited amplification of E2F1, activating mutations of PIK3CA, and loss of TRAF3, indicating abnormal activation of NF- κ B pathway, other oncogenic pathways, and the cell cycle. On the other hand, HPV (-) tumors unveiled amplifications on chromosome 11q, affecting the genes BIRC2, FADD, CCND1 and YAP1, or concurrent mutations of CASP8 with HRAS, pointing to cell cycle, cell death, NF- κ B, and other oncogenic pathways (Cancer Genome Atlas, 2015).

More recent data on single cell sequencing specifically displayed that HNSCC are comprised of heterogeneous mixture of tumor cells with individual RNA transcript signatures (Puram et al., 2017). Puram *et al.* profiled transcriptomes of ~6,000 single cells from 18 HNSCC patients, revealing that malignant cells varied between and within tumors in gene signatures related to partial epithelial-to-mesenchymal transition (pEMT), epithelial differentiation, stress, cell cycle, and hypoxia. Malignant pEMT cells spatially localized to the leading edge of tumor areas. The published data by Puram and colleagues shed more light into the interactions between stromal and a pEMT

program cells, refining HNSCC subclasses by their stromal and malignant composition, and importantly, defined pEMT as an independent predictor of metastasis (Puram et al., 2017). These results clearly accentuated that HNSCC is a heterogeneous malignancy, both at the clinical and molecular level.

1.1.2 Clinical management of head and neck cancer

The multidisciplinary treatment planning for HNSCCs patients is mainly directed by the tumor-node-metastasis (TNM) staging and the anatomical site. The TNM classification has been updated to the newest (eighth) edition which sets more emphasis on the significance of tumor depth of invasion and the HPV status (see Table1). The staging system for HPV-positive oropharynx tumors differs from the previous edition, which results in a lower stage for those tumors compared to that assigned by the seventh edition.

Surgery or radiotherapy is utilized for early-stage tumors. Surgery combined with upfront chemoradiation or postoperative chemoradiotherapy is considered as mainstays of treatment for advanced HNSCCs. Currently, only the classical clinical and histopathological factors are exploited for making therapeutic plans, and these classical methods have met their limitations in the frame of high-precision medicine.

Recent advances in clinical management include image-based and adaptive radiotherapy, transoral robotic resections (TORS), sentinel node biopsy (SNB), and application of the epidermal growth factor receptor (EGFR)-specific antibody (Cetuximab) combined with radiotherapy for HNSCC patients with recurrences and

metastases (Bonner et al., 2006; Montal et al., 2016; Schilling et al., 2015). Notably EGFR is one of the major molecular targets for therapeutic purpose. The optimal application of EGFR inhibitor-based treatment options is under active investigation. HNSCC is proved to be an intrinsically immune-suppressing disease and immune checkpoint inhibitors, which hamper the inhibitory interaction between programmed cell death protein 1 (PD-1) and its ligand PD-L1, have been established as novel and effective therapeutic options in advanced / metastatic HNSCCs (Ferris et al., 2016; Leemans et al., 2018; Saada-Bouزيد, Peyrade, & Guigay, 2019; Seiwert et al., 2016), with both nivolumab and pembrolizumab being granted FDA approval (Forster & Devlin, 2018).

Table 1. Tumour-node-metastasis (TNM) staging of head and neck cancer.

Seventh edition TNM	Eighth edition TNM
Stage I (T1N0)	Stage I (T1-T2N0-N1)
Stage II (T2N0)	Stage II (T1-T2N2 or T3N0-N2)
Stage III (T3N0 or T1-T3N1)	Stage III (T4 or N3)
Stage IVa (T4aN0-N1 or T1-T4aN2)	Stage IV (M1)
Stage IVb (T4b or T1-T4bN3)	—
Stage IVc (M1)	—

1.2 Epithelial-to-mesenchymal transition (EMT)

Epithelial-to-mesenchymal transition (EMT) is a cellular process in which epithelial cells modify the expression of adhesion molecules, lose their epithelial characteristics, and adopt mesenchymal features, which enhance their migratory and invasive

behavior. The reversion of this process mesenchymal-to-epithelial transition (MET), allows cells to acquire an apico-basal polarity and to gain epithelial characteristics, which is associated with a loss of migration. During embryonic development, cells can shift between epithelial and mesenchymal states highly plastically and dynamically, which plays essential role during somitogenesis, gastrulation, and neural crest delamination (Pei, Shu, Gassama-Diagne, & Thiery, 2019; Thiery, Acloque, Huang, & Nieto, 2009). In cancer, EMT has been shown to be associated with tumorigenesis, invasion, cancer cell stemness, metastasis, and treatment resistance (**Fig. 1**) (Lambert, Pattabiraman, & Weinberg, 2017; Nieto, Huang, Jackson, & Thiery, 2016). Although the classic description of EMT has been viewed as a binary shift between epithelial and mesenchymal states, more recent data have disclosed a greater flexibility in this process. EMT may rather proceed in a stepwise manner, through the generation of subpopulations that represent a spectrum of intermediary phases between full epithelial and full mesenchymal states. Hence cancer cells may undergo a partial EMT program (pEMT) and generally be characterized by a high degree of plasticity (Nieto et al., 2016; Pastushenko et al., 2018).

EMT is executed in response to various extracellular stimuli that induce the expression of EMT-inducing transcription factors (EMT-TFs), including Snail, Slug, Zeb, Twist, and others, and specific miRNAs, together with epigenetic and post-translational regulators. In the past several years it has become clearer that EMT is driven by fundamental

regulatory networks, among which the most extensively studied network is built around the transcription factors of the Snail, Slug, Zeb and Twist families.

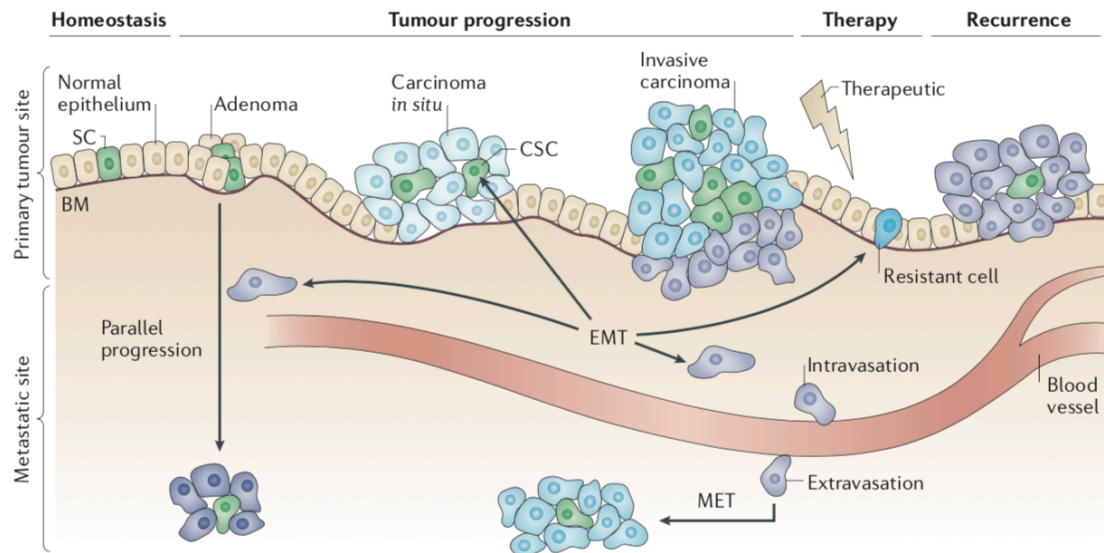


Figure 1. Role of EMT during cancer progression.

In tumors, cells that undergo epithelial-to-mesenchymal transition (EMT) are redefined the epithelial status, and may potentially acquire cancer stem cell-like (CSC) properties, thus associate with malignant phenotypes, such as invasiveness, tumor-initiating ability, and metastatic dissemination. EMT can elicit cancer cell dissemination from primary tumor and successive migration after invading through the basement membrane (BM) and further to secondary site during metastatic colonization. EMT may additionally play a role in parallel progression, in which tumor cells detach early in the disease and metastases progress in parallel to the primary tumor. EMT characters may as well foster treatment resistance, leading to recurrence and poor prognosis. (De Craene & Berx, 2013).

1.2.1 EMT transition states

Unlike the traditional view considering EMT as a binary transformation, the definition of EMT has now been broadened. Recent studies tend to consider that EMT proceeds in a stepwise manner characterized by different cellular phases with different epithelial and mesenchymal markers expression levels and intermediate transcriptional, morphological features, between epithelial and mesenchymal cells (Thiery et al., 2009).

The intermediate phases between fully epithelial and mesenchymal states have been referred to as partial, intermediate, or hybrid EMT.

Hybrid EMT states are evidenced by co-expression of epithelial and mesenchymal markers from multiple studies in various cancer cell lines (Bierie et al., 2017; Hong et al., 2015; R. Y. Huang et al., 2013; Jolly et al., 2016; Yu et al., 2013; J. Zhang et al., 2014). Cells with this hybrid phenotype have been stated as “metastable” (Tam & Weinberg, 2013), reflecting the plasticity and dynamics during EMT process. Tam and Weinberg have hypothesized a linear energy gradient between different EMT states based on epigenetic changes (**Figure 2**) (Tam & Weinberg, 2013). Along with epithelial and mesenchymal traits alteration, an intermediate EMT state is also associated with increased invasion, migration, and cell survival. Similarly, the co-expression of epithelial and mesenchymal markers has been documented *in vivo*, identifying the existence of multiple tumor subpopulations associated with distinctive EMT states, which displayed disparities in cellular plasticity, invasive behavior, and metastatic potential (Pastushenko et al., 2018). Moreover, the correlation between an enrichment of hybrid EMT state RNA signature and poor survival and therapy resistance has been revealed in several tumor types (George, Jolly, Xu, Somarelli, & Levine, 2017; Grosse-Wilde et al., 2015; Yamashita et al., 2018; Yu et al., 2013). It is also worth noting that the existence of partial EMT has been evidenced by single-cell transcriptomics analysis of HNSCC primary tumors, defined by incomplete activation of EMT-TFs. Intriguingly, pEMT cells were spatially localized at the edge of the tumor area

(Baumeister et al., 2018; Puram et al., 2017). In sum, the view of transitional states of EMT process offers a more dynamic interpretation, as depicted in **Figure 2** and has important implications for our understanding of tumor heterogeneity, invasion, metastasis and therapy resistance.

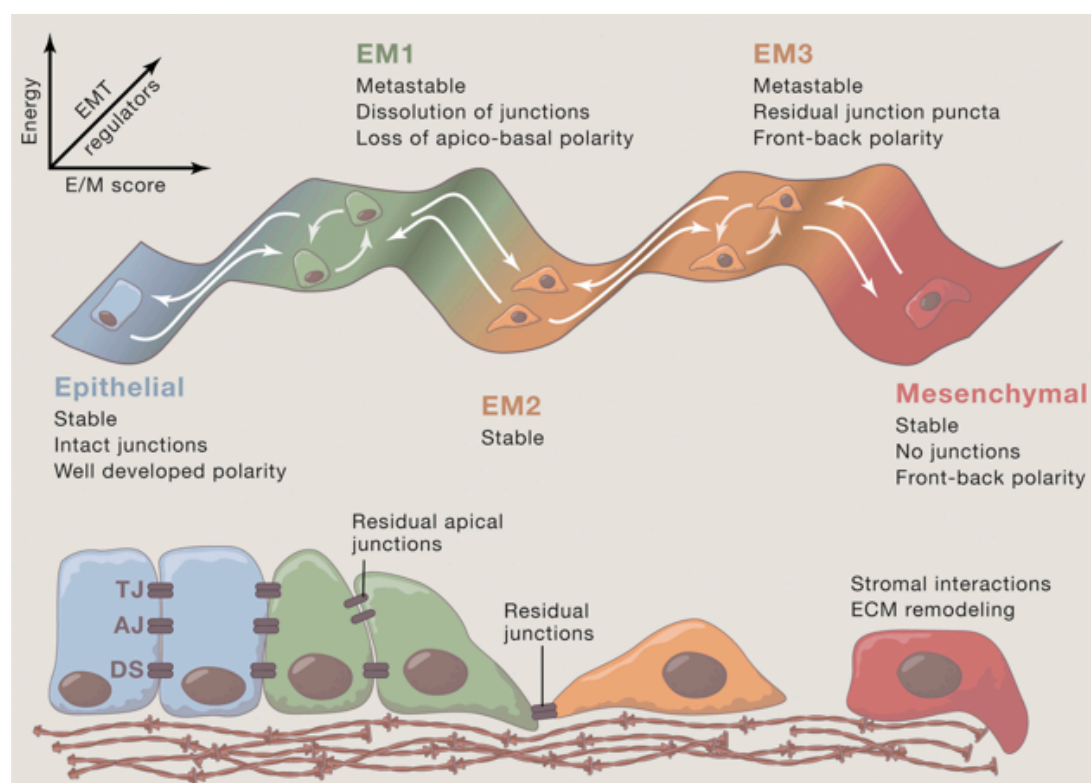


Fig 2. Hypothetical transitional states of EMT.

Induction of EMT can be viewed as a stepwise transition, whereby cells are characterized by epithelial (E), intermediate (EM), and mesenchymal (M) features, reflected by morphology, epithelial and mesenchymal markers, cellular polarity, and junction formation. During phase transition from E to M (x axis), both stability and metastability occur (y axis) in function of EMT regulators (z axis) including EMT-TFs, miRNAs and epigenetic controls. (Nieto et al., 2016)

1.2.2 Regulatory networks of EMT

Various extracellular stimuli, such as EGF and TGF β , can activate signaling cascades and rewire regulatory network to induce EMT. These factors do not only include signals that are secreted by tumor cells, but also “outgoing” signals from stromal cells within

tumors (Thiery et al., 2009). EMT is regulated by complicated networks at different levels by integrating transcriptional control, epigenetic modifications, non-coding RNA regulation, differential splicing (mediated by epithelial-specific regulatory protein ESRP1 and ESRP2) (Warzecha & Carstens, 2012), and post-translational control, which regulate protein stability and subcellular localization, such as phosphorylation and subcellular localization of Snail1 and MAP kinases (De Craene & Berx, 2013; Tam & Weinberg, 2013; Ye et al., 2015). The network built around EMT-TFs is undeniably the most extensively studied, which is supported by various interacting proteins, building up a robust transcriptional control of EMT. The activity of major EMT-TFs, such as SNAIL (zinc finger proteins SNAIL1 and SLUG), ZEB (zinc finger E-box-binding homeobox proteins ZEB1 and ZEB2), and TWIST (twist-related protein TWIST1, TWIST2), play a central role in EMT regulation and are defined as master EMT-TFs (Lamouille, Xu, & Derynck, 2014). The control of these factors relies not only on direct repression of E-Cadherin, the prototypic adhesion molecule that is frequently targeted in EMT, and the simultaneous repression of several other junctional proteins, but also on the activation of mesenchymal genes, which facilitate cellular reprogramming. The list of EMT-TFs further includes PRRX1, fork-head box protein C2 (FOXC2), E47, TCF4 (Ocana et al., 2012) and members of AP-1 (JUN/FOS), for which a role in controlling or contributing to EMT/MET-related cell plasticity has been reported (De Craene & Berx, 2013).

Multiple small non-coding RNAs and microRNAs (miRNAs) are proved to regulate EMT (Diaz-Lopez, Moreno-Bueno, & Cano, 2014). Of the many miRNAs altering their expression during EMT, the miR-200, miR-34, and miR-101 family members were firmly associated with epithelial differentiation and a reduction of their expression could be observed upon EMT induction (Puisieux, Brabletz, & Caramel, 2014). The reciprocal feedback loops between the miR-200 family and the ZEB family, miR-34 family, and the SNAIL family, tightly control both EMT and its reversion, MET (**Figure 3**), not only determining cell morphology along the EMT spectrum, but also controlling cell migration and invasion (Nieto et al., 2016). Furthermore, miR-101 might support E-Cadherin expression by repressing EZH2, thus provides further support for an epithelial phenotype. The networks of such feedback loops between miRNAs and major EMT-TFs serve as molecular switches for cellular fate decision and are important mechanisms to regulate epithelial/mesenchymal cell plasticity.

Yarden, 2011; Lemmon, Schlessinger, & Ferguson, 2014). All four ErbBs family members share a common structure, which consists of an N-terminal extracellular domain, a single transmembrane helix region, a cytoplasmic protein tyrosine kinase domain, and a C-terminal tail with multiple phosphorylation sites (Kovacs, Zorn, Huang, Barros, & Kuriyan, 2015; Lemmon et al., 2014). Despite such general similarity in architecture, the extracellular ligand-binding domains of these receptors and their mechanism of activation differ substantially.

EGFR is a 1,186 amino acid type-I transmembrane glycoprotein that consists of a 621 amino acid (aa) extracellular module (ECM) (comprising domains I, II, III, and IV), a 23 aa helical transmembrane domain (TM), and a 542 aa intracellular module (ICM) that contains a juxtamembrane cytoplasmic domain, a Src homology (SH1) tyrosine kinase domain, and a carboxyterminal tail with multiple phosphorylation sites (**Figure 4**) (Arkhipov et al., 2013; Freed et al., 2017). Besides the intact membrane-bound form of EGFR, soluble extracellular domain of EGFR has been detected, which may be generated by either proteolytic cleavage of full-length EGFR or by alternative splicing. Moreover, an increase of this soluble form has been observed in certain cancers (Adamczyk et al., 2011; Maramotti et al., 2012; Perez-Torres et al., 2008; Wilken et al., 2013).

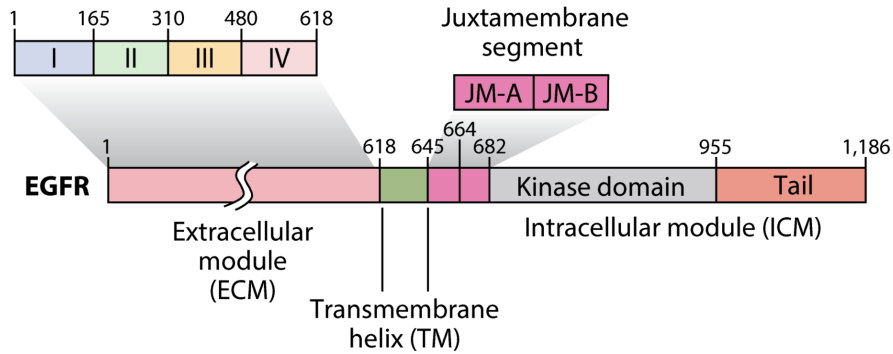


Fig 4. Model for domain architecture of EGFR.

Domain boundaries in EGFR. EGFR is a 1,186 amino acid type-I transmembrane glycoprotein that consists of a 621 amino acid (aa) extracellular module (ECM) (comprising domains I, II, III, and IV), a 23 aa helical transmembrane domain (TM), and a 542 aa intracellular module (ICM) that contains a juxtamembrane segment (JM) cytoplasmic domain, a tyrosine kinase domain, and a carboxyterminal tail with multiple phosphorylation sites (Kovacs et al., 2015)

1.3.2 EGFR ligands and signaling

Activation of EGFR is triggered by ligand binding. So far, seven different growth factors have been identified as EGFR ligands, which can be categorized into two groups based on receptor-binding affinity (Harris, Chung, & Coffey, 2003). The low-affinity ligands include epiregulin (EREG), amphiregulin (AREG), and epigen (EPGN). The high-affinity ligands bind 10- to 100-fold stronger and include EGF, heparin-binding EGF-like growth factor (HB-EGF), transforming growth factor- α (TGF α), and betacellulin (BTC) (Harris et al., 2003). A large body of literature has reported distinct cellular responses to these various EGFR ligands in terms of cell proliferation, survival, and differentiation (Ronan et al., 2016). Different EGFR ligands also produce quantitatively and qualitatively different signatures for downstream signals and are linked to unique cellular phenotypes (Freed et al., 2017).

The dimerization of EGFR initiates upon ligand binding, leading to either homodimerization with an additional EGFR molecule or heterodimerization with another ErbB family member, which results in autophosphorylation of tyrosine residues in the cytoplasmic tail. The phosphorylation of the intracellular domain then triggers a complex program of signaling cascades within the cytoplasm and, ultimately, to the nucleus. The two major EGFR downstream signaling pathways are the RAS-RAF-MEK-ERK pathway and the PI3K-Akt pathway (**Figure 5**), which control cell proliferation, survival, and differentiation (Ciardiello & Tortora, 2008).

In addition to typical signaling pathways activated by EGFR mentioned above, several other EGFR-associated pathways have been identified that may contribute to tumorigenesis and therapy resistance. EGFR has been reported to mediate cellular process by physical interaction with other proteins, such as PUMA, a Bcl-2 family protein (Zhu, Cao, Ali-Osman, Keir, & Lo, 2010) and other signaling molecules that are present in lipid rafts of the plasma membrane (Irwin, Mueller, Bohin, Ge, & Boerner, 2011), thus initiate kinase-independent signaling. A body of evidences suggest that full length of EGFR can be translocated from cell membrane to the nucleus. This nuclear translocation of EGFR signaling has been shown to contribute to cell proliferation, DNA repair ,and treatment resistance (Y. N. Wang et al., 2012). Moreover, upon EGF binding, EGFR can also be translocated to mitochondria and contribute to apoptosis and oncogenesis (Boerner, Demory, Silva, & Parsons, 2004).

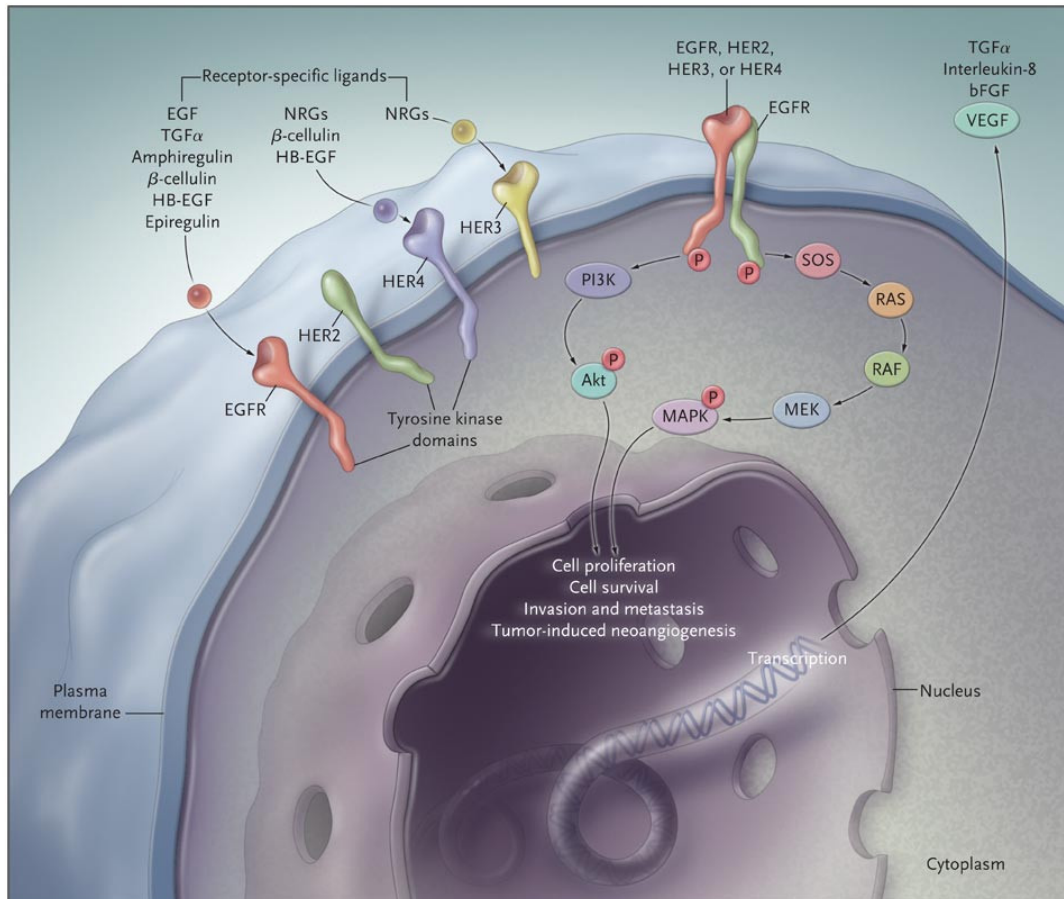


Fig 5. Model for activation of EGFR and downstream signaling pathways.

The dimerization of EGFR initiates upon ligand binding to the extracellular domain, leading to either homodimerization with an additional EGFR molecule or heterodimerization with another ErbB family member, which induces ATP-dependent phosphorylation of tyrosine residues in the intracellular domain. The phosphorylation then triggers a complex program of signaling cascades to the cytoplasm and, ultimately, to the nucleus. The two major EGFR downstream signaling pathways are the RAS-RAF-MEK-ERK pathway and the PI3K-Akt pathway (Ciardiello & Tortora, 2008).

1.3.3 EGFR biology and anti-EGFR treatment in HNSCCs

The EGFR pathway is one of the most frequently dysregulated molecular signaling in human cancers. EGFR is frequently overexpressed and its aberrant activity is implicated in a variety of cancers including HNSCCs (Han & Lo, 2012; Hynes & Lane, 2005) and consequently, EGFR is among the most intensely studied drug targets.

Overexpression of EGFR and its ligand TGF α are extensive in HNSCCs, which has been reported to be elevated in 92% and 87% at mRNA level, respectively (Grandis & Tweardy, 1993). EGFR was proved to be overexpressed at protein level in 38% to 47% of HNSCCs (Bei et al., 2004; Ongkeko, Altuna, Weisman, & Wang-Rodriguez, 2005). Moreover, EGFR levels are upregulated in tumor-adjacent normal epithelium and are further increased in poorly differentiated tumors and advanced-stage tumors. An upregulation of EGFR is further detected during pathogenesis, from dysplasia to squamous cell carcinoma (Molinolo et al., 2009; D. M. Shin, Ro, Hong, & Hittelman, 1994; Trivedi, Rosen, & Ferris, 2016).

HNSCC patients with elevated expression of EGFR have been reported to have poor prognosis (Kalyankrishna & Grandis, 2006). In a study of oropharyngeal cancer, nuclear EGFR was described and high EGFR expression levels, particularly enhanced expression of nuclear-localized EGFR, was proven to disclose a high local recurrence rate and poorer disease-free survival (Psyrrri et al., 2005). EGFR downstream effectors, such as ERK1/2 and Akt, which are highly associated with EMT based on multiple studies, were discovered to be abnormally activated in HNSCC. EGFR overexpression was reported to correlated with enhanced ERK activation in HNSCC by Albanell *et al.* Notably, elevated ERK activation was shown to associated with a higher proliferation and advanced tumor stage in HNSCC (Albanell et al., 2001). Moreover, another EGFR downstream signal, phosphorylated Akt, is discovered to be overexpressed in 57% to 81% of HNSCC tumors (Ongkeko et al., 2005). Thus, EGFR promotes cellular fates

as variable as growth, survival, migration, and EMT, through several oncogenic signaling pathways.

Currently, two types of EGFR antagonists have been successfully assessed in phase III trials and are in clinical use: anti-EGFR monoclonal antibodies and EGFR tyrosine kinase inhibitors (TKIs). Anti-EGFR monoclonal antibodies, with Cetuximab being granted FDA approval, bind to EGFR extracellular domain, blocking the ligand-binding region, and thus leading to blockage of ligand-triggered EGFR tyrosine kinase activation. On the other hand, TKIs, such as Erlotinib and Gefitinib, compete reversibly with ATP to bind to the intracellular EGFR tyrosine kinase domain, and, thereby, exert an inhibitory effect on EGFR auto-phosphorylation and downstream signaling activation. Various additional EGFR inhibitors are currently under investigation in early stages of clinical development.

Despite the overexpression of EGFR in HNSCC and its important role in the pathogenesis of the disease, EGFR inhibitors have only limited success in the therapy of HNSCC. So far, only Cetuximab is primarily implemented into palliative treatment of advanced HNSCC with moderate benefit. The benefits deployed by EGFR antagonists in HNSCC remain insufficient due to high heterogeneity and to the development of multiple resistances (Bertotti & Sassi, 2015; Braig et al., 2017).

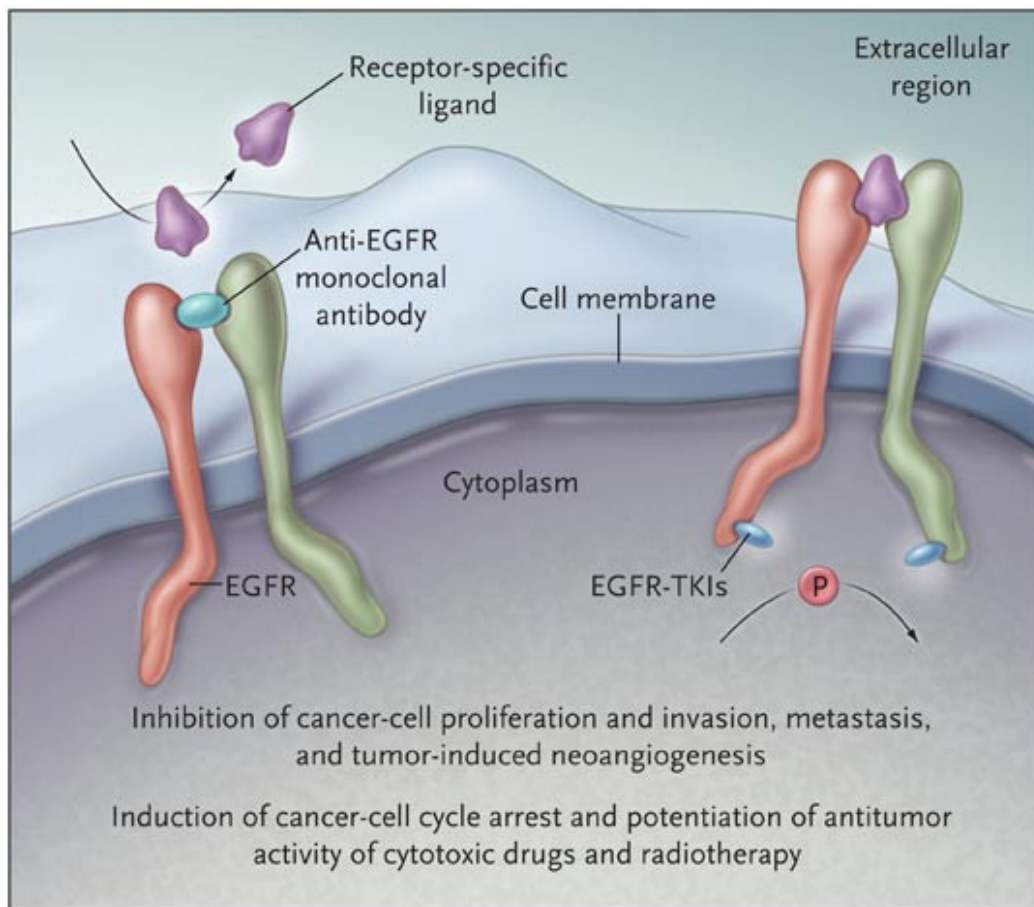


Fig 6. Mechanisms of action of anti-EGFR drugs in cancer cells.

Currently, there are two types of EGFR antagonists: anti-EGFR monoclonal antibodies and EGFR tyrosine kinase inhibitors (TKIs). Anti-EGFR monoclonal antibodies bind to EGFR extracellular domain, blocking the ligand-binding region, and thus leading to blockage of ligand-triggered EGFR tyrosine kinase activation. On the other hand, EGFR-TKIs, compete reversibly with ATP to bind to the intracellular EGFR tyrosine kinase domain, and, thereby, exert inhibitory effects on EGFR auto-phosphorylation and downstream signaling activation. (Ciardiello & Tortora, 2008)

1.4 Epithelial cell adhesion molecule (EpCAM)

1.4.1 Structure of EpCAM

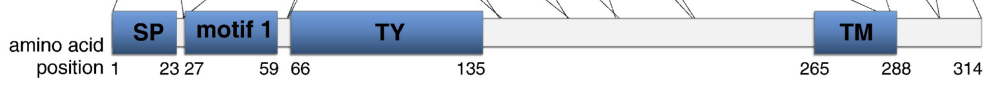
EpCAM is a type I transmembrane glycoprotein, consisting of a large extracellular domain of 265 aa (EpEX, N-terminal) linked to a short intracellular domain of 26 aa (EpICD, C-terminal) by a single transmembrane domain. The EpCAM-encoding gene is located on human chromosome 2 and consists of 9 coding exons (**Figure 7**). The

extracellular domain of EpCAM starts with the signal peptide and is followed by three protein motifs. Unlike initially suggested, EpEX is not comprised of a tandem of EGF-like repeats, since the second motif does not resemble an EGF-like domain but rather a thyroglobulin repeat (Chong & Speicher, 2001). EpEX contains three N-glycosylation sites, of which glycosylation at asparagine residue 198 (Asn¹⁹⁸) was proven to be highly important for the stability of the EpCAM protein at the plasma membrane (Munz, Fellingner, Hofmann, Schmitt, & Gires, 2008). Notably, EpCAM has been reported to be hyper-glycosylated in head and neck cancer compared to healthy tissue (Pauli et al., 2003). The transmembrane domain of EpCAM was shown to be involved in interacting with tight junction protein Claudin7 (Nubel et al., 2009). In the EpICD part, a putative PDZ binding site was described, which can associate with PDZ domain proteins and form complex with signal proteins (Demontis, Habermann, & Dahmann, 2006; Gunawardana, 2016). Whether this is the case for EpCAM is currently unknown. *In vitro*, EpCAM forms a *cis*-dimer where the two subunits laterally interact on the cell surface (Balzar et al., 2001; Trebak et al., 2001). Indeed, crystal structure analysis revealed a prevalent occurrence of EpCAM as a *cis*-dimer (**Figure 8**) (Pavsic, Guncar, Djinovic-Carugo, & Lenarcic, 2014).

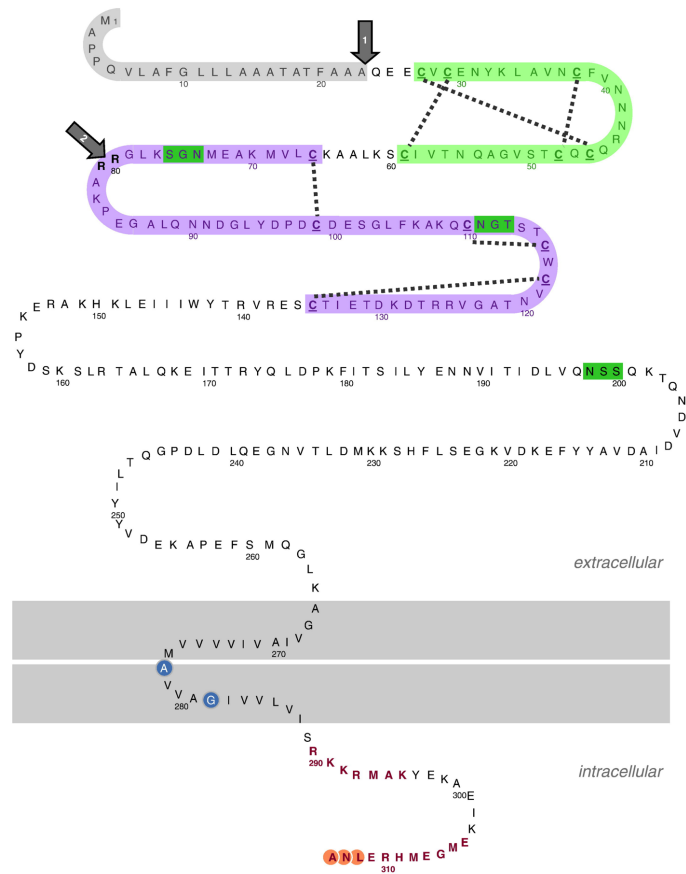
A Chromosome 2



B Protein



C Amino acid sequence



Signal peptide	➔ Cleavage site	● Association with Claudin-7 (Nuebel et al. 2009)
EpCAM motif 1	⋯⋯⋯ Disulphide bond	○ Putative PDZ-binding site
Thyroglobulin type 1-repeat (motif 2)	■ N-glycosylation site	● α-actinin binding sites (Baltzer et al. 1998)

Fig 7. Structure of EpCAM.

EpCAM encoding gene (A), protein (B) and the amino acid sequence (C) and PTM of EpCAM. Adapted from Schnell et al (Schnell, Cirulli, & Giepmans, 2013).

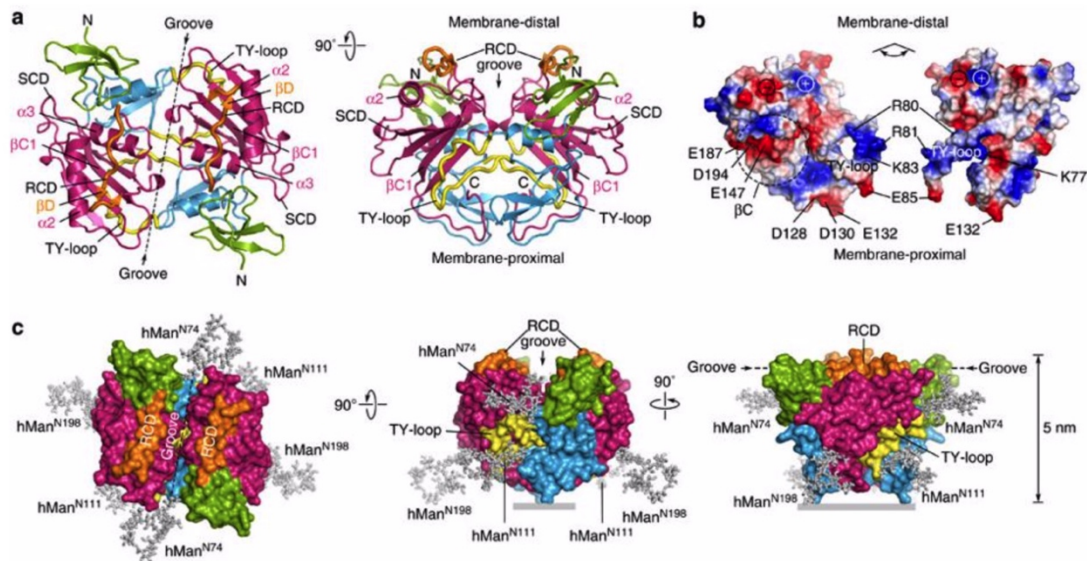


Fig 8. Structure of EpEX cis-dimer.

(a) Representation of EpEX cis-dimer in top and side orientations. (b) The molecular surface of EpEX cis-dimer, color-coded by electrostatic potential. (c) Molecular surface of EpEX cis-dimer with modelled high-mannose chains at N-glycosylation sites of wild-type EpCAM (Asn74, Asn111 and Asn198. (Pavsic et al., 2014)

1.4.2 Regulated intramembrane proteolysis (RIP) of EpCAM and EpCAM-mediated signalling

Regulated intramembrane proteolysis (RIP) is a two-step regulated mechanism combining protease-induced ectodomain shedding with the consecutive liberation of an intracellular domain (ICD) by the gamma-secretase complex. Both, the shed soluble ectodomain and the released ICD of multiple proteins that are subject to RIP, including NOTCH receptors, Amyloid Precursor Protein APP, and others (Brown, Ye, Rawson, & Goldstein, 2000; McCarthy, Coleman-Vaughan, & McCarthy, 2017), may activate signaling events. The proteases implicated in shedding the extracellular domain of EpCAM are members of the “A Disintegrin and Metalloproteinase” ADAM family of sheddases, including ADAM17. Further cleavage is fulfilled by the γ -secretase complex containing presenilin-2 (PS-2). RIP of EpCAM initiates upon cleavage by

ADAM17, shedding of the ectodomain EpEX, which acts as a homophilic ligand for full-length EpCAM (Maetzel et al., 2009). However, other functions remained unidentified. The resulting membrane-tethered C-terminal fragment (CTF) then become a substrate for the γ -secretase complex, which cleaves CTFs at gamma sites (γ -site) to release the A β -like fragment and at epsilon sites (ϵ -site) to liberate EpICD into the nucleus, where it cooperates with β -catenin, FHL2 and Lef1 to regulate gene transcription, including cyclin D1 (Maetzel et al., 2009).

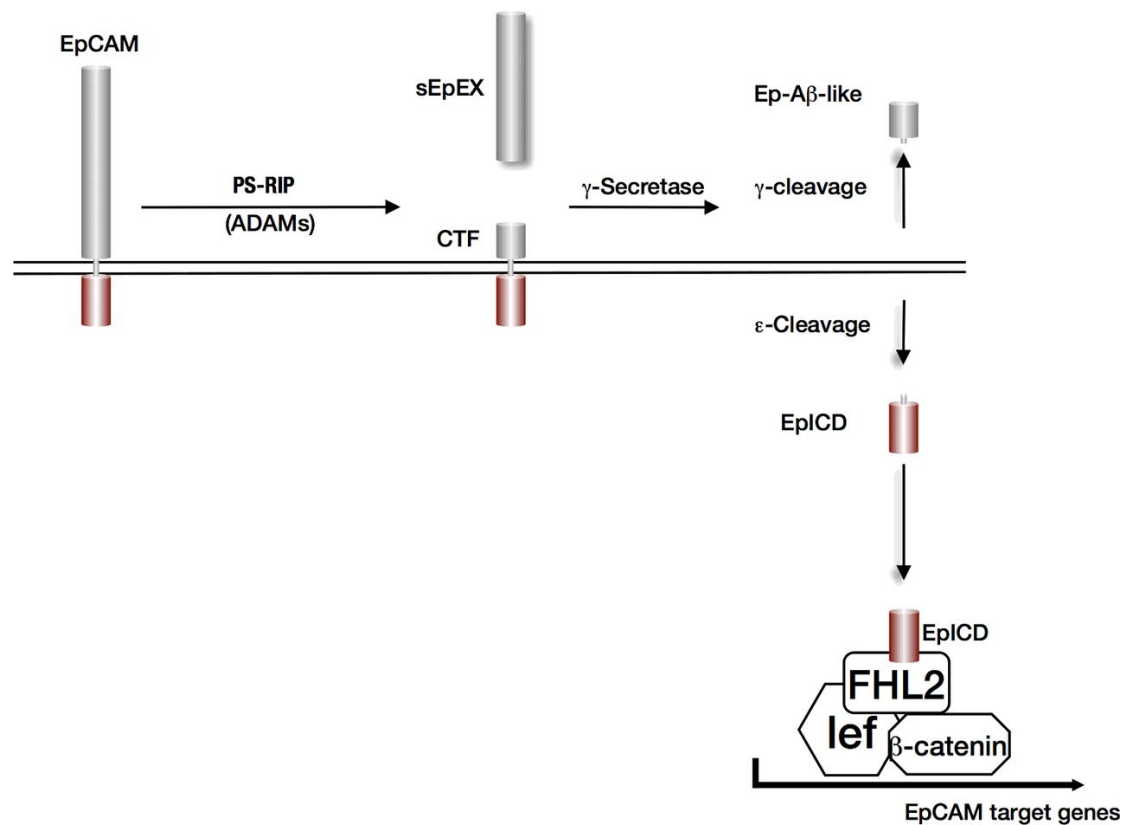


Fig 9. Schematic representation of the regulated intramembrane proteolysis of EpCAM.

Cleavage of EpCAM is initiated upon shedding of the ectodomain EpEX through ADAM proteases. The resulting CTF is a substrate for the γ -secretase complex. Intramembrane cleavage occurs at gamma sites (γ -site) to release the A β -like fragment and at epsilon sites (ϵ -site) to liberate EpICD into the nucleus, where it cooperates with β -catenin, FHL2 and Lef1 to regulate gene transcription (Gires, 2017).

1.4.3 EpCAM in cancer

EpCAM was defined as an epithelial cell adhesion molecule and was also described as a signaling membrane glycoprotein involved in regulating differentiation and proliferation in cancer and stem cells (Chaves-Perez et al., 2013; Kuan et al., 2017; Litvinov, Bakker, Gourevitch, Velders, & Warnaar, 1994; Lu et al., 2010; Maetzel et al., 2009; Sankpal, Fleming, Sharma, Wiedner, & Gillanders, 2017; Sarrach et al., 2018; Slanchev et al., 2009). More recently, EpCAM has been reported to define the degree of epithelial differentiation in HNSCCs and its expression was contrary to genes constituting a pEMT signature, including Slug and vimentin (Puram et al., 2017).

EpCAM expression is elevated in a variety of carcinomas. High expression of EpCAM often, but not always, predicts poor prognosis in breast cancer, esophagus, colorectal cancer, pancreatic cancer, ovarian cancer, as well as in bladder cancer (Fong et al., 2008; Seeber et al., 2016; Spizzo et al., 2002; Spizzo et al., 2004; Stoecklein et al., 2006; van der Gun et al., 2010). However, high levels of EpCAM correlated with improved survival in renal, thyroid, colonic, gastric cancers (Ralhan et al., 2010; Seligson et al., 2004; Went et al., 2005; Went et al., 2006), and in HNSCCs, as shown by Baumeister *et al.* (Baumeister et al., 2018). Notwithstanding, so far, evidence addressing the prognostic value of EpCAM in HNSCC patients remains scarce. Additionally, EpCAM is also considered as an appealing target for tumor diagnosis and therapy because of its tumor-associated overexpression and its role in tumor progression (Baeuerle & Gires, 2007; Munz et al., 2010; Riesenber, Buchner, Pohla, & Lindhofer, 2001).

2. ZUSAMMENFASSUNG

Eine charakteristische Eigenschaft von Plattenepithelkarzinomen des Kopf-Hals-Bereiches (HNSCC; Head and Neck Squamous Cell Carcinomas) ist ihre molekulare Heterogenität, welche zu verstärkter Therapieresistenz und unbefriedigenden klinischen Verläufen führt. Inter- und intratumorale Heterogenität liefern die molekulare Basis für eine Differenzierung von Tumorzellen entlang einer Epithelial-zu-Mesenchymalen-Transition (EMT), welche eine zentrale Rolle bei der Tumorprogression, Therapieresistenz und Metastasenbildung spielt. Die vorliegende Arbeit beschäftigt sich mit der Expression und Funktion des zentralen Marker für epitheliale Differenzierung EpCAM und des therapeutischen Zielantigens EGFR, in klinischen Fällen (n= 180) und in *in vitro* Modellen von HNSCC. Die Beobachtung, dass EGFR^{low}/EpCAM^{high} HNSCC Patienten eine stark verbesserte Überlebensprognose aufweisen, warf die Frage nach der molekularen Grundlage auf, welche im Rahmen dieser Arbeit beantwortet werden konnte. Die EGF/EGFR Signalkaskade besitzt duale Fähigkeiten das zelluläre Schicksal in Bezug auf Proliferation und EMT zu beeinflussen. Durch unterschiedliche Aktivierungsdynamiken der Effektor kinase ERK wird entweder ein zelluläres Programm zur Proliferation (intermediäre ERK Aktivierung) induziert oder die Expression von EMT-Transkriptionsfaktoren wie Snail, Zeb1 und Slug aktiviert, und somit EMT ausgelöst (starke ERK Aktivierung). Weiterhin wurde die extrazelluläre Domäne von EpCAM, genannt EpEX, als neuer Ligand von EGFR identifiziert, welcher pERK1/2 und pAKT aktiviert, wodurch EGFR-abhängige Proliferation eingeleitet, EGF-gesteuerte EMT

jedoch inhibiert wird. EpEX moduliert in kompetitiver Weise die EGF/EGFR-ERK Signalkaskade, unterdrückt die Expression von EMT-Transkriptionsfaktoren und blockiert somit EMT Programm. Dies spiegelt sich in den Expressionsstärken von pERK1/2 und Slug in klinischen Fällen von HNSCC Patienten wieder. Entsprechend bedeutet eine hohe Expression von pERK1/2 und/oder Slug eine schlechtere Prognose von HNSCC Patienten. Die neu identifizierte Wechselwirkung von EGFR und EpCAM, und die Regulation der Effektor kinase pERK stellen somit ein interessantes therapeutisches Ziel dar, um die adjuvante Behandlung von HNSCC Patienten zu verbessern.

3. MATERIALS AND METHODS

3.1 Human samples

The Ludwig-Maximilians-University of Munich, Germany, HNSCC cohort (LMU cohort) included tumor specimens from 180 patients suffering from HNSCC. Distant normal mucosa was available for 87 patients. Clinical samples were obtained after written informed consent during routine surgery based on the approval by the ethics committee of the local medical faculties (Ethikkommission der Medizinischen Fakultät der Ludwig-Maximilians-Universität; #087-03; #197-11; #426-11) and in compliance with the WMA Declaration of Helsinki and the Department of Health and Human Services Belmont Report.

Table 2: Clinical parameters of HNSCC LMU cohort (n=180) including gender, age, p16 expression, TNM stage, smoking habits, and tumor sub-localization.

LMU HNSCC cohort				
Gender	Male	Female		
%	78.9	21.1		
absolute	142	38		
Age	<50	50-69	≥70	
%	14.3	63.4	22.3	
absolute	25	116	39	
P16	Negative	Positive	n.p.	
%	48.9	32.2	18.9	
absolute	88	58	34	
T-Stage	pT1-2	pT3-4	pTx	
%	50.9	48.0	1.1	
absolute	92	86	2	
N-Stage	N0	N+	Nx	
%	39.7	59.7	0.6	
absolute	71	107	12	
M-Stage	cM0	cM+	cMx	
%	96.1	2.2	1.7	
absolute	173	4	3	
Smoking Status	Never	Former	Current	n.d.

%	11.1	57.8	25.0	6.1
absolute	20	104	45	11
Localization	Oral Cavity	Oropharynx	Hypopharynx & Larynx	
%	21.2	58.8	20.0	
absolute	38	106	36	

3.2 Cell lines and treatments

FaDu, Cal27, Cal33, Kyse30, HCT8, HEK293, MCF7, RL95-2, MDA-MB-231 and DU145 cell lines were obtained from ATCC and DSMZ and were confirmed by short tandem repeat (STR) analysis (Helmholtz Center Munich, Germany). Kyse30 and HCT8 cells were stably transfected with EpCAM-YFP fusion in the 141-pCAG-3SIP vectors using MATra reagent (IBA, Goettingen, Germany) following the manufacturer's recommendations and selected with 1ug ml⁻¹ puromycin. Kyse30-shRNA lines were described in (Driemel et al., 2014). Cells were cultured in DMEM or RPMI 1640 supplemented with 10% fetal calf serum, 1% penicillin/streptomycin, in a 5% CO₂ atmosphere at 37°C.

Treatment with EGF (PromoCell PromoKine, Heidelberg, Germany), Cetuximab (Merk Serono, Darmstadt, Germany, 10ug/mL), AG1478 (Selleckchem, 10uM), Erlotinib (Selleckchem, 1uM), AZD6244 (Selleckchem, Munich, Germany; 1uM), MK2206 (Selleckchem, 1uM), β -lactone (Santa Cruz, Heidelberg, Germany, 50uM), recombinant EpEX-Fc, and recombinant Fc (Jackson ImmunoResearch, Baltimore, US) was conducted in standard culture medium.

3.3 siRNA treatment

Ky35 cells were transfected with siRNA targeting EGFR (On-TARGETplus siRNA pool n=4; Dharmacon, Lafayette, CO, US) at 50nM final concentration or cognate control siRNA (non-targeting pool) using Dharmafect Reagent 1 (Dharmacon) according to the manufacturer's instructions. After 24 h incubation at 37°C in 5% CO₂, media containing siRNA and Dharmafect were then replaced with normal culture medium and knockdown was assessed. Cells were then subjected to further assays.

3.4 Immunohistochemistry and immunofluorescence staining

Serial cryosections of primary tumors (n=180) were available for immunohistochemistry (IHC) staining. The sections were incubated with specific primary antibodies, including EpCAM- (1:100, VU1D9, Cell Signaling Technology, NEB, Frankfurt, Germany, #2929), EGFR- (1:200, Dianova, Hamburg, Germany, #DLN-08892), pAKT^{Ser473} (1:400, Cell Signaling technology; #4060), pERK1/2^{Thr202/Tyr204}-specific antibodies (1:200, Cell signaling technology; #4370). These sections were next incubated and stained using the avidin-biotin-peroxidase complex method (Vectastain, Vector laboratories, Burlingame, CA, USA). The slides were finally independently examined by two investigators with light microscopy on a Leica microscope at 100x, 200x, and 400x magnification. Immunohistochemistry scores (IHC score) were evaluated based on staining intensity and percentage, and a 0-300 scoring system was used, where the formula: 3x percentage of strongly staining tumor cells + 2x percentage of moderately staining tumor cells + 1x percentage of weakly staining tumor cells, was used to determine the score. Assessment was performed in a blinded

fashion by two investigators and is given as the mean of both percentages assessed in steps of 5%. (Mack & Gires, 2008).

As for Immunofluorescence staining, cells were plated on glass slides for the indicated time points in growth medium. Cells were washed with cold PBS and fixed with paraformaldehyde. Slides were blocked and then incubated with primary antibodies and then incubated with Alexa Fluor®-488- and Alexa Fluor®-594-conjugated secondary antibodies. Cells were examined and confocal microscopy image acquisition was performed with a TCS-SP5 system (Leica Microsystems; Wetzlar, Germany).

3.5 Flow cytometry, immunoblotting and immunoprecipitation

After trypsinization, aliquots of cells were incubated for 1 h at 4 °C with anti-EpCAM (1:50 dilution in PBS-3% FCS, CD326; BD Biosciences; Heidelberg, Germany,) and anti-EGFR (1:200 dilution in PBS-3% FCS, Dianova, Hamburg, Germany, #DLN-08892) -specific antibodies, or isotype-matched control IgG antibodies. The cells were washed three times in ice-cold PBS-3% FCS, and then stained with FITC-conjugated secondary antibody (1:50 dilution in PBS-3% FCS, Vector Laboratories/Biozol, Eching, Germany; FI-4001) for 30 min at 4 °C. After washing three times with ice-cold PBS-3% FCS, assessment of cell surface expression was performed with a FACSCalibur device (BD Pharmingen, Heidelberg, Germany).

Cells lysates were prepared using PBS containing 1% Triton X-100 supplemented with protease inhibitors (Roche Complete, Roche Diagnostics, Mannheim, Germany).

Protein concentration in cell lysates was determined using BCA-assay (Pierce™ BCA Protein Assay Kit, Thermo Scientific, Rockford, USA). Proteins were separated by 10-15% SDS-PAGE and transferred to PVDF membrane (Millipore, Darmstadt, Germany). After blocking in TBST containing 5% BSA for 1 h at room temperature, membranes were incubated with primary antibodies, including EGFR (1:1000 diluted in TBST containing 5% BSA; Cell signaling technology), EpCAM (1:5000 diluted in TBST containing 5% BSA; DAKO/Biozol; Eching, Germany; #M7239), pERK1/2^{Thr202/Tyr204} (1:1000; Cell signaling technology; #4370), ERK1/2 (1:1000; Cell signaling technology; #137f5), GFP (1:5000; Abcam, Berlin, Germany), phospho-Akt-Ser⁴⁷³ (1:1000; Cell Signaling Technologies; #92725), Akt (1:1000; Cell signaling technology; #9272), and actin antibodies (1:5000; Santa cruz, Santa Cruz US, #sc-47778) overnight at 4 °C. After washing three times, membranes were incubated with horseradish peroxidase (HRP)-conjugated secondary antibodies for 1 h at room temperature. Chemiluminescence signal was visualized with ECL reagent (Millipore, Darmstadt, Germany) in a Chemidoc XRS+ imaging system (Bio-Rad, Munich, Germany).

Indicated cells were lysed in lysis buffer (PBS containing 1% Triton X-100 supplemented with protease inhibitors). Lysates were cleared by centrifugation at 16,000 rcf for 15 min at 4 °C. Post-clearance supernatants were incubated with EpEX-Fc or Fc recombinant proteins (50 µg), EGFR- or EpCAM-specific antibodies (10µg), overnight at 4 °C and then with protein A agarose beads (Thermo scientific Pierce, Munich, Germany, #20333; 100 µl) for 2 h at room temperature. The

Immunocomplexes were washed 5 times in 25mM tris, 150mM NaCl, pH 7.2 and boiled in Laemmli sample buffer and load on SDS-PAGE for protein analysis.

3.6 Protein expression and cross-linking

Human recombinant EpEX (aa 24-265) was expressed in Sf9 insect cells (Thermo Scientific) and was purified as described (Pavsic et al., 2014). EGFR extracellular domain EGFR_{ex} (aa 25-642; gift from Matthew Meyerson; Addgene plasmid # 11011) was expressed and purified as reported (Ferguson, Darling, Mohan, Macatee, & Lemmon, 2000). For cross-linking, EpEX and EGF (250 pmol) and EGFR_{ex} (50 pmol) were mixed in final volumes of 9 µl of 20 mM HEPES pH 8.0, 100 mM NaCl for 1 h at 37 °C at 1000 RPM on a thermomixer. Afterwards, 3,6 µg of BS³ cross-linker (Sigma) were added for 30 min at 37 °C at 1000 RPM on a thermomixer. Reaction was stopped by adding 1 µl of 1 M Tris pH 8.0 and an additional incubation of 15 min.

3.7 Recombinant human EpEX-Fc purification and characterization

Culture the stably transfected HEK-EpEX-Fc cell in selection medium (DMEM+10%FCS+2.5mLP/S+antibiotic) in a T75 flask. At 60-75% confluence, cells were split 1:10 or higher into 3 T75 flasks. When cells reach 75% confluence, split cells and plate on 10 X 15cm dishes. Incubate cells until reaching around 75% confluence, and replace the medium with 25mL of starvation medium per plate (DMEM+ 10%FCS ultra-low IgG+ 2.5mLP/S). Collect media in multiple 50-mL conical falcons (soluble EpEX-Fc in the media). Clarify cellular debris by centrifuge at 4 °C for 20min at 5000rpm. Discard the pellet, pour the supernatant into new 50mL falcons, then

centrifuge again at 4 °C for 20min at 5000rpm. Filter and collect the supernatant and add protease inhibitors inside immediately. Prepare the Protein A agarose-column and wash the resin bed with 50mL cold PBS. Add the conditioned medium to the column and capture the flow-through. Once the media has completely passed through the column, wash the column with 50mL cold PBS. Elute EpEX-Fc proteins with 4-5mL elution buffer (20mM citric acid, PH 2.4). Capture the eluted material and immediately neutralize with 2M Na₂CO₃ solution. Concentrate EpEX-Fc proteins with 30kDa cutoff Ultra centrifuge units at 4 °C for 20min at 3500g. Resuspend EpEX-Fc protein in 600-1000uL Hanks buffer. Recombinant EpEX-Fc were then subjected to further assessment and assays.

3.8 Migration assay, cell proliferation, and BrdU incorporation

Migration was assessed with a standard scratch assay. Cells were seeded in 6-well plates and cultured to a confluence of 80%. Cells were then serum starved for 12h and a scratch was set on the monolayer with a sterile pipette tip across the center of the well. Cells were washed twice with PBS and three random sections of the scratch were marked. Photos were taken for the scratch areas at the indicated timepoints under the Axiovert25 microscope (Zeiss, Jena, Germany) with a Canon EOS 1300D camera (Canon, Schwalbach, Germany). Quantification of the gap distance was performed using ImageJ and MRI wound healing tool. Relative migration was adjusted for proliferation rates.

Serum starved FaDu and Kyse30 cells, treated with different concentrations of EpEX-Fc and EGF, were assayed for cell proliferation using an EVE automatic cell counter (NanoEntek, VWR, Munich, Germany). 1×10^5 cells were plated in 12-well plates before treatment. At time points indicated in the individual figure legends, cells numbers were assessed.

Additionally, to evaluate the proliferative effect of EpEX-Fc, FaDu and Kyse30 cells were plated into a 96-well plate at a density of 5000 cells/well before treatment. After serum starvation cells were treated accordingly for 72h as indicated in the individual figure legends. BrdU assay was performed with the Cell Proliferation ELISA BrdU kit (Roche, Cat.No.11647229001) following the manufacturer's protocol

3.9 Reverse transcriptase polymerase chain reaction analysis

Total cellular RNA was extracted and purified from cultured cells using the RNeasy Mini kit coupled with RNase-free DNase set (Qiagen, Hilden, Germany) and reverse transcribed with Reverse transcription kit (Qiagen). The resulting cDNAs were used for PCR using SYBR-Green PCR MasterMix (Qiagen, Hilden, Germany) in triplicates. PCR and data collection were performed on LightCycler480 (Roche Diagnostics, Mannheim, Germany). All quantifications were normalized to an endogenous control GAPDH. The relative quantitation value for each target gene were calculated according the equation $2^{-\Delta CT}$, where ΔCT was defined as $CT_{\text{gene of interest}} - CT_{\text{endogenous control}}$.

Table 3: Primers used to amplify the genes.

Gene	FW 5'-3'	BW 5'-3'
E-cad	TGC CCA GAA AAT GAA AAA GG	GTG TAT GTG GCA ATG CGT TC
N-cad	GAC AAT GCC CCT CAA GTG TT	CCA TTA AGC CGA GTG ATG GT
Vimentin	GAG AAC TTT GCC GTT GAA GC	GCT TCC TGT AGG TGG CAA TC
Snail	GCG AGC TGC AGG ACT CTA AT	CCT CAT CTG ACA GGG AGG TC
Slug	TGA TGA AGA GGA AAG ACT ACAG	GCT CAC ATA TTC CTT GTC ACA G
Zeb1	TGC ACT GAG TGT GGA AAA GC	TGG TGA TGC TGA AAG AGA CG
Twist	ACA AGC TGA GCA AGA TTC AGA CC	TCC AGA CCG AGA AGG CGT AG
GAPDH	AGG TCG GAG TCA ACG GAT TT	TAG TTG AGG TCA ATG AAG GG

3.10 Statistical analyses

Results represent as means with standard deviations. Significance of differences of two groups was calculated as two-tailed Student's *t* test. Significance of differences between more than two groups was calculated with One-Way or Two-Way ANOVA tests and multiple comparisons including Bonferroni or Tuckey correction using GraphPad Prism version 7.00 for Mac (GraphPad Software).

3.11 Survival analysis

Overall survival (OS) and disease-free survival (DFS) were calculated in months from the date of diagnosis to death due to any cause or to first observations of any recurrence or death (DFS). In the absence of an event, patients were censored at the date of the last follow-up visit.

Analysis was performed in R (R: A Language and Environment for Statistical Computing, R Foundation for Statistical Computing, 2017; 3.4.0) together with the R-survival package (CRAN). For univariate analysis, IHC scores were included into cox-proportional hazard models after stratification into high- and low expressers. Hazard ratios, 95% confidence interval ratios, median survival times and log-rank p-values were included in Kaplan-Meier plots.

4. RESULTS

Head and neck squamous cell carcinomas (HNSCCs) have a dismal overall survival (OS) at 5 years of approx. 45%. Currently, anatomical site, TNM classification and status of infection with high-risk human papillomavirus (HPV) represent the major means of patients' stratification for further therapy. Therefore, novel markers to prognosticate HNSCC progression are in great demand. In the initial experiments of the present doctoral thesis the expression and correlation with clinical endpoints of the two cell surface markers EGFR and EpCAM were assessed. EGFR is a therapeutic target in advanced, metastasized HNSCCs and EpCAM represents as surrogate marker for the epithelial phenotype of these tumors.

4.1 EpCAM and EGFR define subclasses of HNSCCs with disparate clinical outcome

4.1.1 EpCAM and EGFR expression in HNSCCs

First, expression patterns of EpCAM and EGFR were investigated in clinical samples of primary HNSCCs. EpCAM and EGFR expression were assessed by immunohistochemical staining of serial cryosections of primary tumors within an HNSCCs cohort from the head and neck department at the Ludwig-Maximilians-University of Munich, Germany (**LMU cohort; n = 180; Clinical parameters of the cohort in Table 2**). Expression levels of EpCAM and EGFR were quantified using an immunohistochemistry (IHC) scoring system (IHC score 0-300) that implements the

staining intensity and frequency in tumor samples within clinical samples. By comparison, IHC staining of EGFR and EpCAM, revealed heterogeneous in HNSCCs, as illustrated through four representative, distinctive patterns in **Figure 10**. Tumors in **Figure 10A** were characterized by overexpression of both, EGFR and EpCAM, with a frequent co-expression at the single cell level (**Fig. 10A**). Expression of EpCAM and EGFR assessed in tumors in **Figure 10B and C** showed reciprocal patterns, with overexpression of EGFR or EpCAM, respectively (**Fig. 10B, C**). Besides that, tumors depicted in **Figure 10D** exhibited dual low expression of EpCAM and EGFR (**Fig. 10D**). Based on IHC scoring using a cut-off threshold of 150, EpCAM and EGFR expression levels were classified as antigen^{high} and antigen^{low}. High expression of EGFR was present in 112 of 180 cases (62.22%), whereas the remaining 68 cases revealed low expression of EGFR (37.78%). By comparison, 109 carcinomas displayed high expression of EpCAM (60.56%) and EpCAM low expression in 71 cases (39.44%) (**Fig.10E**)

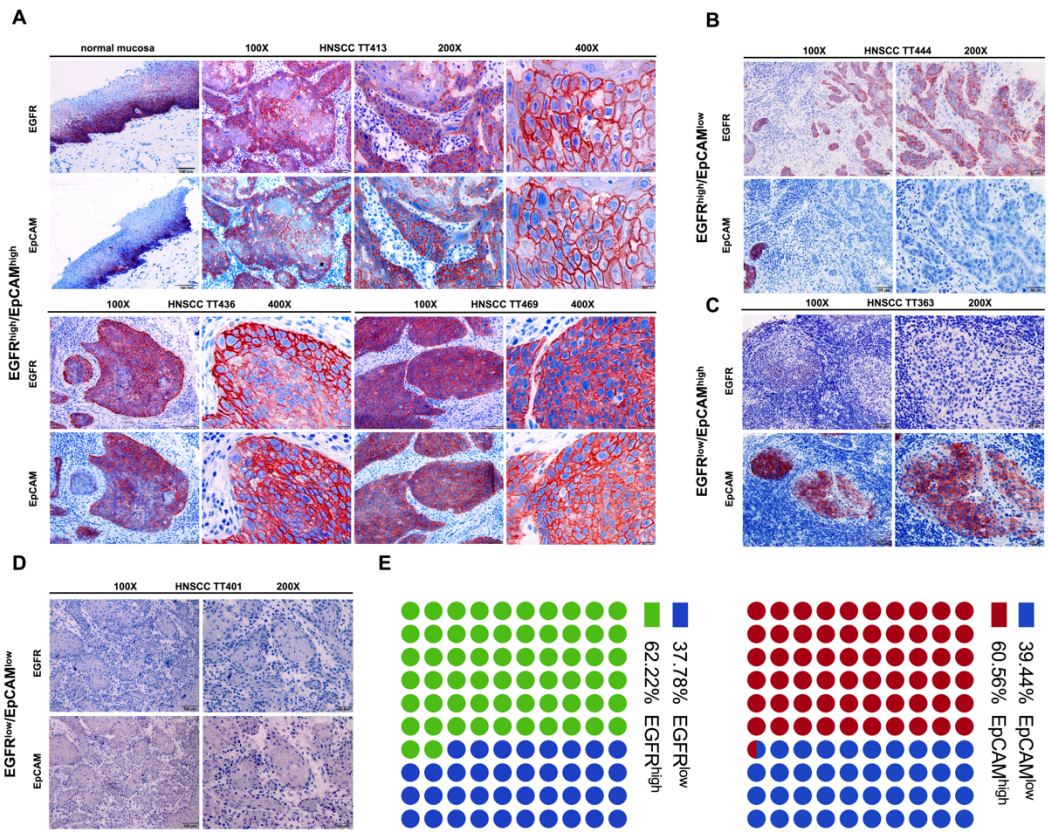


Fig 10. EpCAM and EGFR expression in HNSCCs.

Expression of EpCAM and EGFR was assessed by immunohistochemistry staining of serial cryosections of normal mucosa and primary tumors within the LMU HNSCCs cohort. Shown are representative examples of four distinct patterns: EGFR^{high}/EpCAM^{high} (A), EGFR^{high}/EpCAM^{low} (B), EGFR^{low}/EpCAM^{high} (C) and EGFR^{low}/EpCAM^{low} (D), at 100x, 200x, and 400x magnifications, as indicated. (E) Expression of EpCAM and EGFR is quantified and subclassified according to an IHC scoring cut-off threshold of 150 (0-300).

4.1.2 EpCAM and EGFR expression predict disparate clinical outcomes of HNSCCs

EGFR expression and signaling are important parameters for clinical endpoints of HNSCCs, and EGFR is utilized as a prognostic biomarker in a various of carcinomas, including HNSCCs (Kalyankrishna & Grandis, 2006; Psyrri et al., 2005). To analyze the correlation between EGFR expression and patients' outcome in the LMU HNSCCs cohort, Kaplan-Meier survival curves served to visualize OS of patients stratified

according to EGFR levels defined by IHC scoring (**Fig 11A**). With the third quartile as cut-off threshold, high EGFR expression significantly correlated with a worse OS (HR= 2.99; 95%CI, 1.57 to 5.72) across all patients (n = 180) (**Fig 11A, upper panel**).

It is now well accepted that the outcome of HPV-positive HNSCCs is more favorable compared with HPV-negative cases. The molecular profiles of the patients, the clinical presentation, and, most notably, the prognosis differ between the two subgroups (Ang et al., 2010; Lydiatt et al., 2017; O'Sullivan et al., 2016). In order to analyze the association of the EGFR expression in primary HNSCC with patients' survival independently of the HPV status, we calculated the OS for the HPV-negative LMU sub-cohort (n = 87). In a Kaplan-Meier analysis, the overall survival of patients with high EGFR expression were significantly poorer (HR= 2.78; 95%CI, 1.22 to 6.36), compared with EGFR^{low} patients in HPV-negative cases (**Fig 11A lower panel**), which confirms initial results obtained in the entire cohort.

In order to further confirm results obtained with the LMU-cohort, we analyzed the levels of EGFR expression using reversed-phase protein atlas data (RPPA) from the TCGA HNSCC cohort dataset as a validation cohort (Cancer Genome Atlas, 2015). A similar association between EGFR^{high} tumors and poor OS was observed in both, the full cohort (HR= 1.63; 95%CI, 1.07 to 2.48) and the HPV-negative TCGA sub-cohort (HR=1.66; 95%CI, 1.08 to 2.56), hence yielding results comparable with the LMU cohort (**Fig 11B**).

EpCAM levels have been reported to possess prognostic value in several cancer types, where high expression levels of EpCAM correlated with either poor prognosis (Fong et al., 2008; Seeber et al., 2016; Spizzo et al., 2002; Spizzo et al., 2004; Stoecklein et al., 2006; van der Gun et al., 2010), or with increased survival (Ralhan et al., 2010; Seligson et al., 2004; Went et al., 2005; Went et al., 2006). Furthermore, EpCAM also seems to play a dual role in cancer progression, either promoting or reducing progression (van der Gun et al., 2010). Noteworthy, it has been proposed that EpCAM represents a surrogate marker for epithelial differentiation in HNSCC, as opposed to a partial EMT signature that associated with metastases formation and poorer clinical outcome (Puram et al., 2017). These reports prompted the analysis of the expression of EpCAM in relation to EGFR and prognosis in HNSCC clinical samples.

Based on the expression patterns defined by IHC scoring using a cut-off value of 150, the cohort of patients was sub-classified into four subgroups: EGFR^{high}/EpCAM^{low}, EGFR^{low}/EpCAM^{high}, EGFR^{high}/EpCAM^{high}, and EGFR^{low}/EpCAM^{low}. EGFR^{high}/EpCAM^{high} represented 40.00% of primary tumors (n = 72/180 cases), EGFR^{low}/EpCAM^{low} 17.20% (n = 40/180), and reciprocal expression patterns EGFR^{low}/EpCAM^{high} (n = 37/180) and EGFR^{high}/EpCAM^{low} (n = 31/180) expression accounted for 20.56% and 22.22%, respectively, as shown in a quadrant plot Q1-Q4 (**Fig 11C**). To assess a possible correlation of EpCAM and EGFR expression patterns with the clinical outcome of patients, Kaplan-Meier survival curves were served to analyse OS and disease-free survival (DFS) (median follow-up 23 months) in

subgroups of EGFR and EpCAM expression of patients. The best outcome for the clinical endpoints of OS and DFS was seen in patients whose expression profile was EGFR^{low}/EpCAM^{high} (Q1, red curve), as compared to all other subgroups (**Fig 11D**). To be noted, the outcome of the EGFR^{low}/EpCAM^{high} subgroup (Q1, red curve) is most outstanding in comparison with the EGFR^{high}/EpCAM^{low} subgroup (Q3, green curve), with OS above 90% and below 10%, respectively (**Fig 11D**).

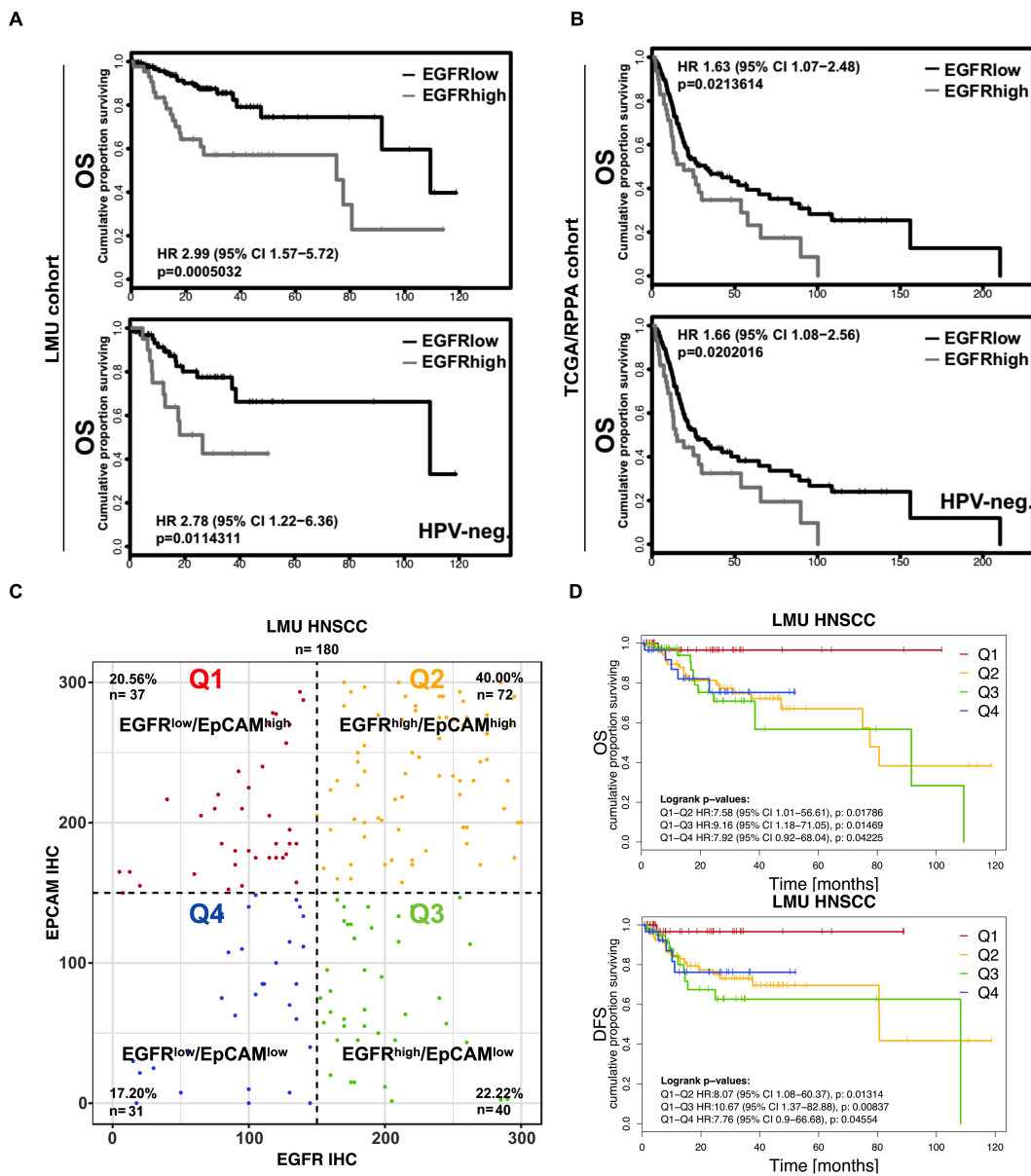


Fig 11. EpCAM and EGFR expression predict disparate clinical outcomes of HNSCC patients.

(A) Kaplan-Meier survival analysis of overall survival (OS) probability of HNSCC patients from the entire Ludwig-Maximilians-University of Munich cohort ($n = 180$) (upper panel) and the HPV-negative sub-cohort (lower panel) was performed to assess the correlation between EGFR expression and clinical outcome of patients. EGFR^{high} and EGFR^{low} subgroups were subclassified based on EGFR IHC score, (cut-off threshold at 3rd quartile). (B) Overall survival analysis of patients from the TCGA HNSCC cohort ($n = 279$) (upper panel) and HPV-negative sub-cohort (lower panel). Patients were stratified according to EGFR expression levels from the reversed-phase protein atlas (RPPA) data (cut-off threshold at 3rd quartile). (C) Based on the expression patterns defined by IHC scoring using a cut-off value of 150, patients from the LMU HNSCCs cohort ($n = 180$) were subclassified into four subgroups, and are indicated in a quadrant plot. (D) Kaplan-Meier survival analysis served to calculate overall survival (upper panel) and disease-free survival (DFS)(lower panel) of all four subgroups defined in C.

4.1.3 Correlation of EGFR and EpCAM expression subtypes with clinical parameters

Clinical parameters including HPV-infection status, tumor localization, T stage, N stage, grading, and age, were analyzed and determined in EGFR and EpCAM expression subgroups of patients. There was a slight enrichment of HPV-positive patients within the subgroup of EGFR^{low}/EpCAM^{high} tumors, although statistically not significant ($p=0.055$) (**Fig 12A**). In order to rule out an impact of the HPV-infection status on prognostic values based on EGFR and EpCAM expression profiles, OS and DFS (median follow-up 19 months) were assessed in a separate analysis of HPV-negative patients within the LMU cohort ($n = 87$). The expression patterns of EGFR and EpCAM of HPV-negative tumors in all four subgroups disclosed a similar distribution, in comparison with the full cohort (**Fig 12B**) and confirmed a significantly improved OS

and DFS of EGFR^{low}/EpCAM^{high} (red curve) over EGFR^{high}/EpCAM^{low} (green curve)

(Fig 12C).

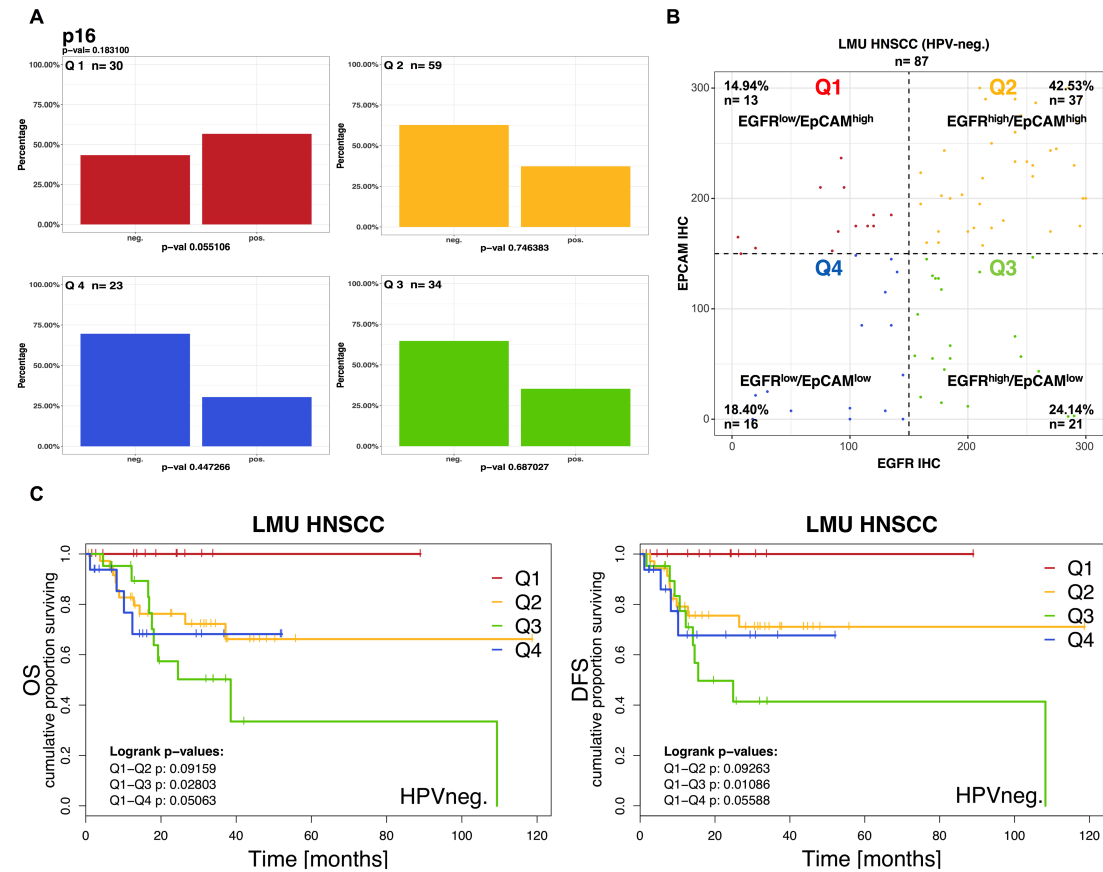


Fig 12. EpCAM and EGFR expression predict disparate clinical outcomes of HPV-negative HNSCC patients.

(A) HPV-statuses of each EpCAM and EGFR expression sub-populations are depicted in percent. The Chi square p-value for differences across all four quadrants is calculated (upper left). Individual p-values for differences of single quadrants versus the remaining three quadrants are indicated underneath. (B) Based on the expression patterns defined by IHC scoring using a cut-off value of 150, HPV-negative primary HNSCCs of the LMU cohort (n = 87) were subclassified into four subgroups, and indicated in a quadrant plot. (C) Kaplan-Meier survival analysis served to calculate overall survival (left) and disease-free survival (right) of all four subgroups defined in B.

In a separate study, we further analyzed the effect of the sub-localization of tumors on the clinical outcome. It is noteworthy that oral cavity carcinomas were significantly enriched in the subgroup of EGFR^{high}/EpCAM^{low} tumors, whilst EGFR^{low}/EpCAM^{high}

subgroup comprised of significantly less oral cavity carcinomas (**Fig 13A**). In order to exclude a possible contribution of sub-localizations of tumors to the disparate clinical outcomes of patients from the four EGFR and EpCAM expression subgroups, Kaplan-Meier survival analysis was performed in the most abundant entity within the LMU cohort, *i.e.* oropharyngeal carcinomas (n = 105). The four subgroups were repartitioned similarly to the full LMU cohort, as shown in a quadrant plot (**Fig 13B**). In conformity with all results aforementioned, EGFR^{low}/EpCAM^{high} patients displayed noticeably more favorable outcome, with significantly improved OS and DFS in comparison with EGFR^{high}/EpCAM^{low} patients (**Fig 13C**).

Hence, EpCAM and EGFR expression predicted disparate clinical outcomes of HNSCC patients. Furthermore, high expression of EpCAM and low expression of EGFR generally were associated with improved survival of HNSCC patients.

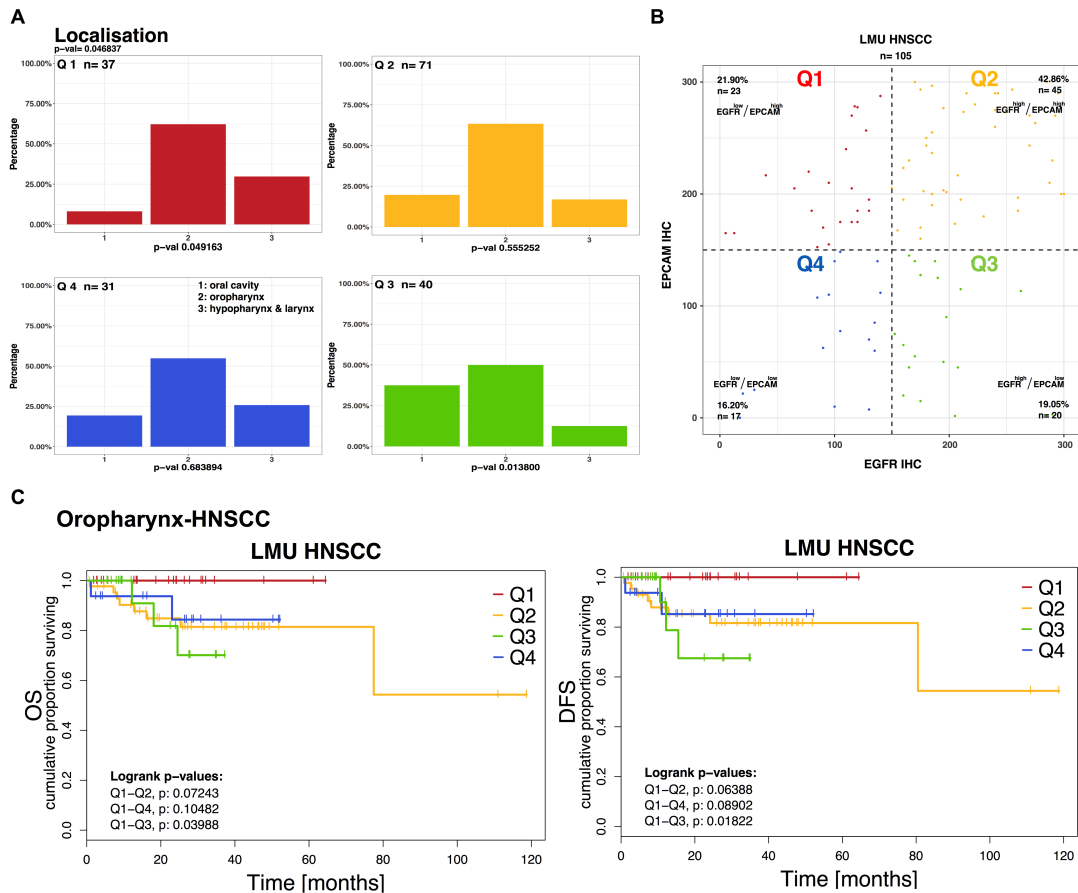


Fig 13. EGFR and EpCAM expression predict disparate clinical outcomes of oropharyngeal HNSCC patients.

(A) Tumor localization of each EpCAM and EGFR expression subgroups are depicted in percent. The Chi square p-value for differences across all four quadrants is calculated (upper left). Individual p-values for differences of single quadrants versus the remaining three quadrants are indicated underneath. (B) Based on the expression patterns defined by IHC scoring using a cut-off value of 150, primary oropharyngeal HNSCCs of the LMU cohort (n = 105) were subclassified into four subgroups, and indicated in a quadrant plot. (C) Kaplan-Meier survival analysis served to calculate overall survival (left) and disease-free survival (right) of all four subgroups defined in B.

4.2 EGF induces EMT in HNSCC cell lines, but induction of EpCAM RIP by EGF is not a common mechanism in HNSCC cells

The EGF/EGFR signaling axis has been repeatedly reported to tightly associate with carcinogenesis and most importantly, induction of EMT in various carcinoma cell lines

in a dosage dependent manner, including HNSCC, endometrial cancer, cervical cancer, lung cancer, breast cancer, colon cancer, esophageal cancer, pancreatic cancer, ovarian cancer, gastric cancer, thyroid cancer, skin cancer, and prostate cancer cell lines (Buonato, Lan, & Lazzara, 2015; Chandra Mangalhara et al., 2017; Cui et al., 2017; Fu et al., 2017; Fukuda et al., 2016; Grassi et al., 2017; Holz et al., 2011; J. Li et al., 2014; Y. Li et al., 2017; Muthusami, Prabakaran, Yu, & Park, 2014; Saito, Mine, Kufe, Von Hoff, & Kawabe, 2017; Sheng et al., 2017; Tashiro, Henmi, Otake, Ino, & Imoto, 2016; Vergara et al., 2011; P. Wang, Ma, & Zhang, 2017; Xu et al., 2017; Xue et al., 2015; Y. Zhang et al., 2015; Z. Zhang, Dong, Lauxen, Filho, & Nor, 2014; Zuo et al., 2011). Activation of EGFR downstream signaling pathways, *i.e.* Ras/Raf/MEK/ERK and PI3 kinase/AKT may play different role in proliferation, anti-apoptotic features, and EMT regulation. The regulatory role of EGFR in EMT offers a hint to understand the association between EGFR^{high} and poor clinical outcome. However, the explanation for EpCAM^{high} predicting improved survival is still in veil. It has been reported recently that EGF/EGFR mediated EMT is related to the regulated intramembrane proteolysis (RIP) of EpCAM. EGF treatment was demonstrated to induce RIP of EpCAM, resulting in shedding of the ectodomain of EpCAM (EpEX), and the release of the intracellular domain of EpCAM (EpICD) that induces an EMT program in an endometrial carcinoma cell line (Hsu et al., 2016). This prompted me to explore a potential functional crosstalk between EGFR and EpCAM, which could

provide a molecular basis for the observed disparate clinical outcomes in the HNSCCs cohort.

4.2.1 Characterization of HNSCC cell lines with a high co-expression of EGFR and EpCAM

The expression patterns of EGFR and EpCAM were analysed in HNSCC cell lines (FaDu and Cal27) and esophageal carcinoma cell line (Kyse30), and in the colon carcinoma cell line (HCT8). EGFR and EpCAM were highly expressed and co-expressed on the cell membrane of FaDu, Cal27, Kyse30, and HCT8 cell, as determined by immunostaining and flow cytometry (**Fig 14A**). Membranous co-localization of EGFR and EpCAM was confirmed with dual immunofluorescence staining and laser scanning confocal microscopy analysis of FaDu and Cal27 cells (**Fig 14B**).

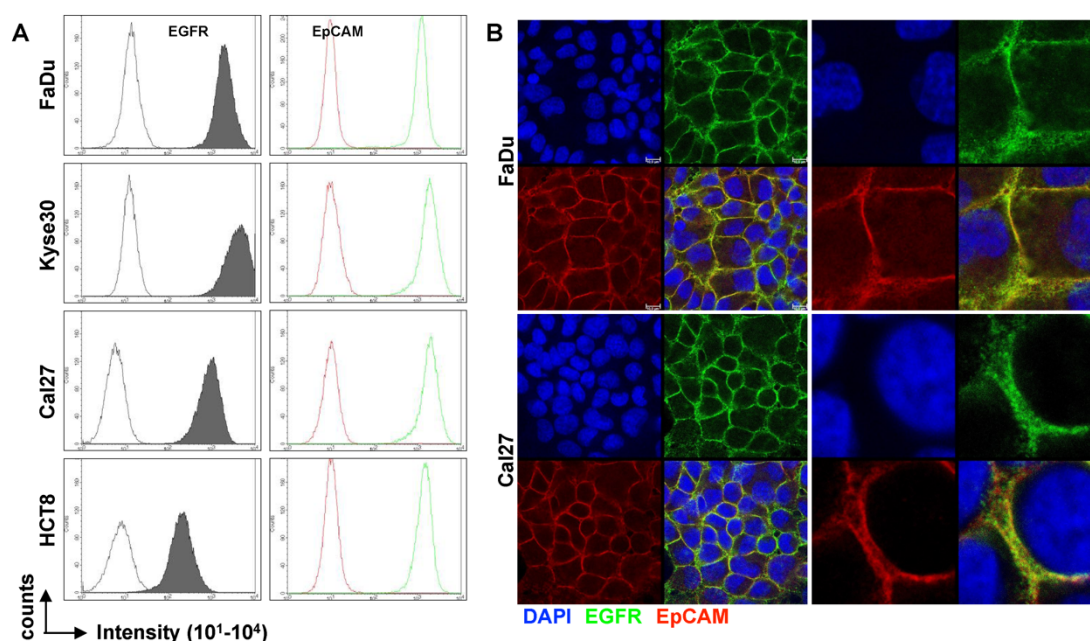


Fig 14. High Co-expression of EGFR and EpCAM in HNSCC cell lines.

(A) Cell surface EGFR and EpCAM were measured on FaDu, Kyse30, Cal2,7 and HCT8 cells by immunostaining and flow cytometry. Shown are representative

histograms of EpCAM and EGFR expression. (B) Double immunofluorescence staining of EGFR (green) with EpCAM (red) to assess co-localization of EGFR and EpCAM on FaDu and Cal27 cells. DAPI was used to stain nuclei (blue). Representative images in low (left) and high (right) magnifications are shown. All data were combined and generated from three independent replicates.

4.2.2 EGF treatment results in disruption of cell-cell contact and EMT in HNSCC cell lines that overexpress EGFR

In order to investigate whether EGF/EGFR signaling induces EMT in HNSCC carcinoma cells, FaDu and Kyse30 cells, which express high levels of EGFR, were treated with low (1.8 nM) and high (9 nM) concentrations of EGF for 72 hours. Following treatment, EGF^{high} (9 nM)-treated cells exhibited an elongated fibroblast-like morphology and decreased cell-cell contact. Contrarwise, EGF^{low} (1.8 nM)-treated cells, which corresponded to concentration reportedly inducing EMT in endometrial carcinoma cells, and control cells appeared cuboidal and displayed a cobblestone-like epithelial morphology (**Fig 15A**). The mesenchymal-like morphology with decreased cell-cell contact evident in EGF^{high}-treated cells, compared with control cells, was indicative of cells undergoing an EMT.

To validate this EMT, expression of E-Cadherin, which is considered as a hallmark associated with EMT (Lamouille et al., 2014), was examined by immunofluorescence staining and confocal imaging (**Fig 15B**) and immunoblotting (**Fig 15C**) with whole cell extract. Cells treated with EGF^{high} displayed reduced expression of E-Cadherin in comparison with control cells (**Fig 15B-C**). These data suggested that EGF^{high}

treatment induces morphological and biological alterations in HNSCC cell lines that are in conformity with EMT.

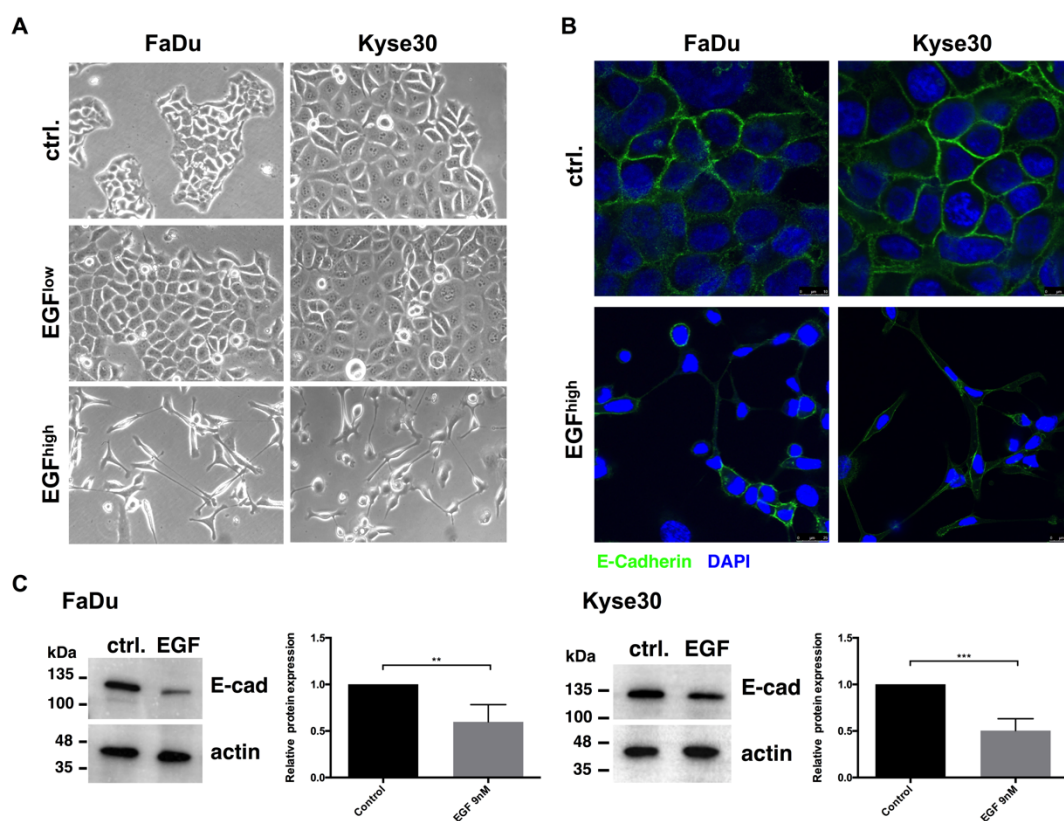


Fig 15. EGF promotes EMT in HNSCC cell lines.

(A) FaDu and Kyse30 cells were serum-starved and treated with control media, EGF^{low} (1.8 nM), and EGF^{high} (9 nM). Representative micrographs of cell morphology were recorded after 72 h at 100x magnification. (B) E-cadherin expression was measured on control- and EGF^{high}-treated FaDu and Kyse30 cells, by immunofluorescence staining and confocal laser scanning microscopy after 72 h. (C) Representative immunoblots and analyses of E-cadherin in control and EGF^{high} treated FaDu and Kyse30 cells after 72 h. Results are presented as mean values with standard deviations (SD). All data were combined and generated from three independent replicates.

4.2.3 EGF stimulation does not promote RIP of EpCAM in HNSCC cell lines

It has been reported that EGF treatment induces RIP of EpCAM in EGFR-dependent manner in endometrial carcinoma cell line RL95-2, resulting in shedding of soluble

extracellular domain (EpEX) and in the release of the intracellular domain of EpCAM (EpICD), which further functions as a nuclear transcriptional inducer of an EMT program (Hsu et al., 2016). Therefore, evaluating a potential link between EGF/EGFR signaling and RIP of EpCAM in HNSCC cell lines or discovering a possible alternative crosstalk between EGFR and EpCAM, which contributes to the disparate clinical outcomes of HNSCCs patients defined in **Fig 11**, was of high interest.

I aimed to examine whether EGF treatment in carcinoma cells would lead to alteration in events of EpCAM RIP, at the level of EpEX shedding, C-terminal fragment (CTF) on the membrane, and EpICD generation. To do so, human EpCAM was fused to yellow fluorescent protein (YFP) to increase the size of cleavage fragments and to facilitate their detection (see scheme in **Fig 16A**).

Ky30 and HCT8 cells stably expressing human EpCAM-YFP were maintained untreated or were treated with EGF (9 nM) for 72 h in serum-free condition. Extracellular shedding is accepted as a prerequisite for subsequent cleavage by the γ -secretase complex (Fig 16A). Therefore, I first investigate EpEX levels naturally shed in cell culture supernatant. A soluble ectodomain EpEX of EpCAM was detected in cell-free supernatant of both Ky30 and HCT8 cells. However, EGF^{high} treatment and controls groups did not reveal any difference (**Fig 16B**). Formation of a membrane-associated CTF-YFP was analyzed in membrane fraction, showing no alteration between EGF-treated cells and control cells (**Fig 16C**). Generation of intracellular fragment EpICD was detected in whole cell lysates, and further in cytoplasmic and

nuclear extracts. No accumulation of EpICD was observed following EGF treatment in comparison with untreated cells within the different subcellular fractions in the presence of proteasome inhibitor (β -lactone) (**Fig 16D, E**). β -lactone served to stabilize EpICD from proteasome-mediated degradation (Hachmeister et al., 2013; Y. Huang et al., 2019).

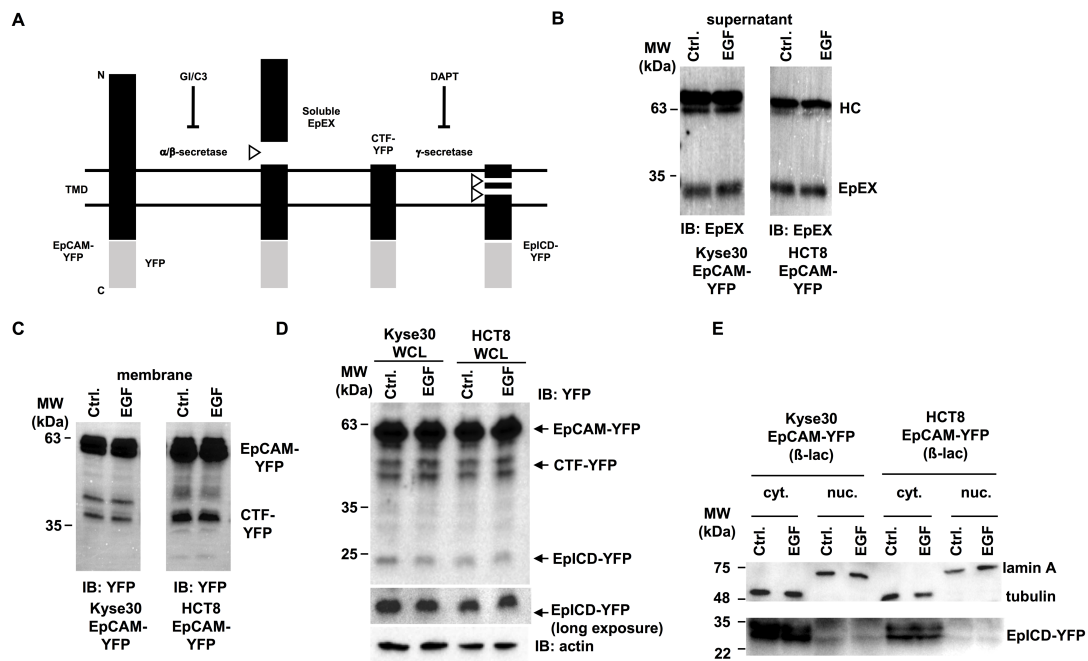


Fig 16. EGF^{high} promotes EMT but does not induce regulated intramembrane proteolysis of EpCAM.

(A) Schematic representation of EpCAM regulated intramembrane proteolysis including proteases involved and inhibitors. Kyse30 and HCT8 stably expressing EpCAM-YFP cells were maintained untreated or were treated with EGF 9 nM for 72 h. (B) Expression of soluble extracellular domain of EpCAM (EpEX) in supernatants were assessed by immunoprecipitation and immunoblot with EpCAM ectodomain specific antibody, and (C) membrane isolates were used to assess the formation of CTF-YFP by immunoblot with YFP specific antibody. (D) Whole cell lysates were used to visualize EpCAM-YFP, CTF-YFP, and EpICD-YFP by immunoblot with an anti-YFP antibody. (E) Generation of EpICD-YFP was detected by immunoblot with a YFP specific antibody in cytoplasmic (cyt.) and nuclear fractions (nuc.) of cells in the presence of proteasome inhibitor (β -lac). Tubulin and lamin A staining served to control fractionated samples. All data were combined and generated from three independent replicates.

In order to certify that the concentration of EGF utilized on endometrial carcinoma cells in the study of Hsu *et al.* would not impact on RIP of EpCAM, despite no effects on EMT in the cell lines studied here, I repeated the treatment of Kyse30 cells and HCT8 cells with 1.8 nM EGF for 24 h, which corresponds to conditions used by Hsu *et al.* In line with data shown in **Fig 16**, neither an alteration in EpEX shedding (**Fig 17A**), nor CTF formation (**Fig 17B**), nor accumulation of EpICD (**Fig 17C**) could be observed.

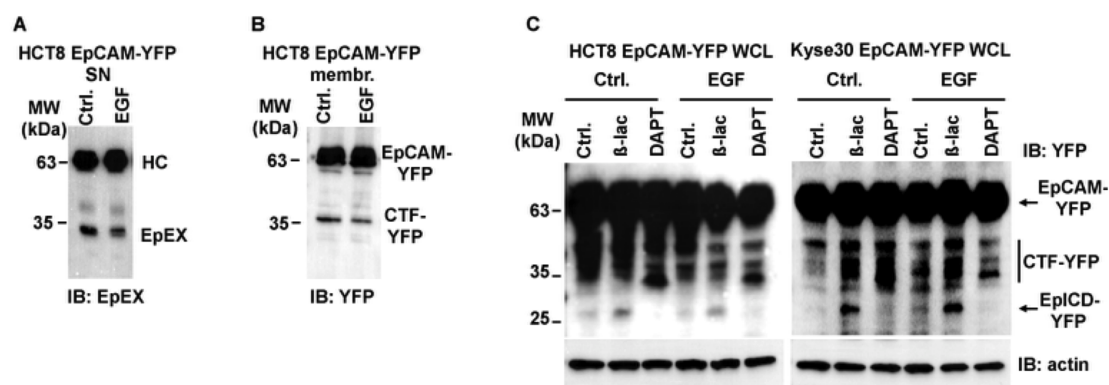


Fig 17. EGF^{low} does not induce EpCAM cleavage.

Kyse30 and HCT8 stably expressing EpCAM-YFP cells were maintained untreated or were treated with EGF 1.8 nM for 24 h. (A) Expression of soluble extracellular domain of EpCAM (EpEX) in supernatants were assessed by immunoprecipitation and immunoblot with EpCAM ectodomain specific antibody and (B) membrane isolates were used to assess formation of CTF-YFP by immunoblot with YFP specific antibody. (C) Whole cell lysates were used to visualize EpCAM-YFP, CTF-YFP, and EpICD-YFP by immunoblot with anti-YFP antibody. Actin staining served as control for equal protein loading. All data were combined and generated from three independent replicates.

4.3 EGF treatment does not result in reduction of EpCAM in a panel of carcinoma cell lines

To further explore an impact of EGF/EGFR signaling on the expression of EpCAM in a broader panel of carcinoma cell lines, EpCAM expression levels were examined in a

panel of nine cancer cell lines including HNSCC (FaDu, Kyse30, Cal27, Cal33), breast (MCF7, MDA-MB-231), colon (HCT8), prostate cancer cells (Du145), and endometrial (RL95-2), following EGF treatment with different concentration and for different duration. To be noted, these chosen nine carcinoma cell lines cover EGFR/EpCAM expression patterns from high, moderate, to weak for both molecules.

4.3.1 Expression of EpCAM assessed by flow cytometry

Using an antibody recognizing EpEX, flow cytometry analysis comparing cell surface expression of EpCAM between EGF-treated and untreated cells were conducted. Quantification of cell surface expression of EpCAM did not reveal any significant difference between EGF-treated cells and control cells, independently of initial expression levels of EGFR and EpCAM (**Fig 18A, B, D, E**). Nine cancer cell lines assessed herein exhibited no significant difference in EpCAM expression after EGF 1.8 nM or 18 nM treatment for 24 hours, compared to untreated cells (**Fig 18A, D**). In order to rule out dosage effect and possible contribution from duration of treatment, I further utilized prolonged treatment with EGF 9 nM for 72 hours in a separate analysis. No changes in EpCAM expressions were observed in the cell lines tested either, except for RL95-2 cell line, showing a slight increase of EpCAM expression on cell surface (**Fig 18B, E**). TGF α treatment was additionally conducted to certify that the lack of EpCAM reduction was not due to requirements for different EGFR ligands in the tested carcinoma cell lines. The results disclosed no reduction of EpCAM after TGF α 1.8 nM treatment for 24 hours (**Fig 18C, F**).

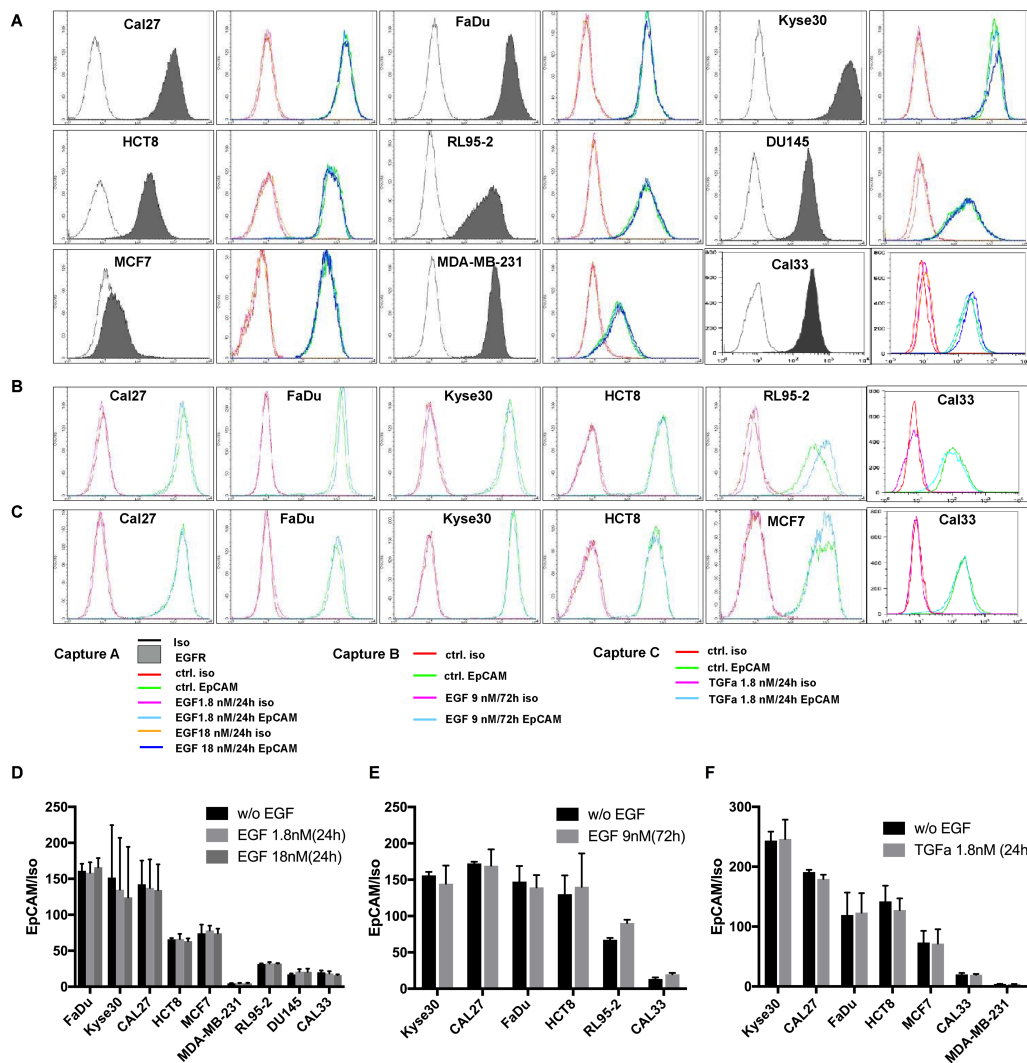


Fig 18. EGF and TGF α treatment does not reduce surface expression of EpCAM in an array of carcinoma cell lines.

(A-C) Indicated cell lines were maintained untreated or treated with (A) EGF 1.8 nM, 18 nM for 24 h (B) EGF 9 nM for 72 h or (C) TGF α 1.8 nM for 24. Cell surface expression of EpCAM was measured by flow cytometry. (D-F) Quantification of EpCAM expression was assessed by flow cytometry on indicated cell lines treated with EGF 1.8 nM and 18 nM for 24 h (D), and 9 nM for 72 h (E), and TGF α 1.8 nM for 24 h (F). Results are shown as ratios of EpCAM mean fluorescence intensities divided by control intensities (EpCAM/iso), means with standard deviations (SD). All data were combined and generated from three independent replicates.

4.3.2 Expression of EpCAM assessed by Western blot analysis

To further investigate the effects of EGF treatment on EpCAM protein expression, immunoblot analysis were performed with whole cell lysates of FaDu, Kyse30, Cal27,

Cal33, HCT8, MCF7, RL95-2, and Du145 cells to assess EpCAM levels. Cells were kept untreated or were treated with EGF 1.8 nM and 18 nM for 24 h, and EGF 9 nM for 72 h. Quantification of immunoblot results did not reveal any change in EpCAM expression levels (**Fig 19**), except for the treatment of RL95-2 cells with EGF 9 nM for 72 h, which confirmed an induction of EpCAM (**Fig 19B, D, right panel**).

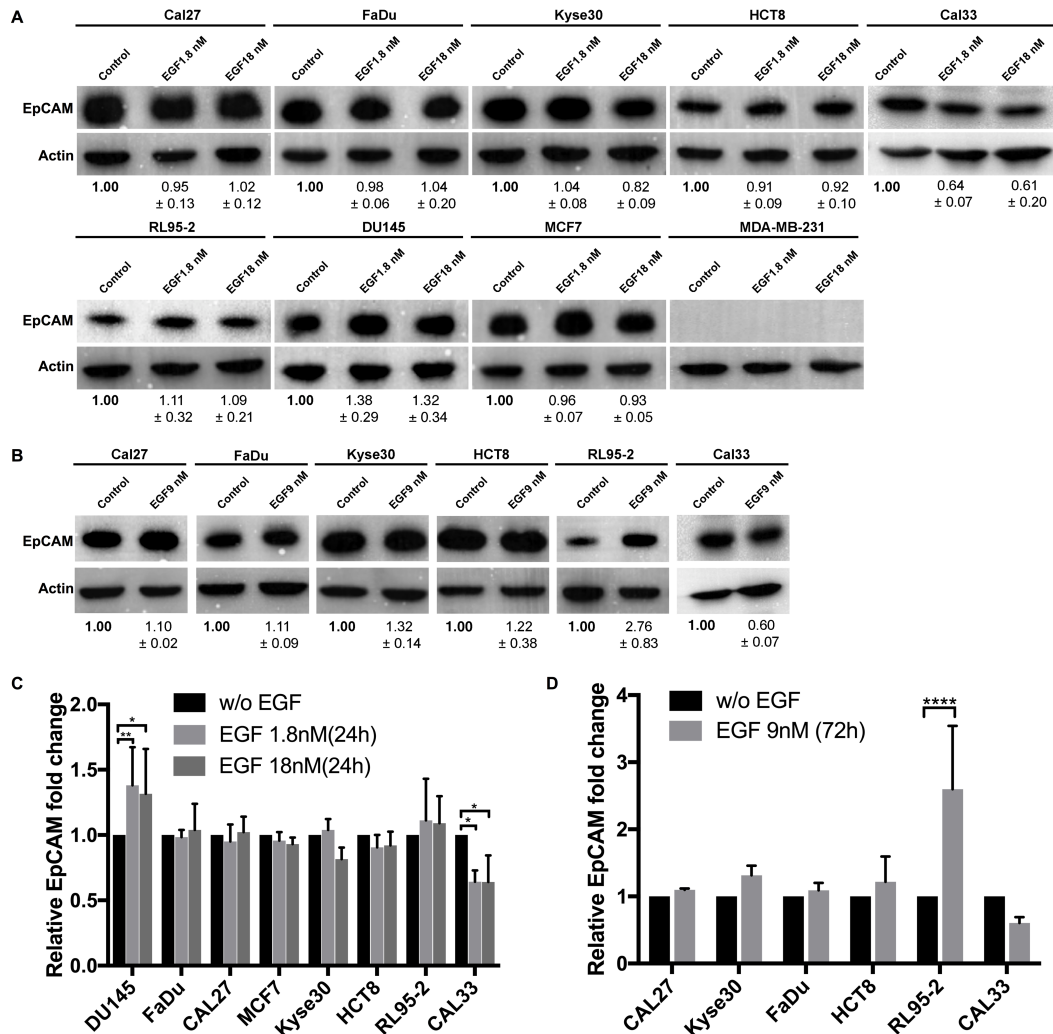


Fig 19. EGF treatment does not reduce EpCAM expression in a panel of carcinoma cell lines.

(A-B) Indicated cell lines were maintained untreated or treated with EGF 1.8 nM, 18 nM for 24 h (A) or EGF 9 nM for 72 h (B). Expression of EpCAM was measured by immunoblot with whole cell lysates. EpCAM expression levels normalized for actin and standardized to control are indicated below the immunoblots. (C-D) Quantification of EpCAM expression assessed by immunoblot on indicated cell lines treated with EGF

1.8 nM and 18 nM for 24 h (C), and 9 nM for 72 h (D). Results are shown as relative fold changes of EpCAM expression, where expression levels in control cells were set to one for comparison, means with standard deviations (SD). All data were combined and generated from three independent replicates. * p-value <0.05, ** p-value <0.01; paired student's T-test.

4.3.3 Expression of EpCAM assessed by IFS-confocal analysis

Next, immunofluorescence staining and confocal laser scanning microscopy analysis was performed to assess cell surface expression of EpCAM on FaDu, Kyse30, Cal27, HCT8 and RL95-2 carcinoma cells with EpEX-specific antibodies. The results confirmed a retention of EpCAM at the cell surface after treatment with EGF 1.8 nM or 18 nM for 24 h (**Fig 20A**) or with EGF 9 nM for 72 h (**Fig 20B**), which is consistent with results from flow cytometry measurements (**Fig 18**) and immunoblot staining (**Fig 19**). Of note, treatment of FaDu, Kyse30 and RL95-2 cells with EGF 9 nM for 72 hours induced a mesenchymal cell-like appearance, whereas Cal27 and HCT8 cells did not exhibit signs of EMT following the same treatment. The reason for such cell type-specific response to EGF^{high} treatment will be explored in further experiments.

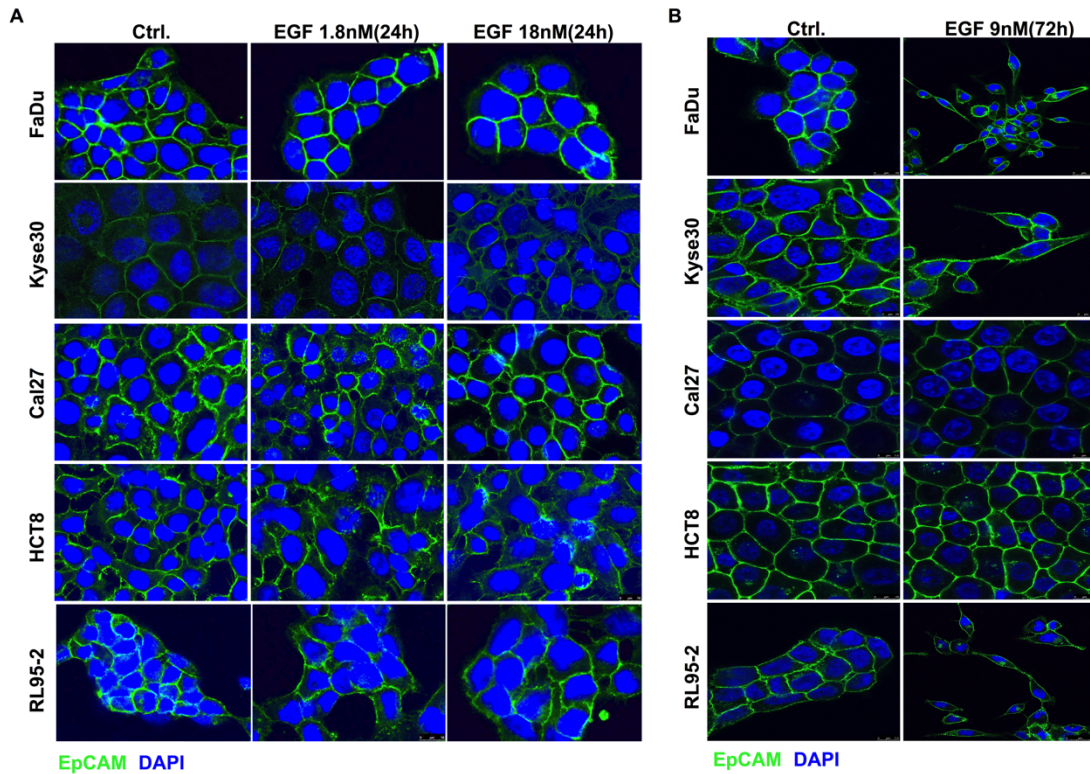


Fig 20. EGF treatment does not reduce expression of EpCAM assessed by IFS-confocal analysis.

Immunofluorescence staining and laser scanning confocal microscopy analysis of EpCAM expression on indicated cells treated with EGF 1.8 nM and 18 nM for 24 h (A), and 9 nM for 72 h (B) EpCAM: green, nuclei: blue (DAPI). Shown are representative images from $n = 3$ independent experiments with multiple areas analyzed.

4.4 EpEX is an EGFR ligand that induces downstream signaling pathways

EGFR activity is largely dependent on the accessibility of ligands. Upon ligand binding, homodimers or heterodimers of EGFR with further ErbB family members are formed, and multiple intracellular signaling pathways are triggered, mainly ERK and AKT activation. EGFR ligands are synthesized as type I transmembrane proteins and the most important post-translational modification for these ligands is their proteolytic release from the plasma membrane (Blobel, 2005). Via proteolytic processing, a soluble ectodomain containing the EGF motif (also known as the EGF domain or

module) can be released into the extracellular milieu and the EGF motif is the central structural and functional feature responsible for the interaction with the EGFR.

EGF motifs are not confined to EGFR ligands but are also present in single or multiple copies in dozens of structurally and functionally unrelated proteins. Several proteins containing EGF motif such as Thrombospondin (TSP) and tenascin-C have been identified associating with EGFR and may act as ligands for EGFR (Liu et al., 2009; Swindle et al., 2001)

EpCAM ectodomain EpEX shedding as a soluble fragment occurs in response to cleavage by ADAM proteases and, furthermore, EpEX molecules are also comprised of an EGF motif, the function of which is largely unknown. These findings and similarities mentioned above provided the rationale to further investigate potential interaction between EpCAM/EpEX and EGFR.

4.4.1 Endogenous EpCAM associates with EGFR

In order to address potential crosstalk between EGFR and EpCAM, an association between endogenous EpCAM and EGFR was determined. Whole cell extracts from FaDu, Cal27 and HCT8 cells were immunoprecipitated with EpCAM-specific antibodies and analyzed by immunoblotting using EGFR-specific antibodies. The results showed that immunoprecipitation of EpCAM allowed for the co-precipitation of EGFR, and *vice versa* (**Fig 21**). Hence, the bi-directional co-immunoprecipitations revealed an association between endogenous EpCAM and EGFR.

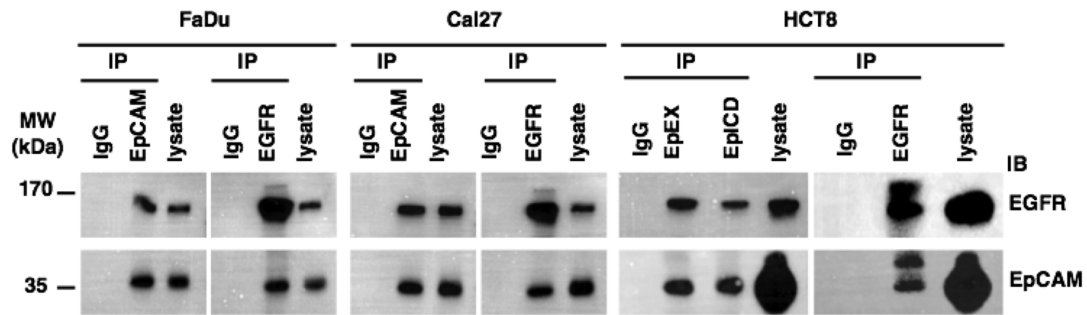


Fig 21. Protein-protein interaction of endogenous EpCAM and EGFR.

Bidirectional co-immunoprecipitation (Co-IP) of endogenous EGFR and EpCAM in whole cell lysates of FaDu, Cal27, and HCT8 cells using EGFR- and EpCAM-specific antibodies. Isotype control antibody (IgG) served as control. Co-immunoprecipitated EGFR and EpCAM were visualized in immunoblotting with specific antibodies as indicated. All data were combined and generated from three independent replicates.

4.4.2 Naturally shed EpEX molecules are present in supernatant of cancer cells in multimeric form

RIP of EpCAM is a process that occurs in cancer cells (Maetzel et al., 2009), and that results in the presence of EpEX in the serum of cancer patients (Abe et al., 2002; Gebauer et al., 2014; Kimura et al., 2007; Petsch et al., 2011). In order to confirm the release of EpEX by HNSCC and colon cancer cell lines, cell-free supernatants from Cal27, FaDu, Kyse30, and HCT8 cultures were immunoprecipitated with EpEX-specific antibodies. Immunoblotting of EpEX-IPs confirmed the presence of EpEX in cell culture supernatants (**Fig 22B, left panel**). Native gel electrophoresis of immunoprecipitated EpEX from Cal27, FaDu, Kyse30, and HCT8 supernatants further demonstrated that naturally shed EpEX was present in monomeric, dimeric, and multimeric forms (**Fig 22B, right panel**).

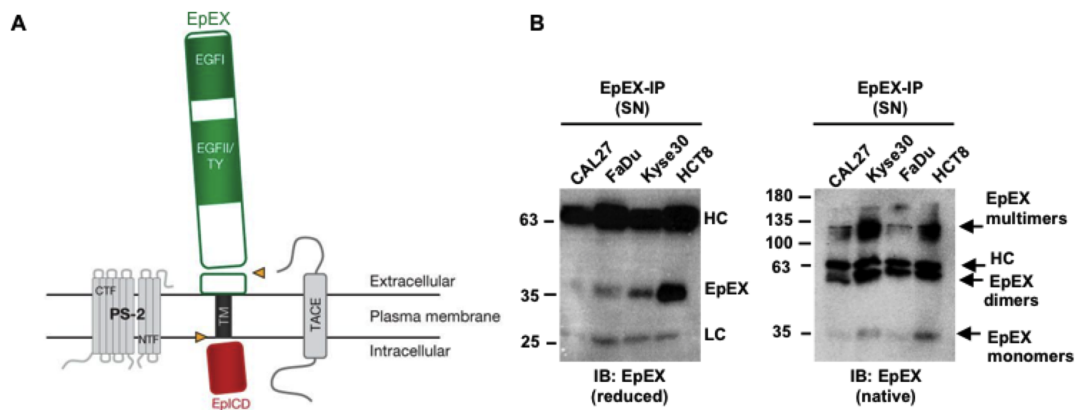


Fig 22. Oligomeric status of naturally shed EpEX.

(A) Schematic picture of EpCAM structure and RIP adapted from Maetzel et al (Maetzel et al., 2009). (B) Supernatants (SN) of Cal27, FaDu, Kyse30, and HCT8 cells were immunoprecipitated with EpEX-specific antibodies. Immunoprecipitated complexes were separated under reduced (left) and non-reduced native conditions (right) and EpEX was detected with specific antibodies. Antibody heavy chains (HC), light chains (LC), EpEX mono-, di-, and multimers are indicated. All data were combined and generated from three independent replicates.

4.4.3 Generation of recombinant soluble EpEX-Fc fusion protein

I next analysed a potential binding of EpEX to EGFR. For this purpose, my approach started with the generation of a recombinant protein that contains the extracellular domain of EpCAM (EpEX) fused to the Fc region of human immunoglobulin 1. EpEX-Fc was produced by stable transfection of HEK293 cells with the according expression plasmid and was purified from the culture medium by gravity flow with protein A beads resin (**Fig 23A**). Subsequently, EpEX-Fc protein were eluted, concentrated, and further characterized biochemically. The purity of recombinant EpEX-Fc was assessed by SDS-PAGE with Coomassie staining (**Fig 23B**) and the integrity and identity were assessed by immunoblotting with anti-EpEX and anti-Fc specific antibody (**Fig 23C**). Under physiological conditions, endogenous EpCAM form dimers and multimers, and

is glycosylated, which is reported to be important for EpCAM protein stability (Munz et al., 2008). The oligomeric state and N-glycosylation status of recombinant EpEX-Fc protein were confirmed native gel electrophoresis and PNGase assay, respectively. Oligomerization through Fc mimics the dimeric/oligomeric state of EpEX, with monomers, dimers and oligomers as observed in cell culture supernatants (**Fig 23D, E**).

The data indicated that recombinant EpEX-Fc is similar to naturally shed EpEX with respect to oligomerization and post-translational modification, and can thus be used for further assessment of a potential impact of EpEX on EGFR activation and functional consequences.

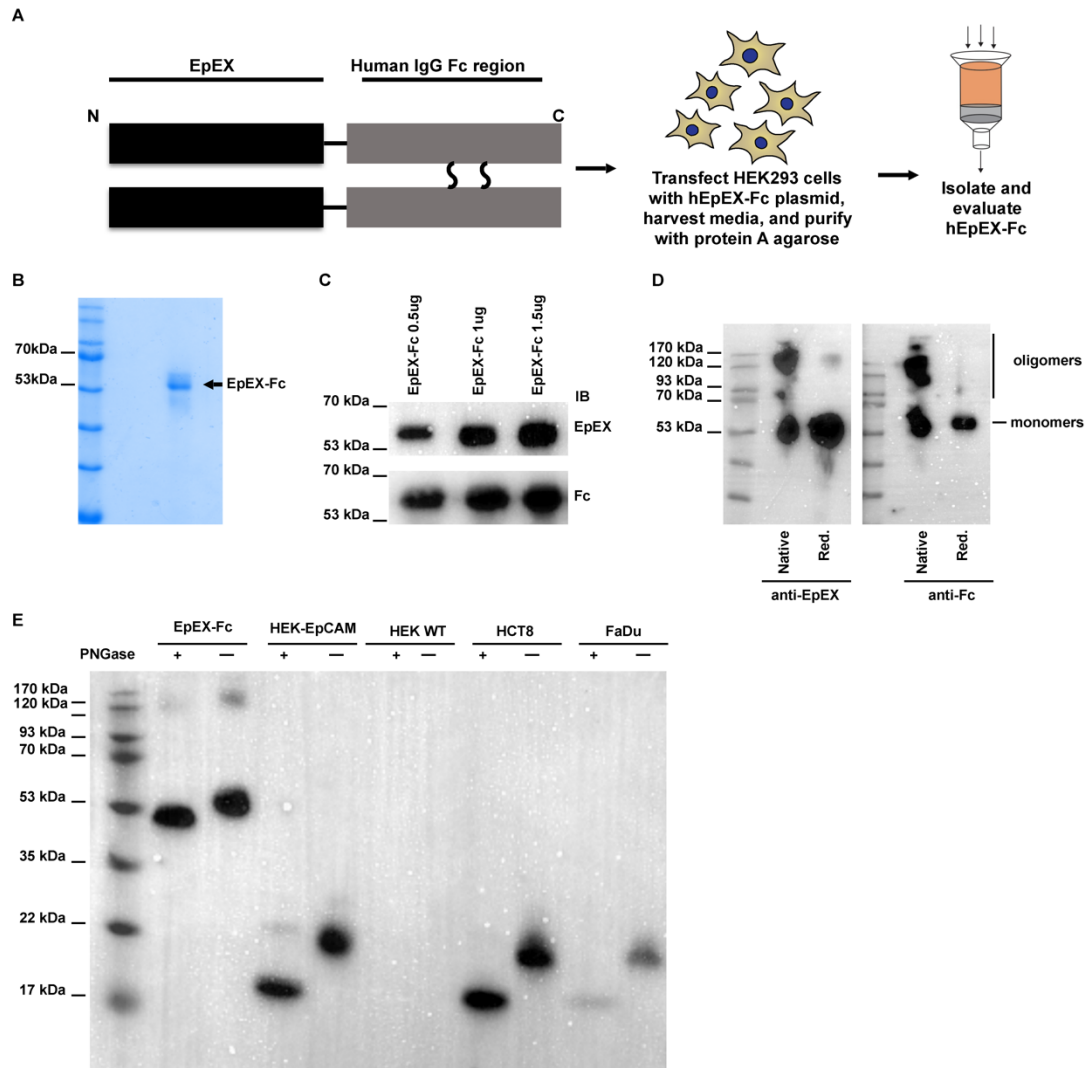


Fig 23. Generation, purification and assessment of EpEX-Fc.

(A) Schematic workflow of EpEX-Fc generation and purification. A fusion consisting of the extracellular domain of EpCAM (EpEX) and the Fc region of human IgG1 was stably expressed in HEK293 cells. Cell culture media were harvested and recombinant EpEX-Fc protein was purified by gravity flow with protein A beads resin. Subsequently, EpEX-Fc protein was eluted and concentrated. (B) The purity of recombinant EpEX-Fc was assessed by SDS-PAGE with Coomassie staining. (C) EpEX-Fc is composed of both EpEX and Fc and immunoblotting experiments with anti-EpEX and anti-Fc specific antibody confirmed the integrity and identity. (D) Native and reducing immunoblot experiments with anti-EpEX and anti-Fc specific antibodies were performed to assess oligomeric state of recombinant EpEX-Fc protein, showing EpEX-Fc oligomerizes to form dimers and trimers. (E) PNGase assay and immunoblot with anti-EpEX antibody indicate that EpEX-Fc is glycosylated, which is similar to full-length EpCAM in HEK293 cells and endogenous EpCAM in HCT8 and FaDu cells. All data were combined and generated from three independent replicates.

4.4.4 Soluble EpEX directly binds to the extracellular domain of EGFR

In order to assess a potential interaction between EpEX and EGFR, recombinant EpEX-Fc protein was utilized as a bait to isolate potential interacting proteins from cell lysates. Fc served as a control for unspecific binding of proteins within the same settings. Whole cell lysates of FaDu and Cal27 cells were immunoprecipitated with EpEX-Fc or Fc, and thereafter immunoprecipitated complexes were immobilized on protein A agarose beads, and further separated on SDS-PAGE. Immunoprecipitated proteins were detected by immunoblotting with Fc- and EGFR-specific antibodies. EpEX-Fc, but not Fc, allowed for the co-precipitation of full-length EGFR, suggesting that EpEX-Fc binds to EGFR (**Fig 24A**).

To address whether the interaction of EpEX-Fc with EGFR occurred directly and through binding to the extracellular domain of EGFR, purified recombinant extracellular domains of EGFR (EGFR_{ex}) and EpCAM (EpEX) were co-incubated and cross-linked (cross-linking assay performed in collaboration with Aljaž Gaber, Miha Pavšič, Brigita Lenarčič at the Department of Chemistry and Biochemistry, Faculty of Chemistry and Chemical Technology, University of Ljubljana, Slovenia). Cross-linking of EGFR_{ex} alone resulted in dimerization of EGFR_{ex} (**Fig 24B; lane 2**), which was further increased by adding EGF (**Fig 24B; lane 5**). Cross-linking of EpEX induced dimerization (**Fig 24B; lane 4**), as has been described (Pavsic et al., 2014). Furthermore, a protein-protein interaction complex of approx. 120 kDa was detected after incubation and cross-linking of EGFR_{ex} and EpEX, corresponding to a 1:1

complex of EGFR_{ex} binding to EpEX. Additionally, a second, weaker band of ~155 kDa, corresponding to a protein-protein interaction complex of one EGFR_{ex} molecule and an EpEX dimer was detected (**Fig 24B; lane 6**). It must be noted that in the presence of EGF, the intensity of the ~120 kDa band was reduced and that the second band of ~155 kDa disappeared (**Fig 24B; lane 7**), indicating that EGF compete with EpEX binding to EGFR_{ex}.

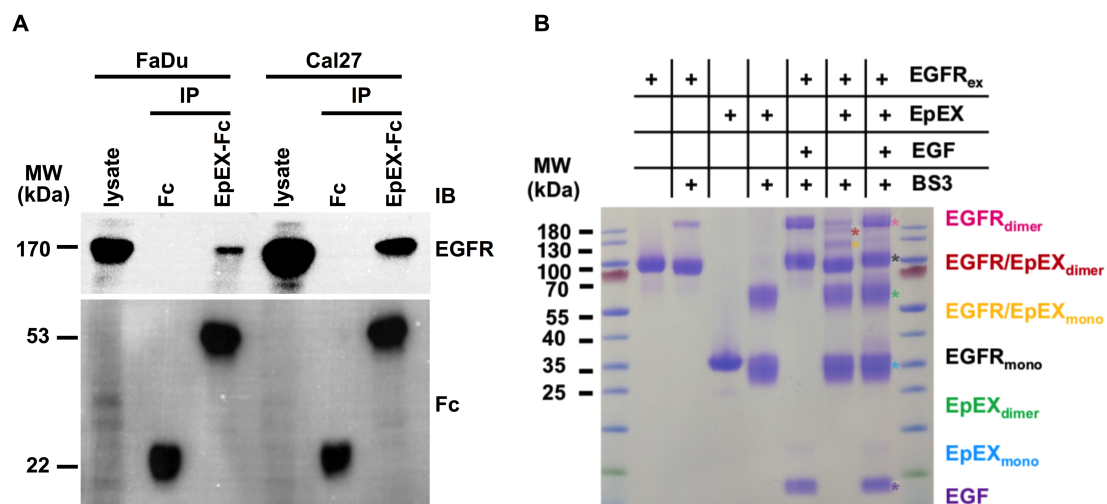


Fig 24. Soluble EpEX directly binds to EGFR extracellular domain.

(A) Whole cell lysates of FaDu and Cal27 cells were immunoprecipitated with EpEX-Fc or Fc, and thereafter immunoprecipitated complexes were separated on SDS-PAGE. Immunoprecipitated proteins were detected by immunoblotting with Fc- and EGFR-specific antibodies. (B) Extracellular domain of EGFR (EGFR_{ex}) and EpEX were incubated in the presence or absence of crosslinker (BS3). Where indicated, EGF was added. Monomers, dimers, and EGFR_{ex}/EpEX complexes are marked. All data were combined and generated from three independent replicates.

4.4.5 EpEX-Fc specifically activates EGFR downstream signaling pathways

Based on the binding of EpEX-Fc to the extracellular domain of EGFR, the activation of EGFR downstream signaling was evaluated in serum-starved FaDu, Kyse30, and

Cal27 cells treated with EpEX-Fc (10 nM) or Fc (10 nM). As controls, cells were either kept untreated (negative control) or were treated with EGF (1.8 nM) as positive control. Both ERK MAP kinases ERK1 and ERK2 were dually phosphorylated in response to EpEX-Fc, but not Fc treatment. The degree of ERK phosphorylation following treatment of cells with EpEX was inferior to treatment with EGF (**Fig 25A**). Phosphorylation of AKT was also detected upon EpEX-Fc treatment (**Fig 25B**). Direct inhibition of EGFR kinase activity using EGFR tyrosine kinase inhibitor (TKI) AG1478 demonstrated its requirement for downstream signaling by EpEX-Fc through EGFR. The AG1478 TKI entirely (Cal27) or partially (FaDu, Kyse30) blocked ERK1/2 activation by EpEX-Fc and EGF (**Fig 25C**).

The foregoing results may also rely on an indirect activation of EGFR by EpEX-Fc through a potential interaction of EpEX-Fc with an unknown receptor, which secondarily transmits signals via EGFR kinase activation. To probe this possibility, the external binding of EGFR was blocked using the therapeutic anti-EGFR antibody Cetuximab (Bonner et al., 2006). Cetuximab abrogated ERK and AKT activation induced by EpEX-Fc (**Fig 25A, B lane 6**), indicating that activation of EGFR signaling by EpEX-Fc occurs directly through binding to the extracellular domain of EGFR.

The effect of EpEX-Fc and EGF on ERK1/2 and AKT activation was further validated by immunofluorescence staining and laser scanning confocal microscopy of FaDu and Cal27 cells. Imaging of phospho-ERK1/2 confirmed the activating capacity of EpEX-Fc and the inferior induction in comparison with EGF, whereas AKT activation by EGF

or EpEX-Fc was similar (**Fig 25D, E**). Due to differential voltage adjustments, comparison across cell lines was not feasible. Furthermore, EpEX-Fc and EGF induced ERK1/2 activation was entirely blocked by an inhibitor of the upstream kinase MEK1 (AZD6244) in FaDu, Cal27, and Kyse30 cells (**Fig 25C lane 6**). These results provide evidence that EpEX-Fc specifically induces ERK1/2 activation through EGFR signaling and MEK activity.

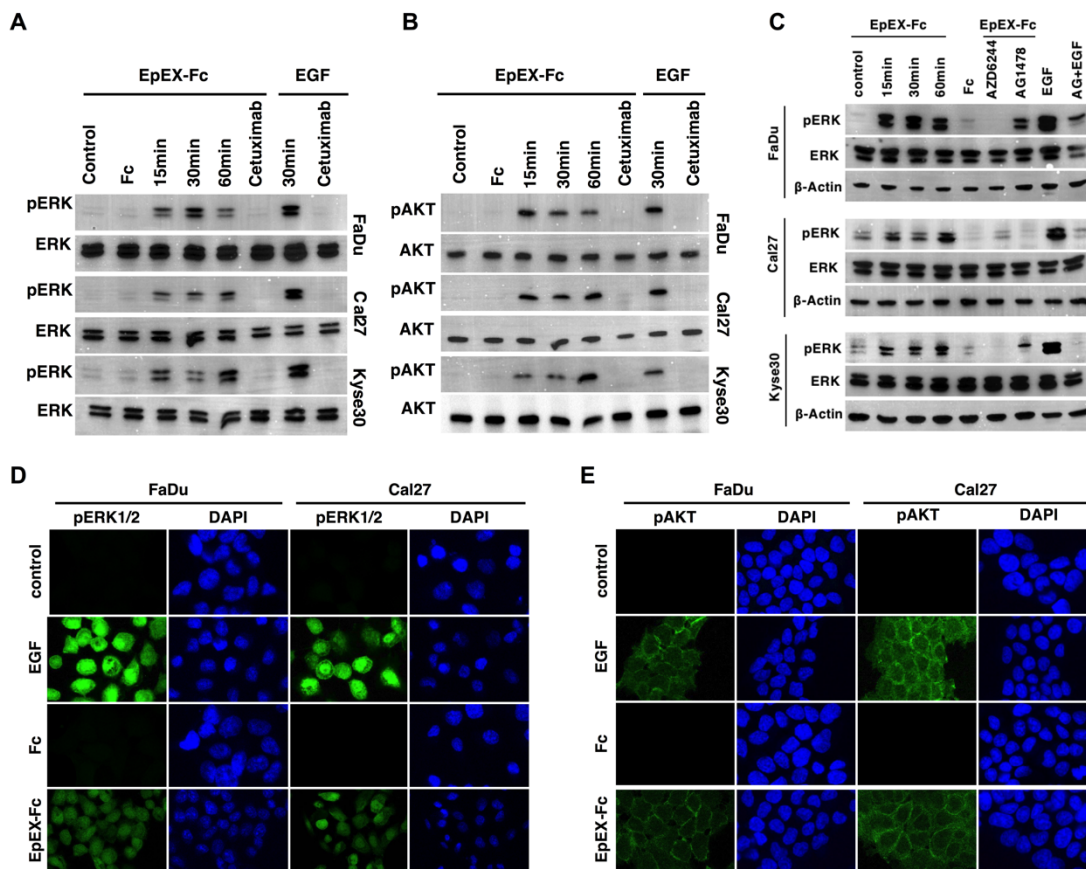


Fig 25. Soluble EpEX-Fc binds to EGFR and activates EGFR downstream signaling towards ERK and AKT.

(A, B, C) FaDu, Cal27, and Kyse30 cells were maintained untreated (control), treated with EpEX-Fc, Fc (10 nM) for the indicated time points or EGF (1.8 nM) for 30 min. Whole cell lysates from treated cells were utilized for immunoblotting with specific antibody. Assessment of phosphorylation of ERK1/2 (pERK1/2) (A) and phosphorylation of AKT (pAKT) (B) following EpEX-Fc and EGF stimulation. Where indicated, cells were additionally treated with the EGFR-inhibitory monoclonal antibody Cetuximab. Levels of ERK1/2 and AKT served as controls. (C) pERK1/2 was assessed

by immunoblot. Where indicated, MEK1 inhibitor AZD6244 or EGFR inhibitor AG1478 were added. ERK1/2 and Actin were used as controls. (D, E) Immunofluorescence laser scanning confocal microscopy analysis of pERK1/2 and pAKT on FaDu and Cal27 cells treated with EGF (9 nM), Fc or EpEX-Fc (10 nM) for 30 min (ERK1/2 or AKT: green, nuclei: blue (DAPI)). All data were combined and generated from three independent replicates.

4.4.6 Activation of EGFR downstream signaling by EpEX-Fc is EGFR-dependent, but does not require full length EpCAM

To further assess EpEX/EGFR signaling, a requirement for EGFR expression for the induction of ERK phosphorylation by EpEX-Fc treatment was analyzed in HEK293 cells, which do not express detectable amounts of EGFR. Accordingly, activation of ERK1/2 was not observed in HEK293 cells with EpEX-Fc or EGF treatment (**Fig 26A left panel**). Transient expression of EGFR restored the phosphorylation of ERK1/2 induced by EGF and EpEX-Fc, confirming a requirement of EGFR expression for the observed effects of EpEX-Fc on ERK1/2 activation (**Fig 26A right panel**).

A possible involvement of full-length EpCAM and its downstream signaling, instead of EpEX as a novel ligand of EGFR, in EpEX-Fc induced ERK1/2 activation was addressed in the CRISPR-Cas9 EpCAM knockout HCT8 cell line (Tsaktanis et al., 2015). HCT8 EpCAM-knockout cells entirely lacked EpCAM expression, but retained EGFR levels comparable to wild-type and CRISPR-Cas9 control cell lines (**Fig 26B**). EpEX-Fc-induced ERK1/2 activation was still observed in EpCAM-knockout cells, which completely lacked EpCAM expression but with comparable EGFR level (**Fig 26B, C, D**), demonstrating full-length EpCAM is not required in EpEX-induced ERK1/2

activation. Hence, EpEX-Fc is a novel EGFR ligand that activates EGFR downstream signaling specifically.

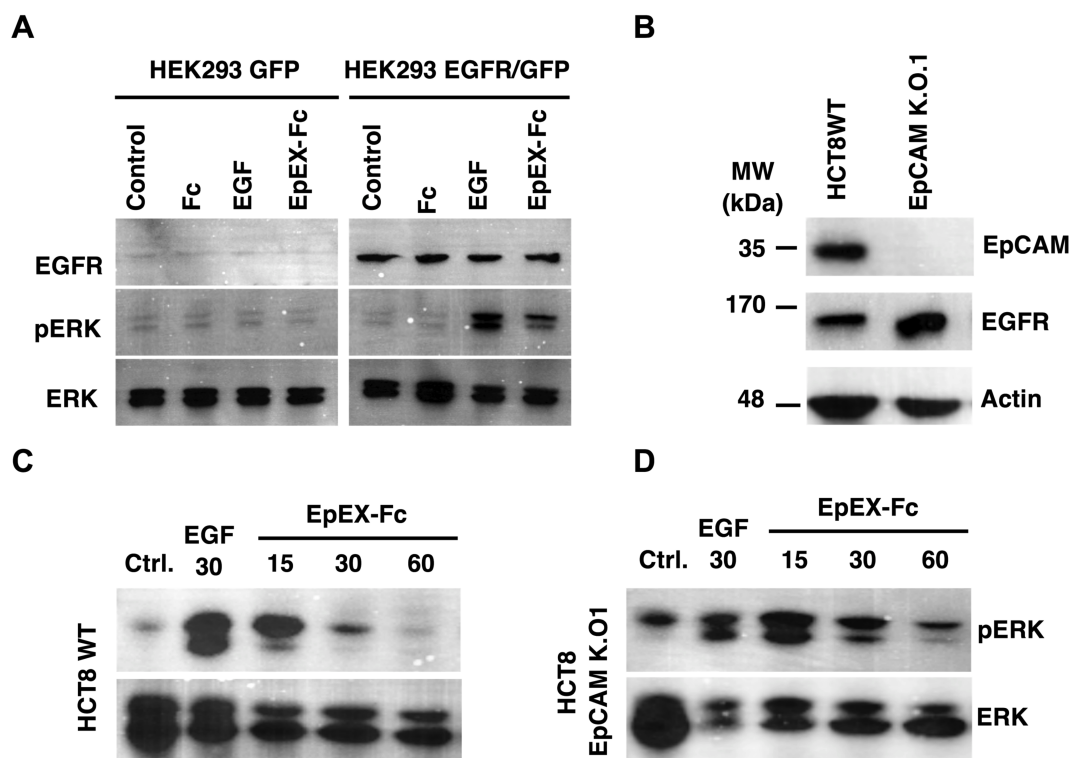


Fig 26. Activation of ERK1/2 and AKT by EpEX-Fc is EGFR-dependent, but does not require full length EpCAM.

(A) Immunoblot analysis of EGFR and pERK1/2 expression on GFP or EGFR-GFP transiently transfected HEK293 cells, following EpEX-Fc, Fc (10 nM) or EGF (1.8 nM) treatment for 30 min. (B) Immunoblot characterization of EpCAM and EGFR expression on HCT8 wild-type (HCT8WT) and CRISPR-Cas9 EpCAM knockout clone 1 (EpCAM K.O.1) cells. (C) Immunoblot assessment of pERK1/2 activation on HCT8 WT cells and EpCAM-knockout cells treated with EpEX-Fc, Fc (10 nM) or EGF (1.8 nM) for 30 min. Levels of ERK1/2 were assessed in parallel as controls. All data were combined and generated from three independent replicates.

4.5 Effects of EpEX-Fc and EGF are dosage-dependent and differ in cellular outcome

Because EGFR signaling is known to mediate various cellular fates including proliferation, cell migration, epithelial-to-mesenchymal transition (EMT), amongst

others (Yarden & Sliwkowski, 2001), we aimed to assess the functional consequences of treatment with EpEX-Fc.

4.5.1 Proliferation assay

First, I set out to determine and compare abilities of EGF and EpEX-Fc to stimulate the proliferation of HNSCC cells. In order to rule out the effects from further growth factors present in fetal calf serum, all cell lines were serum-starved and maintained in serum-free condition throughout the experiment. Serum-starved FaDu and Kyse30 cells were treated with different concentrations of EpEX-Fc and EGF for 24, 48, and 72 h. Both, EpEX-Fc and EGF stimulated HNSCC cells in a dose-dependent manner. Treatment of FaDu with low-dose EGF (1.8 nM) resulted in cell proliferation with a 2.2-fold increase in cell number at 72 h compared with control (**Fig 27A, yellow curve**). Treatment of FaDu cells with high-dose EpEX-Fc (10 nM) also induced cell proliferation, which was inferior to EGF^{low} treatment (1.5-fold increase in cell numbers, respectively after 72 h) (**Fig 27A, blue curve**). Neither high-dose EGF (9 nM), nor low-dose EpEX-Fc (1 nM) or Fc (10 nM) did induce FaDu cell proliferation (**Fig 27A, red, light and dark grey curves**). To be noted, the effect of EpEX-Fc on cell proliferation was entirely blocked upon co-treatment with Cetuximab (**Fig 27A green curve**). In parallel, a proliferation assay with Kyse30 cells certified the proliferation-inducing effect of high-dose EpEX-Fc (10 nM) and the inferior induction compared to low-dose of EGF, disclosing 2-fold and 2.5-fold increases, respectively. Conversely, high-dose EGF also induced 2.2-fold increase and low-dose EpEX-Fc did not have any significant

mitogenic effect (**Fig 27D**). Similarly, EpEX-Fc-induced proliferation was blocked upon co-treatment with Cetuximab (**Fig 27D, green curve**). To further confirm the proliferation-inducing effects of high-dose EpEX-Fc, DNA synthesis was examined by measuring BrdU incorporation in Kyse30 and FaDu cells following treatment with EpEX for 72 h. In line with aforementioned cell counting results (Fig 27A, B, D, E), high-dose EpEX-Fc (10 nM) treated FaDu and Kyse30 cells exhibited a significant 30% and 50% induction in BrdU uptake after 72 h, respectively, in comparison with control-treated cells. Consistently, BrdU incorporation induced by EpEX-Fc was blocked by co-treatment with Cetuximab (**Fig 27C, D**).

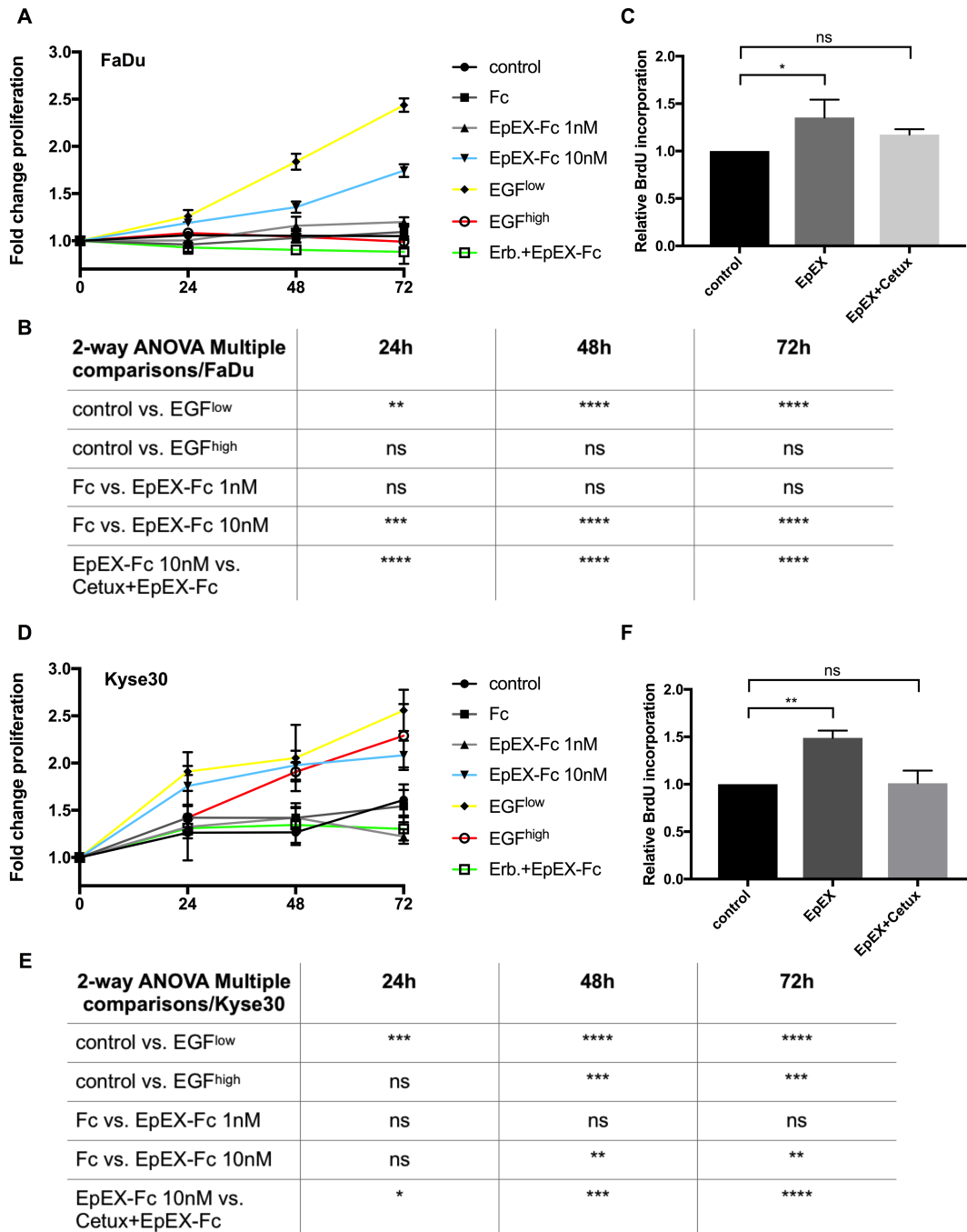


Fig 27. EpEX-Fc induces EGFR-dependent proliferation.

(A, D) Serum starved FaDu and Kyse30 cells were treated with low (1 nM) and high dose (10 nM) of EpEX-Fc, Fc (10 nM), EGF^{low} (1.8 nM), EGF^{high} (9 nM) or a combination of EpEX-Fc (10 nM) with Cetuximab for 24, 48, and 72 h and cell numbers were assessed. Data shown represent fold changes in cell numbers, means with standard deviations (SD) from $n = 3$ independent experiments. Two-Way ANOVA with posthoc multiple testing and Bonferroni correction (B, E). ns: not significant; * 0.05, ** 0.01; *** 0.001; **** 0.0001. (C, F) DNA synthesis was examined by measuring BrdU incorporation in FaDu and Kyse30 cells following treatment with EpEX-Fc (10 nM) or a combination of EpEX with Cetuximab for 72 h. Shown are means with standard

deviations (SD) from $n = 3$ independent experiments. Two-Way ANOVA with posthoc multiple testing and Bonferroni correction. ns: not significant; * 0.05.

4.5.2 Migration assay

Next, the influence of high-dose EGF (9 nM) and EpEX-Fc (10 nM) on the cell migration was assessed in a wound-healing assay on FaDu and Kyse30 cells (**Fig 28 A, B**). Relative migration was quantified (**Fig 28C, D**) and corrected for proliferation rates, demonstrating that EGF treatment at concentrations inducing EMT (9 nM) resulted in significantly enhanced relative migration of serum-starved FaDu cells (at 48h, 3.1-fold increase in cell migration) (**Fig 28A red lines, Fig 28C red bar**) and Kyse30 cells (at 24 h, 2.6-fold increase in cell migration) (**Fig 28B red lines, Fig 28D red bar**) compared with control-treated cells. Within the same time period, no increases in cell migration could be detected in cells treated with EpEX-Fc or Fc. The increased cell migration in response to EGF^{high} was diminished significantly by co-treatment with EpEX-Fc (diminished by 32.3% and 42.2% for FaDu and Kyse30, respectively) (**Fig 28C, D yellow bars**), and by Cetuximab (diminished by 59% and 70.8% for FaDu and Kyse30, respectively) (**Fig 28C, D, green bars**).

Thus, EGF has dual capacities to drive distinct cellular fates in a dosage-dependent manner, inducing proliferation at low concentration (1.8 nM) and promoting EMT and migration at high concentration (9 nM) in HNSCC cell lines, whereas EpEX-Fc induces proliferation at high concentration and exhibits an inhibitory effect on EGF-induced cell migration.

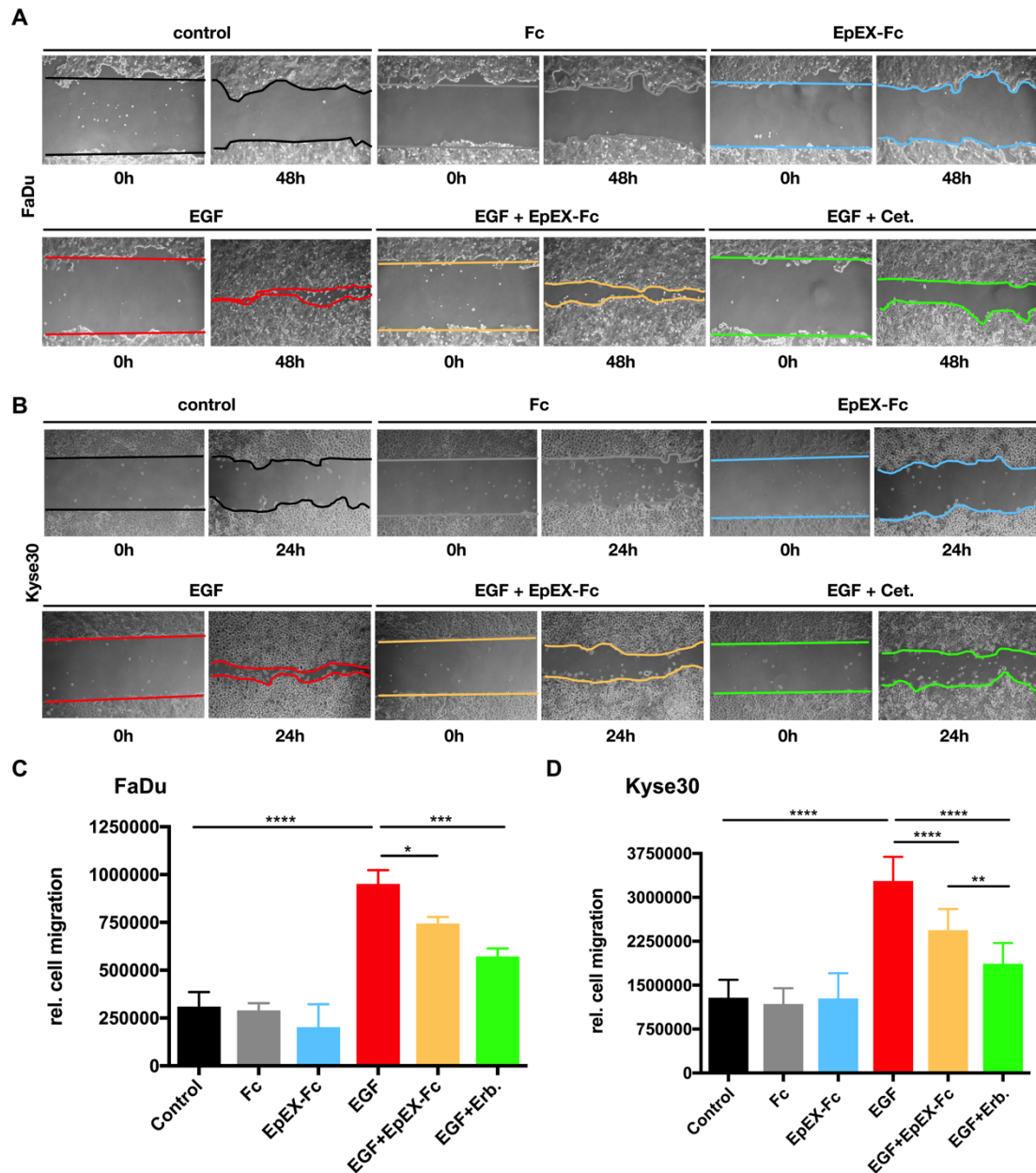


Fig 28. EpEX-Fc inhibits high-dose EGF-induced cell migration in HNSCC cells. (A, B) Wound-healing assay with FaDu, and Kyse30 cells treated with Fc (10 nM), EpEX-Fc (10nM), EGF (9nM), EGF (9nM) in combination with EpEX (10 nM), or EGF (9nM) with Cetuximab for indicated time or untreated (control). Shown are representative micrograph pictures of cells after 24 h (Kyse30) and 48 h (FaDu). (C, D) Quantification of the gap distance from representative micrographs was performed using ImageJ and MRI wound healing tool. Relative migration was adjusted for proliferation rates. Shown are means with standard deviations (SD) from $n = 3$ independent experiments. One-Way ANOVA with posthoc multiple testing and Bonferroni correction * 0.05, ** 0.01; *** 0.001.

4.6 EpEX-Fc impedes EGF-induced EMT in HNSCC cell lines

4.6.1 EGF^{high} drives mesenchymal characteristics, but EpEX-Fc sustains an epithelial phenotype and impedes EGF-induced EMT in HNSCC cells

The foregoing results demonstrate that EpEX-Fc acts as a ligand for EGFR activating downstream signaling, supporting proliferation, however, partially inhibiting cell migration induced by the classical EGFR ligand EGF. This suggested that EpEX-Fc might have the capacity to repress EGF-mediated EMT in HNSCC cell lines. However, it could so far not be ruled out that EpEX-Fc may drive EMT less potently. In order to assess this possibility, serum-starved FaDu, Kyse30, and Cal27 cells were treated with increased doses of EpEX-Fc up to 50 nM for 48 to 72 h, corresponding to a five-fold molar excess compared to previous experiment.

As shown in **Fig 29A, B, upper panel**, EpEX-Fc-, as well as Fc- and EGF^{low}-treated cells sustained an epithelial morphology. In contrast, treatment of FaDu and Kyse30 cells with EGF^{high} resulted in the acquisition of a spindle-shaped morphology and loss of cell-cell contact. To further evaluate the function of EpEX-Fc in EGF-induced EMT, FaDu and Kyse30 cells were simultaneously treated with an EMT-inducing dose of EGF (9 nM) and increasing doses of EpEX-Fc (1nM, 5nM, 10nM, and 50 nM) for 72 h. As shown in **Fig 29A, B lower panel**, cells co-treated with increasing amount of EpEX-Fc were unable to undergo EGF^{high}-induced EMT, as evidenced by the retention of an epithelial morphology in EGF and EpEX-Fc co-treated cells compared to EGF^{high}-

treated cells. Hence, high-dose of EpEX-Fc precludes EGF-induced EMT in HNSCC cell lines.

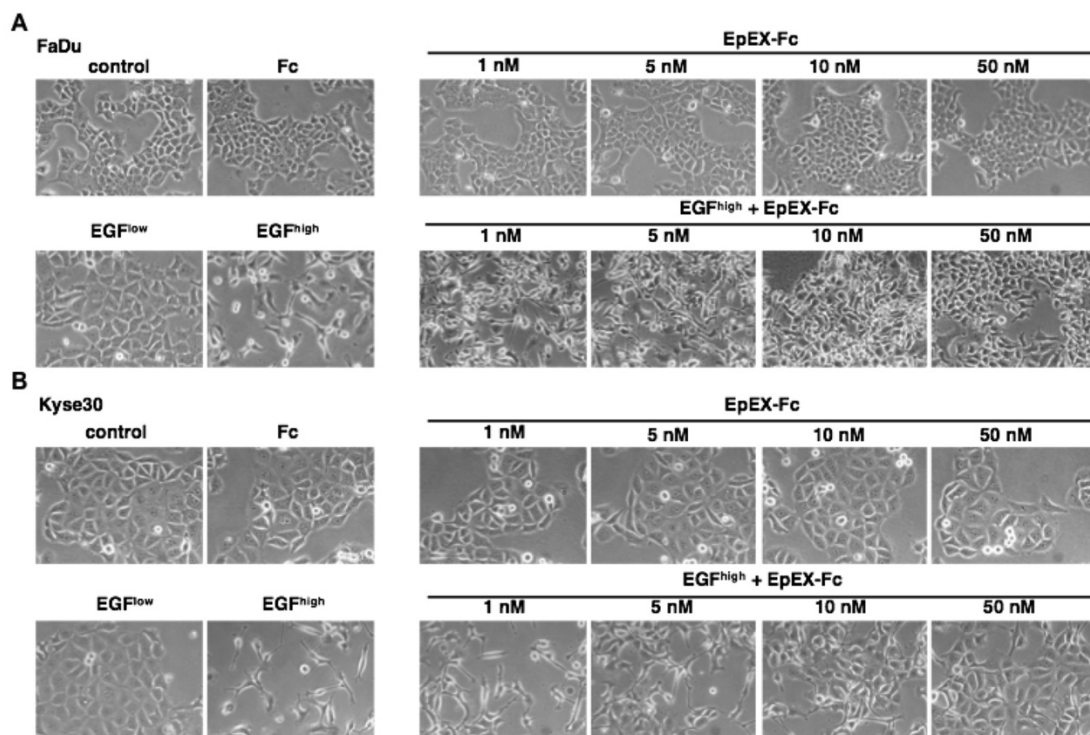


Fig 29. EpEX-Fc impedes EGF-mediated EMT in dosage dependent manner.

Serum starved FaDu (A) and Kyse30 (B) cells were treated with control media, Fc (10 nM), EGF^{low} (1.8 nM), EGF^{high} (9 nM), EpEX-Fc (1-50 nM), or with EGF^{high} in combination with increasing concentrations of EpEX-Fc (1-50 nM). Representative micrographs of cell morphology were recorded after 72 h (FaDu) or 48 h (Kyse30) at 100x magnification. All data were combined and generated from three independent replicates.

4.6.2 EGF does not induce EMT in Cal27 cells

While performing EGF and EpEX co-treatment experiments, it became obvious that EGF^{high} (9 nM) did not drive mesenchymal characteristics in the HNSCC cell line Cal27. In a complementary experiment, Cal27 cells were treated with EGF^{high} (9 nM) and a two-fold higher EGF concentration (18 nM) for 72 h. As shown in **Fig 30**, Cal27 cells

did exhibit neither EMT-like morphology changes, nor loss of E-cadherin after high-dose EGF, which pinpoints at differences in cellular response towards EGF treatment.

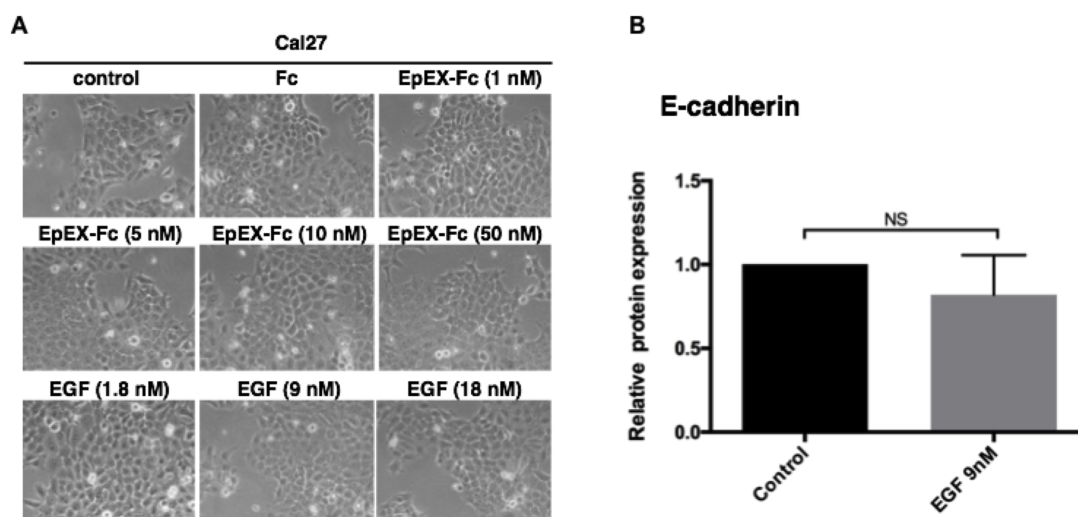


Fig 30. EGF does not induce EMT in Cal27 cells.

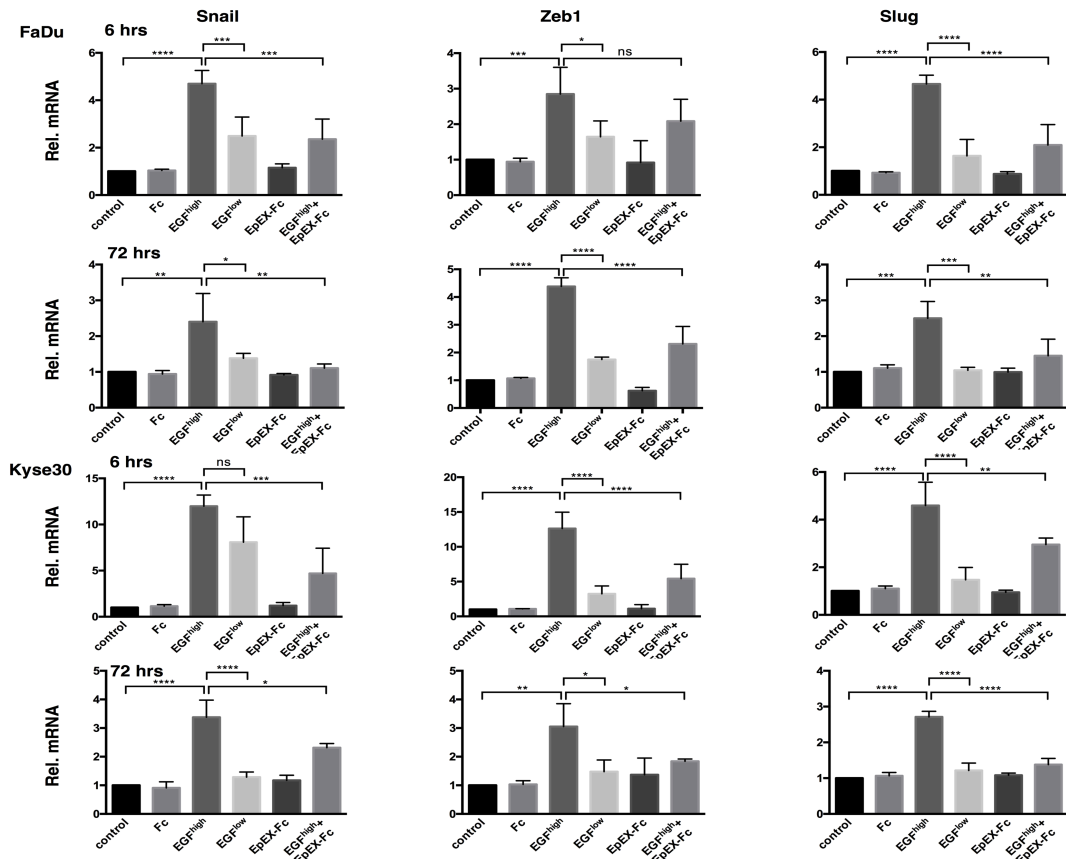
(A) Micrographs of Cal27 cells treated with control media, EpEX (1-50 nM), and high (9 nM and 18nM) doses of EGF for 72 h. (B) Immunoblot assessment of E-cadherin expression on untreated and EGF (9 nM, 72 h) treated Cal27 cells. Shown are mean values with standard deviations (SD). NS, not significant. All data were combined and generated from three independent replicates.

4.6.3 EpEX-Fc impedes EGF-induced EMT via modulation of EMT-TFs levels

To understand the specific biological functions exerted by EpEX-Fc when inhibiting EGF-induced EMT, the expression of classical EMT markers, including EMT-associated transcription factors, was further examined. To do so, FaDu and Kyse30 cells were serum-starved and were either kept untreated (control), treated with EGF^{low} (1.8 nM), EGF^{high} (9 nM), EpEX-Fc (10 nM), Fc (10 nM), or with EGF^{high} in combination with EpEX-Fc (10 nM). Regulation of epithelial marker E-cadherin, mesenchymal marker N-cadherin, vimentin, and EMT transcription factors (EMT-TF) Snail, Slug,

Zeb1, and Twist were assessed at the transcriptional levels after 6 and 72 h following treatment. A substantial induction of EMT-associated transcription factors, including Snail, Zeb1 and Slug, the upregulation of the latter has been shown as master driver and to correlate positively with EMT, was observed at both time points and in both HNSCC cell lines treated with EGF^{high} (**Fig 31A**). Importantly, Snail, Zeb1, and Slug induction was significantly repressed in the presence of EpEX-Fc at 10 nM in both cell lines treated with EGF (9 nM) (**Fig 31A**). Furthermore, a downregulation of E-Cadherin and an upregulation of N-Cadherin was observed in EGF^{high}-treated FaDu cells at 72 h and an induction of vimentin was observed in EGF^{high}-treated Kyse30 cells, which could also be counteracted by EpEX-Fc co-treatment (**Fig 31B upper panel**). Fc or EpEX-Fc (10 nM) treatment did not result in changes in transcription of any of the genes analyzed by quantitative RT-PCR. E-cadherin, N-cadherin, and Twist expression was only slightly or not affected in Kyse30 cells (**Fig 31B lower panel**). Thus, EGF^{high} induces EMT-associated morphological changes along with the enhanced expression of the EMT-TFs Snail, ZEB1 and Slug, and partial loss of E-cadherin. Importantly, soluble EpEX-Fc impedes EGF-induced EMT *via* repression of the abovementioned EGF-activated EMT-TF transcription. Hence, morphological and molecular characterization of EGF and EpEX co-treated cells demonstrated that EpEX-Fc impedes EGF-induced EMT in HNSCC cells.

A



B

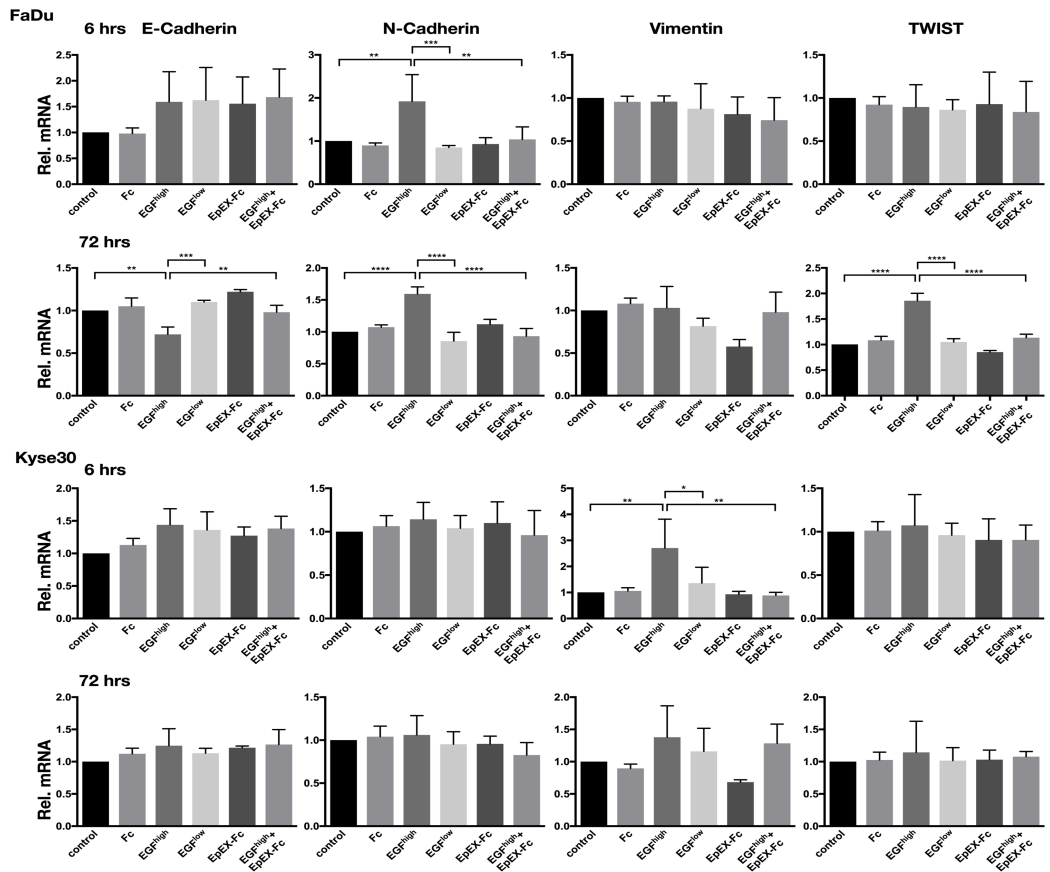


Fig 31. EpEX-Fc inhibits EGF-mediated EMT via control of EMT-TFs levels

*FaDu and Kyse30 cells were either kept untreated (control), treated with Fc (10 nM), EGF^{low} (1.8 nM), EGF^{high} (9 nM), EpEX-Fc (10 nM), or with EGF^{high} in combination with EpEX-Fc (10 nM). After 6 hrs and 72 hrs, mRNA levels of the indicated transcripts were assessed by qRT-PCR with GAPDH as house-keeping gene. mRNA levels are represented as relative levels compared to control-treated cells. Shown are means with standard deviations (SD) from n = 3 independent experiments performed in triplicates. One-Way ANOVA with posthoc multiple testing and Bonferroni correction p-values * 0.05, ** 0.01; *** 0.001.*

4.7 MEK-ERK, but not AKT signalling is required for EGF-induced EMT

EGF/EGFR and downstream signaling activation (mainly MEK-ERK signaling and PI3K-AKT signaling axis) are able to drive cancer cells to undergo EMT, as was shown in the present thesis and as has been reported by other groups in different cancer cell types (Buonato et al., 2015; Chandra Mangalhara et al., 2017; Cui et al., 2017; Fu et al., 2017; Fukuda et al., 2016; Grassi et al., 2017; Holz et al., 2011; J. Li et al., 2014; Y. Li et al., 2017; Muthusami et al., 2014; Saito et al., 2017; Sheng et al., 2017; Tashiro et al., 2016; Vergara et al., 2011; P. Wang et al., 2017; Xu et al., 2017; Xue et al., 2015; Y. Zhang et al., 2015; Z. Zhang et al., 2014; Zuo et al., 2011). Consequently, I aimed at determining the signaling pathway(s) that play(s) a key role in EGF-induced EMT, in order to further explore molecular mechanisms of EpEX-Fc-mediated inhibition of EGF-induced EMT.

4.7.1 Systematic evaluation of cell signaling contributions to EGF/EGFR-mediated EMT

Cellular decision making and acquisition of EMT in response to EGF is controlled by networks of intracellular signaling pathways. EGF binding to EGFR leads to activation of downstream signaling pathways mainly as the mitogen-activated protein kinase (MAPK)/ERK pathway and phosphoinositide 3-kinase (PI3K)/AKT pathways. Signals originating at the plasma membrane eventually exert effects on cell behavior through transcriptional changes orchestrated in the cell nucleus. In order to investigate signaling pathways implicated in EGF-dependent EMT, I performed a systematic review on EGF/EGFR-mediated EMT based on published literature to determine which signaling, *i.e.* MEK-ERK signaling or PI3K-AKT signaling, reportedly plays a central role in EGF/EGFR mediated EMT.

The electronic PubMed and EMBASE databases were searched for relevant articles published between January 1, 2000 and January 1, 2019 using the following search strategy with medical subject heading (MESH) terms; (“Epidermal growth factor” OR “Epidermal growth factor receptor”) AND (“Epithelial mesenchymal transition” OR “Epithelial mesenchymal transformation”). No language limitations were used. The retrieved results were collected and articles with unavailable full-text and duplicates were removed. Titles and abstracts served as an initial screen to determine their relevance to the review topic. Inclusion and exclusion criteria were developed as following: *In vivo* and *in vitro* studies examining the mechanistic pathway between

EGF/EGFR and EMT were included. Human studies examining the diagnostic, prognostic, and therapeutic significance of molecules downstream of EGFR signaling in patients with cancer were included in the review.

Initially, 391 records were identified from the database searches with the abovementioned screening strategy. Thirty-five records were excluded because they were in review publication type instead of original reports. 356 records were further analyzed for inclusion in the review. 278 records were excluded because they were irrelevant to analyze the topic since they reported on resistance to anti-EGFR therapy, represented studies of growth factors other than EGF, reported on EMT induced independently of EGF/EGFR, or due to an inability to obtain the full-length article. Eventually, 78 studies were included for detailed examination, in which MEK-ERK or PI3K-AKT signaling were reported as the main mediator in EGF/EGFR-induced EMT (MEK-ERK n=22; PI3K-AKT n=14). The remaining studies reported on other signaling such as Smad, JAK, STAT3, NF- κ B or undetermined main mediators. In conclusion, the systematic review of literature associated with EGF/EGFR-induced EMT could not reach an unequivocal agreement on determining which signaling pathway, MEK-ERK or PI3K-AKT, was the central mediator in EGF/EGFR induced EMT.

4.7.2 MEK-ERK signaling is the central mediator in EGF-induced EMT in HNSCC

Since we could not draw a conclusion based on literature research and in order to determine signaling pathways responsible for EGF-mediated EMT in HNSCC cell lines, treatment of EMT-responsive FaDu and Kyse30 cells with high-dose EGF in

combination with Cetuximab (EGFR specific antibody), Erlotinib (EGFR specific TKI), AZD6244 (MEK1 inhibitor), and MK0026 (pan-AKT inhibitor) was performed and morphological evidence was recorded. High-dose EGF induced pronounced EMT, as shown in **Fig 15, 29 and 32**, which was completely abolished by Cetuximab and Erlotinib. Importantly, MEK inhibitor AZD6244, but not AKT-inhibitor MK0026, significantly inhibited EGF-induced EMT in both cell lines, as evidenced by morphology. Hence, these data demonstrated that EGF executes EMT through induction of ERK1/2, but not AKT (**Fig 32**).

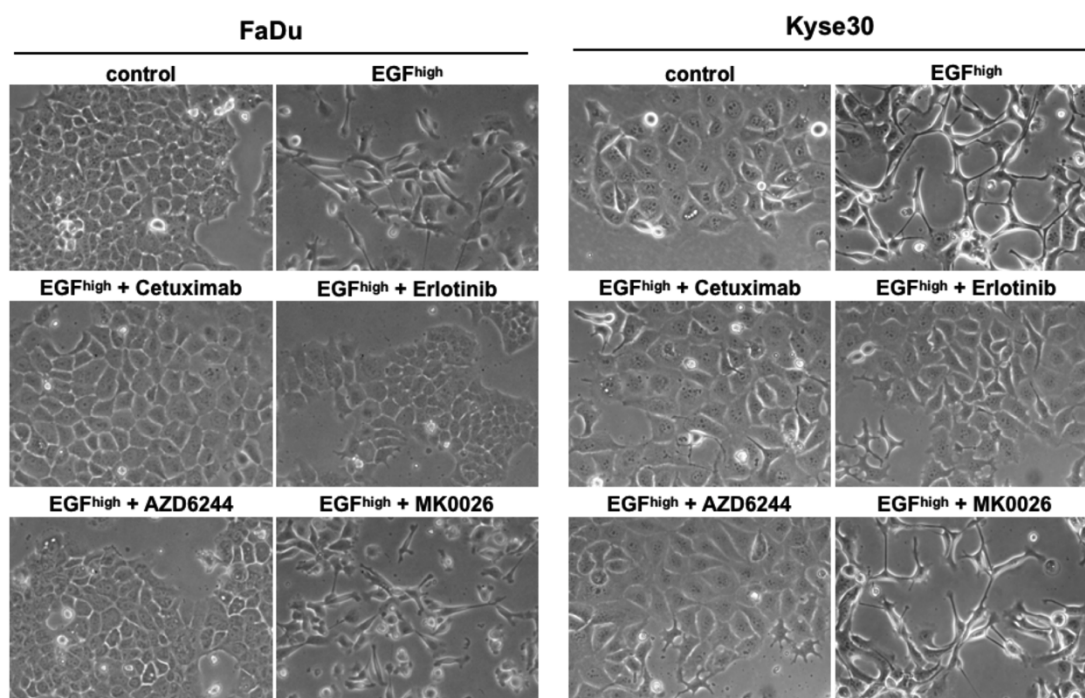


Fig 32. ERK1/2 signaling acts as the major mediator of EGF-induced EMT. FaDu and Kyse30 cells were either maintained untreated (control), or treated with EGF^{high} (9 nM), and in combination with Cetuximab (EGFR specific antibody), Erlotinib (EGFR specific TKI), AZD6244 (MEK1 inhibitor), and MK0026 (pan-AKT inhibitor). Shown are representative morphological micrograph pictures of cells after 48 h (Kyse30) and 72 h (FaDu) from *n* = 3 independent experiments.

4.8 Strength and duration of ERK1/2 activation integrates differential cellular fates

4.8.1 Differential responsiveness of HNSCC cell lines to EGF determines disparities in cellular outcome

Treatment of HNSCC FaDu and Kyse30 cells with EGF^{high} drives mesenchymal characteristic, whereas HNSCC Cal27 cells did neither induce EMT after treatment with EGF^{high} at 9 nM nor at 18 nM. Since activated ERK1/2 was determined as the major effector in EGF-induced EMT, potential differences in EGF-induced ERK1/2 phosphorylation between EMT-responsive FaDu and non-responsive Cal27 cells were assessed. Both cell lines were serum-starved and treated with high-dose EGF (9 nM), and subsequently activating phosphorylation of ERK1/2 was assessed by immunoblotting after 10, 60, and 180 minutes. Three different quantitative measures could be utilized to assess ERK signaling: signal amplitude, duration (transient or sustained), and integral strength (a composite of the other two measures) (Hornberg, Binder, et al., 2005; Hornberg, Bruggeman, et al., 2005). As shown in **Fig 33A**, activation kinetics of ERK1/2 phosphorylation differed between FaDu and Cal27 cells in both signal amplitude and duration. In contrast to a strong and sustained ERK1/2 phosphorylation in EGF^{high}-treated FaDu cells, Cal27 cells exhibited weaker and more transient activation (**Fig 33A**). ERK signaling remained strong for at least 3 h in FaDu cells, but returned to basal level 60 min after addition of EGF in Cal27 cells. Quantification of integral signal strength, derived from intensity and duration of ERK1/2

activation, revealed 3-fold higher in FaDu cells than Cal27 cells (**Fig 33B, red versus black curves and bars**). Thus, integrated signal strength of phospho-ERK1/2 in response to EGF functions as a major switch in decision-making towards EMT induction.

4.8.2 EGF and EpEX shape different ERK activation dynamics, rewiring different cell fates

Prompted by these observation, next, in order to straighten out whether the different cellular outcomes driven by EGF and EpEX-Fc, *i.e.* EMT and proliferation, were related to the ERK1/2 activation dynamics, EGF^{high}-induced ERK phosphorylation was compared with that induced by EpEX-Fc (10 nM) in FaDu cells by immunoblotting at indicated timepoints over a 6 h period of time. The amplitude of EGF^{high}-induced ERK phosphorylation was substantially higher than that induced by EpEX-Fc, with significant differences at all time points examined. Furthermore, EGF^{high} elicited sustained ERK activity, remaining strong at least for 360 min after addition of EGF, whereas ERK signaling returned to basal levels 180 min after addition of EpEX (**Fig 33C**). Quantification revealed that the 6h-integrated signal strength of ERK in EGF^{high}-stimulated cells was 4-fold higher than that in EpEX-Fc-stimulated cells (**Fig 33D, red versus blue curves and bars**). In contrast, in low-dose EGF (1.8 nM) and high-dose EpEX-Fc (10 nM) treated cells, which both trigger proliferation, the activation kinetics and amplitude of ERK were almost identical after treatment for 180 min (**Fig 33E and**

F; blue versus green curves and bars). Hence, EGF and EpEX-Fc shape different ERK dynamics, rewiring divergent cell fates.

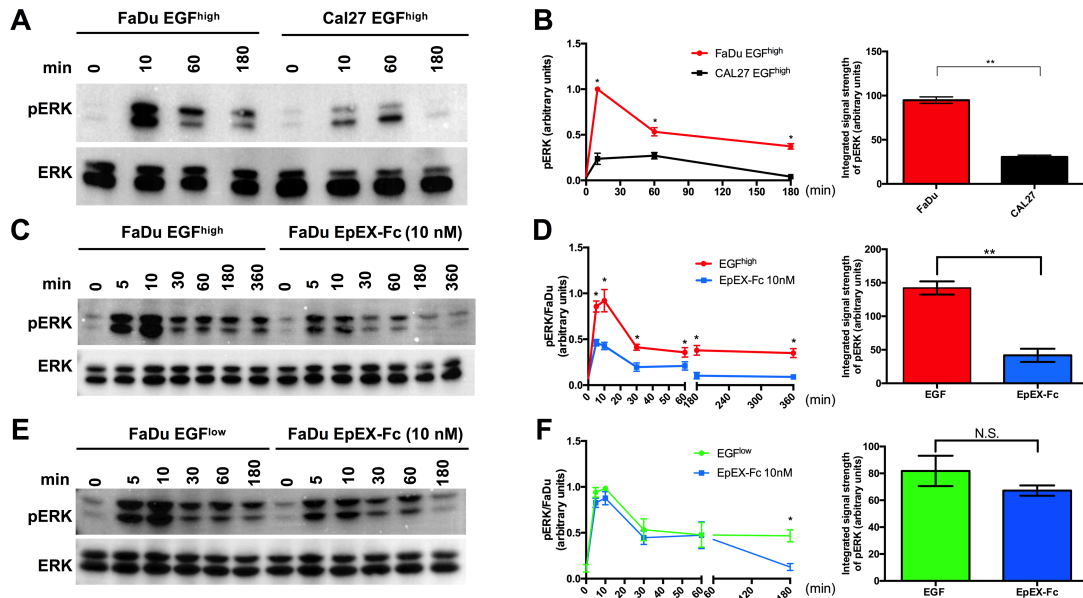


Fig 33. Integrated signal strength of phospho-ERK1/2 represents a major switch in decision-making towards EMT induction and proliferation.

(A, B) Immunoblot assessment of pERK expression level with whole cell lysates from FaDu and Cal27 cells treated with EGF^{high} (9 nM) for the indicated time points. Levels of ERK1/2 were used as controls. Shown are (A) representative results and (B) relative quantifications from immunoblot results. (C, D) Immunoblot assessment of pERK expression level in whole cell lysates from FaDu cells treated with EGF (9 nM) or EpEX-Fc (10 nM) for the indicated time points. Shown are (C) representative results and (D) relative quantifications from immunoblot results. (E, F) Immunoblot assessment of pERK expression level in whole cell lysates from FaDu cells treated with EGF (1.8 nM) or EpEX-Fc (10 nM) for the indicated time points. Shown are (E) representative results and (F) relative quantifications from immunoblot results. Shown are mean values with standard deviations (SD). All data were combined and generated from three independent replicates. Statistical analysis performed as One-way ANOVA, multiple testing with Bonferroni correction and significance shown as: * p-value <0.05, ** p-value <0.01, NS, not significant.

4.8.3 EpEX impedes EGF-induced EMT by altering the signal strength of ERK1/2 activation

In the present thesis, EpEX was identified as a new ligand for EGFR, which competes with EGF binding to EGFR, induced different ERK dynamics compared to EGF, and impedes on EGF-induced EMT. Thus, it was hypothesized that the inhibitory effect of EpEX on EGF-induced EMT might be associated with altered ERK signaling. To address this hypothesis, phospho-ERK1/2 levels were compared among EGF^{high}-treated, high-dose EpEX-Fc-treated, and a combination of both treatments FaDu cells by immunofluorescence staining and confocal laser scanning microscopy analysis. Treatment with EGF^{high} resulted in a strong activation of phospho-ERK1/2 and a predominant nuclear localization of the activated kinase, whereas EpEX-Fc induced a more moderate activation. Noteworthy, EGF and EpEX-Fc co-treatment resulted in diminished ERK1/2 activation, compared with single EGF^{high} treatment (**Fig 34A**). Quantification of phospho-ERK1/2 disclosed a 3-fold reduction of ERK1/2 activation by EpEX-Fc compared to EGF^{high}, and, importantly, a 2-fold reduction upon EGF^{high} and EpEX-Fc co-treatment, in comparison with the strong induction by EGF^{high} solely (**Fig 34B**). Thus, EpEX-Fc potentially impedes EGF-induced EMT by altering the integrated strength of ERK1/2 activation.

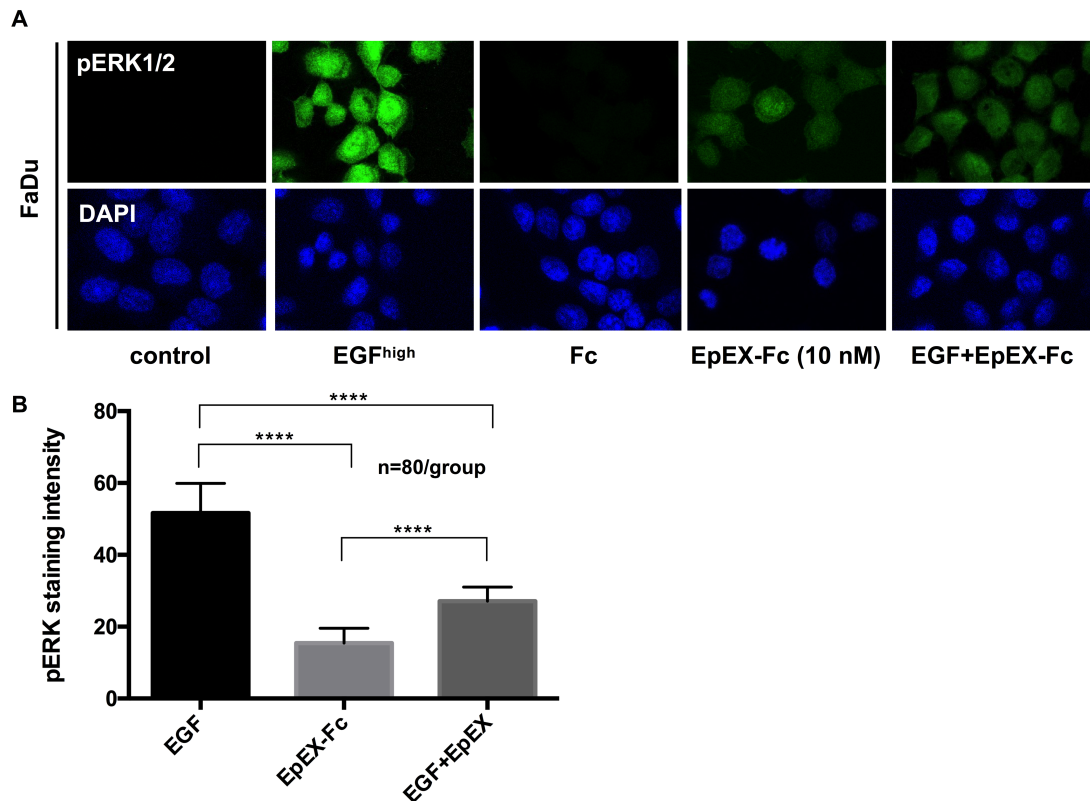


Fig 34. EpEX-Fc impedes EGF-mediated EMT through modulation of ERK1/2 activity.

pERK1/2 expression was assessed on control- and EGF^{high}- (9 nM) treated, high-dose EpEX-Fc- (10 nM) treated, and a combination of both treatments on FaDu cells by immunofluorescence staining and confocal laser scanning microscopy analysis after 72 h. Shown are (A) representative images and (B) relative quantifications of *pERK1/2* intensity from *n* = 3 independent experiments. One-way ANOVA, multiple testing with Bonferroni correction. **** *p*-value <0.0001. Phosphorylated ERK1/2 (*pERK1/2*): green, nuclei: blue (DAPI).

4.9 EGFR and EpCAM expression levels control EMT induction *in vitro* and mimic the *in vivo* situation

EGFR and EpCAM expression levels correlated with the clinical outcome of HNSCC patients (see Fig 10 and Fig 11). *In vitro* data provided evidence that the soluble ectodomain of EpCAM, EpEX, which is naturally shed in the extracellular milieu and found in serum of cancer patients, was able to impede EGF/EGFR mediated EMT through modulation of ERK1/2 activity by competitive binding to EGFR. The distinct

morphology and biological events resulting from EGF^{high} and EGF^{high} and EpEX co-treatment of HNSCC cells might also determine the significant discrepancy of clinical outcome of tumors patients characterized by differential EGFR and EpCAM expression *in vivo*.

4.9.1 Establishment of an *in vitro* system to mimic EGFR and EpCAM expression profiles in primary HNSCC

In order to test whether the results obtained *in vitro* might be the basis for strongly differing clinical outcome in patients, an *in vitro* system to mimic the situation in the primary tumor cohort was established. To do so, the expression of EGFR and EpCAM in Kyse30 cells, which express high levels of both, was down-regulated using siRNA and shRNA molecules, respectively. By doing so, EGFR and EpCAM expression patterns corresponding to the four quadrants of expression observed in primary HNSCC were reconstituted. Kyse30 cells were treated with an EGFR-specific siRNA pool (n=4), an EpCAM-specific shRNA, and the cognate controls. Double-knockdown of endogenous EGFR and EpCAM was achieved in EpCAM-knockdown Kyse30 cells via additional EGFR-specific siRNA transfection. Single- and double-knockdown were confirmed by immunoblotting, exhibiting diminished expression levels of the targeted molecules and no cross-interference (**Fig 35A**). Based on these expression levels, EGFR-knockdown Kyse30 cells mimicked tumor quadrant 1 (Q1, EGFR^{low}/EpCAM^{high}) of primary HNSCC observed in the LMU cohort. Wildtype Kyse30 cells mimicked tumor quadrant 2 (Q2, EGFR^{high}/EpCAM^{high}), EpCAM-knockdown Kyse30 cells mimicked

tumor quadrant 3 (Q3, EGFR^{high}/EpCAM^{low}), and double-knockdown Kyse30 cells mimicked tumor quadrant 4 (Q4, EGFR^{low}/EpCAM^{low}).

4.9.2 EGFR and EpCAM levels associated with differential responsiveness to EGF in ERK activity

Previous data in the present thesis have demonstrated that the integrated strength of ERK1/2 activity represents the major molecular switch regulating cellular fates of proliferation versus EMT (**see Fig 33**), upon which EpEX exert its inhibitory effect on EGF-induced EMT. Thus, it was of interest to determine whether a recapitulation of EGFR and EpCAM expression profiles reminiscent of the *in vivo* situation in HNSCC would affect EMT induction and cell functionality. To investigate this possibility, ERK activation in response to EGF^{low} (1.8nM) was assessed on serum-starved Kyse30 cell variants mimicking clinical quadrants 1-4. The results indicated that in EGFR^{high}/EpCAM^{high} wildtype Kyse30 cells (Q2 equivalent) EGF^{low} treatment resulted in intermediate ERK1/2 phosphorylation (**Fig 35B lane8**), while knockdown of EGFR in Kyse30 cells rendered the cells refractory to the ERK-activating effect of EGF treatment. As a result, EGFR-knockdown Kyse30 cells (EGFR^{low}/EpCAM^{high}, Q1 equivalent) exhibited strongly reduced ERK1/2 activity (**Fig 35B lane7**) and ERK1/2 activation was entirely abolished in EGFR and EpCAM double-knockdown Kyse30 cells (EGFR^{low}/EpCAM^{low}, Q4 equivalent) (**Fig 35B lane10**). Oppositely, hyperactivation of ERK1/2 phosphorylation was observed in EpCAM-knockdown cells with high levels of EGFR (EGFR^{high}/EpCAM^{low}, Q3 equivalent) (**Fig 35B lane9**). Overall,

these results demonstrated that tumor cells with different EGFR/EpCAM expression patterns exhibited different responsiveness to EGF, resulting in different integrated strength of ERK signaling. The results showed that EGF-mediated ERK1/2 activation depended on high levels of EGFR, and that EGFR^{high} tumor cells have stronger ERK signaling. However, EpCAM expression could hamper hyperphosphorylation of ERK in EGFR^{high} cells. Combined with our foregoing *in vitro* data, I assumed that EGFR^{high}/EpCAM^{low} tumor cells have more potential to undergo EMT, whereas EGFR^{low}/EpCAM^{high} tumor cells are more refractory to the EMT-driving effect of EGF.

4.9.3 EGFR and EpCAM levels control EMT induction in tumor cells

Given that EGFR and EpCAM can regulate ERK activity and that high ERK activity promotes an EMT, the relationship between differential EGFR/EpCAM expression patterns and EMT induction was examined. All cell lines recapitulating quadrants 1-4 of the LMU cohort were treated with EGF^{low} (1.8 nM) (**Fig 35C, E**) and EGF^{high} (9 nM) for 72 h (**Fig 37D, F**), and cell morphology, Slug expression, and cell migration were assessed to certify an EMT induction. EGF^{low} treatment is not able to drive mesenchymal characteristic in HNSCC FaDu and Kyse30 cells, as has been repeatedly shown (**see Fig15; Fig29 and Fig35C**). Strikingly, treatment of EpCAM-knockdown Kyse30 cells (EGFR^{high}/EpCAM^{low}, Q3 equivalent) with EGF^{low} resulted in a fusiform cellular morphology (**Fig 35C, Q3-green**) and increased expression of Slug (**Fig 35E, green bar**). Hence, EGFR^{high}/EpCAM^{low} cells undergo EMT after treatment with a five-fold reduced concentration of EGF as compared to EGFR^{high}/EpCAM^{high}

cells (**Fig 35D, F yellow bar**). In contrast, EGFR-knockdown in Kyse30 cells (EGFR^{low}/EpCAM^{high}, Q1 equivalent) and double-knockdown of EGFR and EpCAM in Kyse30 cells (EGFR^{low}/EpCAM^{low}, Q4 equivalent) lacked any evidence of EMT induction following EGF treatment. Neither morphology nor Slug expression were affected following EGF treatment (**Fig 35D, F**). Importantly, EpCAM knockdown (Q3 equivalent) exhibited an even stronger EMT induction following EGF^{high} treatment, showing enhanced Slug expression compared to wildtype (Q2 equivalent) cells (**Fig 35F, green bar**). Accordingly, wildtype and EpCAM-knockdown Kyse30 cells (Q2 and Q3 equivalent) acquired enhanced migratory ability after EGF^{high} treatment, in comparison with that of EGFR-knockdown and EGFR/EpCAM double-knockdown Kyse30 cells (Q1 and Q4 equivalent) (**Figure 35G**).

Hence, loss of EGFR abolished, whereas loss of EpCAM facilitated EGF-induced EMT, through modulation of ERK activation and Slug expression. These differences were further corroborated at the level of cellular behavior. Overall, EGFR^{high}/EpCAM^{low} tumor cells have more potential to undergo EMT, while EGFR^{low}/EpCAM^{high} tumor cells were more refractory to the EMT-driving effect of EGF.

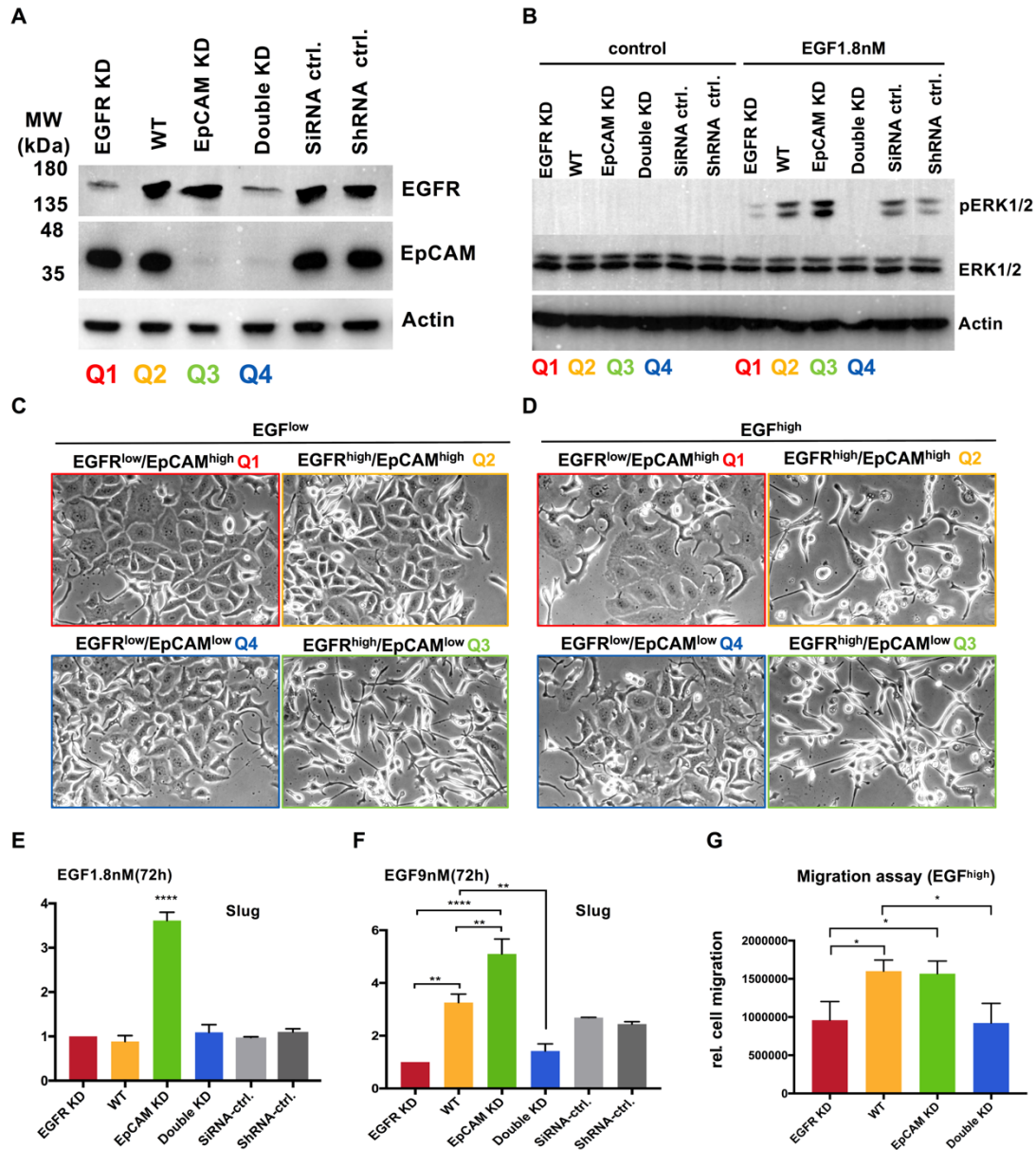


Fig 35. EGFR and EpCAM levels are molecular determinants of EMT induction, ERK activation, and migration.

(A) Establishment and characterization of an *in vitro* system mimicking EGFR and EpCAM expression patterns corresponding to primary HNSCCs. EGFR and EpCAM single- and double-knockdown of Kyse30 cells were confirmed by immunoblotting. Clinical quadrants equivalents are indicated. (B) Immunoblot assessment of pERK1/2 activation following EGF 1.8 nM stimulation on quadrant 1 to 4 equivalents of Kyse30 cell variant. Levels of ERK1/2 were assessed in parallel as controls. (C, D) Quadrant 1 to 4 equivalents of Kyse30 cell variants were treated with EGF^{low} (1.8 nM) (C) and EGF^{high} (9 nM) (D) for 72 h and cell morphology was assessed. Shown are representative images. (E, F) qRT-PCR assessment of Slug transcription levels in quadrant 1 to 4 equivalents of Kyse30 cell variants untreated (control) or treated with EGF^{low} (1.8 nM), or treated with EGF^{high} (9 nM) for 72 h. Results are present as means

\pm SD from $n = 3$ independent experiments performed in triplicates. (G) Scratch assay was performed with quadrant 1 to 4 equivalents of Kyse30 cell variants treated with EGF^{high} (9 nM) and relative migration was quantified from representative micrographs and adjusted for proliferation rate of each cell line. Results are present as means \pm SD. All data were combined and generated from three independent replicates. Statistical analysis performed as One-way ANOVA with posthoc multiple testing and Bonferroni correction and significance shown as: * p -value < 0.05 , ** p -value < 0.01 , *** 0.001, **** 0.0001.

4.10 pERK1/2 and Slug define HNSCC patients with poor outcome

The aforementioned data have shown that integrated signal strength of phospho-ERK1/2 functions as a major molecular switch in decision-making towards EMT induction (**Fig 33**). High integrated strength of ERK1/2 activity correlated with increased Slug expression and enhanced cell migration, as shown in **Fig 35** and reported in breast cancer (Chen et al., 2009). Moreover, as reported in single cell transcriptomic study of HNSCC, Slug was the only up-regulated EMT-TF in the pEMT-signature, and appears as an early EMT-inducing factor compared to other EMT-TFs. The foregoing *in vivo*-mimicking Kyse30 system data indicated that EGFR^{high}/EpCAM^{low} tumor cells were characterized by a stronger ERK phosphorylation and Slug induction following EGF stimuli, and thus have enhanced potential to undergo EMT. Oppositely, EGFR^{low}/EpCAM^{high} tumor cells exhibited substantially lower ERK phosphorylation and Slug transcription in response to EGF, and were accordingly more refractory to EMT induction (**see Fig 35**). These findings prompted the analysis of phospho-ERK and Slug expression in human HNSCCs, in which it might play a role in tumor progression and metastasis, and might thus correlate with prognosis.

4.10.1 Concurrent expression pattern of phospho-ERK and Slug in HNSCC samples

Phospho-ERK and Slug expression levels were analysed in EGFR^{low}/EpCAM^{high} tumors (Q1, n=37) and EGFR^{high}/EpCAM^{low} tumors (Q3, n=39) of the LMU HNSCCs cohort by IHC staining in consecutive sections specimens. Remarkably, EGFR^{high}/EpCAM^{low} tumors were characterized by relatively high level of phospho-ERK1/2, whereas EGFR^{low}/EpCAM^{high} tumors exhibited low to moderate phospho-ERK levels (**Fig 36A**). Likewise, Slug IHC staining results showed low Slug levels in EGFR^{low}/EpCAM^{high} specimens and elevated expression in EGFR^{high}/EpCAM^{low} specimens. To be noted, pERK1/2 and Slug were frequently expressed concurrently in cells located at the edge of tumor areas in our cohort (**Fig 36A upper panel**), in conformity with the published intratumoral localization of pEMT-program cells at the leading edge of HNSCCs (Puram et al., 2017). Quantification using IHC scoring revealed that pERK1/2 and Slug were 2.14-fold and 2.1-fold higher in EGFR^{high}/EpCAM^{low} tumors than in EGFR^{low}/EpCAM^{high} tumors (**Fig 36B**). Therefore, IHC analyses of phospho-ERK and Slug supported preceding *in vitro* data and indicated that ERK activity and Slug, which regulated EMT, were controlled by EGFR/EpCAM levels in HNSCCs.

4.10.2 Slug correlates with ERK activation.

I next aimed at identifying the overall correlation between pERK1/2 and Slug. Slug and pERK1/2 expression were assessed by IHC staining with consecutive sections of all

available patients' specimens of the LMU HNSCC cohort (n=169/180) and quantified using the IHC scoring system (IHC score 0-300). Spearman correlation analysis of IHC scores disclosed a robust positive correlation of pERK1/2 and Slug expression ($r=0.5784$, $p<0.0001$) in the HNSCC cohort (**Fig 36C**).

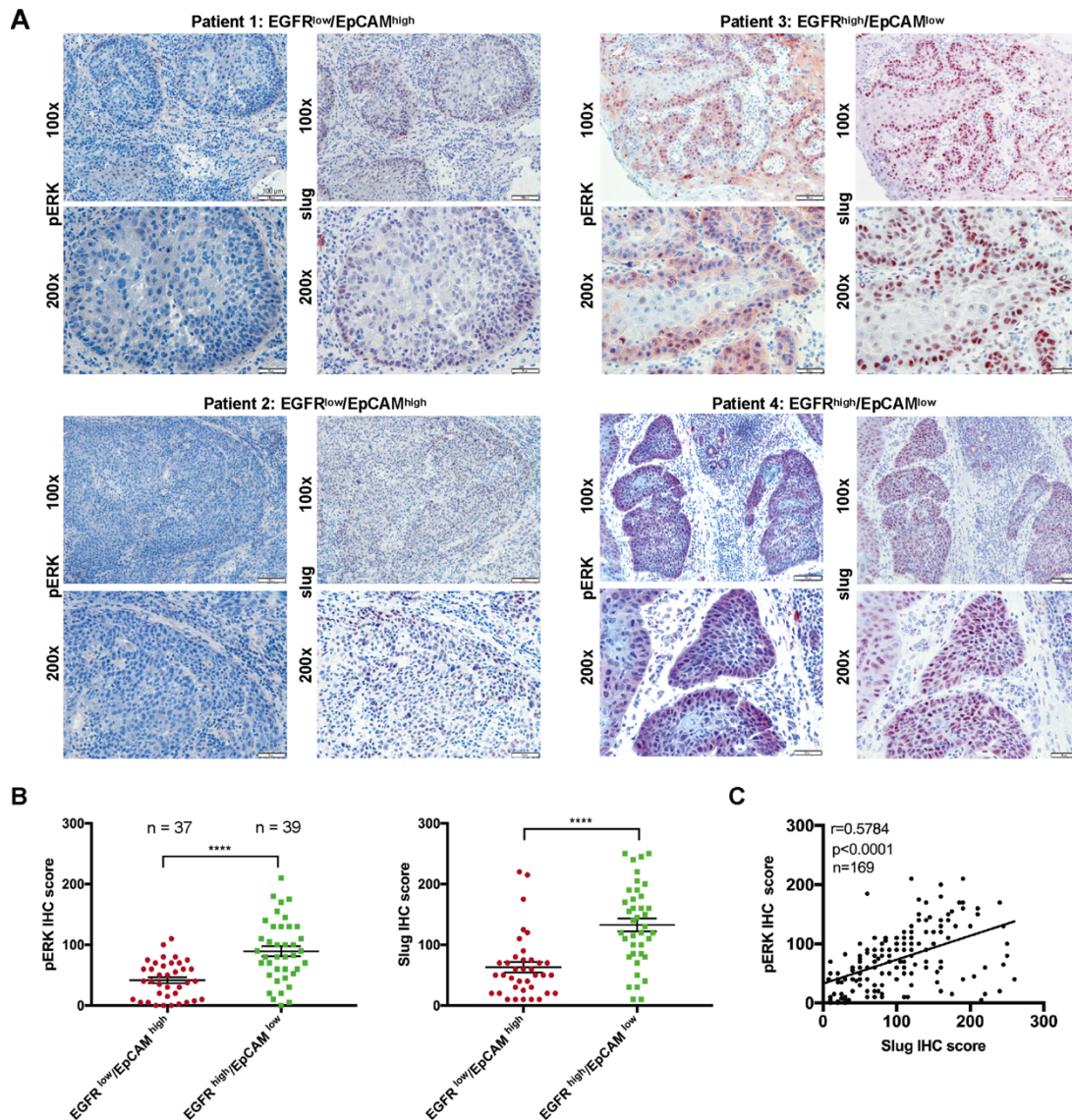


Fig 36. pERK and Slug are co-expressed and correlate in HNSCCs.

(A) Expression of pERK1/2 and Slug were assessed by immunohistochemistry staining of serial cryosections of primary tumors from the LMU HNSCCs cohort. Shown are two representative examples of EGFR^{low}/EpCAM^{high} (patients 1 and 2) (left panel) and EGFR^{high}/EpCAM^{low} (patients 3 and 4) (right panel) HNSCC at 100x and 200x magnification. (B) Expression of pERK1/2 and Slug were quantified (IHC score 0-300) and compared between EGFR^{low}/EpCAM^{high} (n=37) and EGFR^{high}/EpCAM^{low} (n=39)

HNSCC. Results are presented as IHC score values means \pm SEM. Statistical analysis performed as Student's T-test and significance shown as: **** p -value <0.0001 . (C) Spearman correlation analysis of pERK and Slug expression based on IHC scores with r -value and p -value for the entire HNSCC cohort ($n=169/180$).

4.10.3 Phospho-ERK and Slug predict poor survival of HNSCC patients

Next, the capacity of pERK1/2 and Slug expression levels to prognosticate the clinical outcome of HNSCC patients was assessed. To do so, Kaplan-Meier survival analysis served to calculate OS and DFS of patients with EGFR and EpCAM IHC scores below 125 (antigen^{low}) or above 175 (antigen^{high}). Patients with high expression of pERK1/2 and/or Slug (IHC score >175) correlated with poor OS ($n=98$) and DFS ($n=97$) (**Fig 37**). Hence, EGF/EGFR/pERK1/2/Slug represents a signaling axis that impacts on cell differentiation towards EMT and defines HNSCC patients with poor clinical outcome.

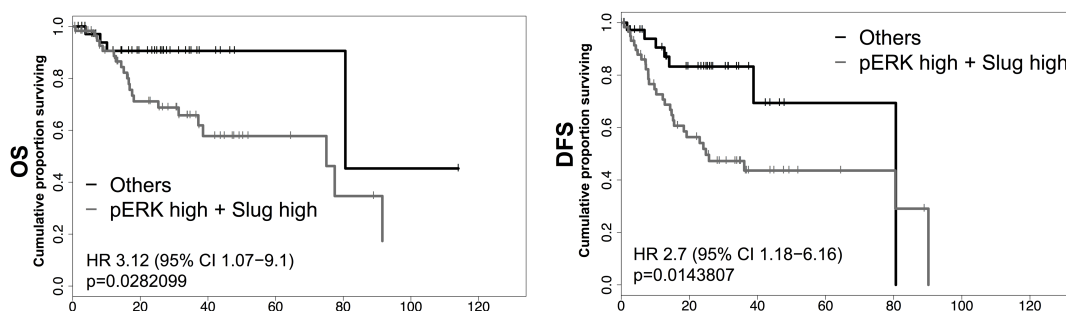


Fig 37. pERK and Slug predict poor survival of HNSCC patients.

Kaplan-Meier survival analysis served to calculate OS and DFS of patients with EGFR and EpCAM IHC scores below 125 (antigen^{low}) or above 175 (antigen^{high}). Patients were stratified according to pERK and Slug expression and patients with expression of pERK1/2 and/or Slug >175 are considered as high expressors (pERK high + Slug high). OS ($n=98$) and DFS ($n=97$) are compared between pERK high + Slug high subgroup and all remaining patients.

5. DISCUSSION

HNSCC is a common malignancy characterized by frequent recurrences and poor clinical outcome (Leemans et al., 2011). Recent studies revealed a remarkably high clinical, cellular and genetic heterogeneity of HNSCC (Cancer Genome Atlas, 2015; Mroz et al., 2015; Puram et al., 2017; Stransky et al., 2011). The importance of intratumoral heterogeneity in tumor development, treatment resistance, and metastasis formation was documented (Almendro et al., 2013; Bedard et al., 2013; Burrell et al., 2013; Gerashchenko et al., 2013; Hiley et al., 2014; Murugaesu et al., 2013). Accordingly, the degree of intratumoral heterogeneity correlates with poor survival in HNSCC patients (Mroz et al., 2015; Mroz et al., 2013). Especially, high intratumoral heterogeneity allows for the development of a pEMT phenotype of cancer cells, which is considered as central to foster metastasis formation and therapy resistance (Brabletz, Kalluri, Nieto, & Weinberg, 2018; Lambert et al., 2017; Puram et al., 2017). Consequently, metastatic disease and therapy resistance remain central challenges in HNSCC. So far, molecular risk factors with clinical utility for risk stratification of HNSCC are of limited value, therefore, generating an integrated evaluation system of molecular risk factors to prognosticate HNSCC progression is in great demand.

5.1 Duality of EGF/EGFR signaling in HNSCC

The EGFR pathway is one of the most frequently dysregulated signaling pathways in human cancers. EGFR is frequently overexpressed and its aberrant activity is implicated in a variety of cancers including HNSCC (Han & Lo, 2012; Hynes & Lane,

2005). Consequently, EGFR is among the most intensely studied drug targets across numerous cancer entities. Currently, EGFR is, along with PD1/PD-L1 checkpoint inhibitors, a major therapeutic target in palliative treatment regimens for recurrent and metastatic HNSCCs (Bonner et al., 2006; Goldberg, 2005; Price & Cohen, 2012; Zimmermann, Zouhair, Azria, & Ozsahin, 2006). Additionally, elevated expression of EGFR has been reported to associate with poor prognosis in HNSCC patients (Kalyankrishna & Grandis, 2006; Psyrri et al., 2005). In the present thesis, I confirmed that HNSCCs characterized by high expression of EGFR (EGFR^{high}) were associated with poor OS in the LMU_cohort of HNSCC patients (**Fig 11A**), and further validated these results in the HNSCC TCGA cohort (**Fig 11B**). Even after accounting for the HPV status of the patients, which is a predictor of improved survival, the analysis still disclosed a significantly poorer OS of EGFR^{high} versus EGFR^{low} tumors (**Fig 11A, B**). Moreover, main downstream effectors of EGFR such as ERK1/2 and Akt, which are highly associated with EMT based on multiple studies, were discovered to be abnormally activated in HNSCCs (Albanell et al., 2001; Ongkeko et al., 2005). Thus, EGFR may promote an EMT cellular fate through strong and maintained activation of downstream signaling pathways, which contributes to HNSCCs progression and poor survival.

In vitro, EGF/EGFR and downstream signaling activation (mainly MEK-ERK signaling and PI3K-AKT signaling axis) are able to drive cancer cells to undergo EMT, as has been reported in different cancer cell types (Buonato et al., 2015; Chandra Mangalhara

et al., 2017; Cui et al., 2017; Fu et al., 2017; Fukuda et al., 2016; Grassi et al., 2017; Holz et al., 2011; J. Li et al., 2014; Y. Li et al., 2017; Muthusami et al., 2014; Saito et al., 2017; Sheng et al., 2017; Tashiro et al., 2016; Vergara et al., 2011; P. Wang et al., 2017; Xu et al., 2017; Xue et al., 2015; Y. Zhang et al., 2015; Z. Zhang et al., 2014; Zuo et al., 2011). The present study demonstrated that EGF/EGFR signaling also induced EMT in HNSCC carcinoma cells, FaDu and Kyse30, which express high levels of EGFR. EMT was evidenced by mesenchymal-like morphology, decreased epithelial marker, EMT-TFs upregulation, and enhanced migratory ability (**Fig 15, 28, 29, 31**). Particularly intriguing was the finding that activation of EGFR through EGF in HNSCC cells results in distinct cellular outcomes in a dosage dependent manner. EGFR activation in response to low doses of EGF (EGF^{low}, 1.8 nM) led to cell proliferation, whereas EGFR activation by EGF^{high} (9 nM) induced EMT (**Fig 15, 27, 29, 31**). This raised the question, how the activation of a particular EGFR signaling pathway by the same ligand provides different biological consequences. In other words: How does a cell distinguish between EGF^{low}- and EGF^{high}-induced signaling and how does it interpret the differences at the molecular level? Answering these questions required a cautious probing of the EGF-induced EGFR downstream signaling pathways, *i.e.* the RAS-RAF-MEK-ERK pathway and the PI3K-Akt pathway. By doing so, the aim was to uncover the central effector that controls cellular decision-making and acquisition of EMT, as this would further facilitate exploring molecular mechanism of the observed dual capacity of EGF/EGFR in cellular outcomes. In the tested HNSCC cell lines, I

found that MEK inhibitor AZD6244, but not AKT-inhibitor MK0026 significantly inhibited EGF-induced EMT (**Fig 32**), demonstrating that EGF executes EMT through induction of ERK1/2, but not AKT in these cell lines. Multiple lines of evidence conform to results of the present thesis, demonstrating a decision-making role of the ERK1/2 pathway in EGF-induced EMT (Blaj et al., 2017; Chiu et al., 2017; Ichikawa et al., 2015; S. Shin et al., 2010). However, in contrast, AKT has also been reported to function as the central effector in EMT induction in prostate cancer cell lines (Gan et al., 2010), in nasopharynx carcinoma (M. H. Wang et al., 2018), and in mammary MCF7 cells (Gao, Yan, Wang, Liu, & Yang, 2015). The heterogeneity of tumor types and the diversity of stimuli triggering EMT might account for the disparity. Notwithstanding, more lines of evidences conform to the central role of the ERK1/2 pathway in EGF-induced EMT, as documented in the aforementioned systematic review of literature, in which MEK-ERK or PI3K-AKT signaling were reported as the main mediator in EGF/EGFR-induced EMT (MEK-ERK n=22; PI3K-AKT n=14). Hence, ERK1/2 signaling is the major effector in EGF-induced EMT in various cancer cell lines, as well as demonstrated in the present thesis, in HNSCCs. Furthermore, a central role of ERK1/2 signaling is also demonstrated in FGF- and HGF-induced EMT (Nagai et al., 2011; Said & Williams, 2011), and in TGF β -mediated EMT in a variety of epithelial cancer cell types (Amatangelo, Goodyear, Varma, & Stearns, 2012; Janda et al., 2002; Xie et al., 2004). Moreover, overexpression of active variants of mediators of the Ras-Raf-MEK-ERK axis was shown to be sufficient to provoke EMT in multiple types of cancer cell lines

(Herr, Wohrle, Danke, Berens, & Brummer, 2011; Lemieux et al., 2009; Makrodouli et al., 2011; S. Shin et al., 2010; Voisin et al., 2008).

Activation of the MAPKs ERK1/2 signaling pathway exerts a prominent influence on cell proliferation, differentiation, and EMT induction. Distinct ERK dynamics were revealed to trigger different cellular fate decisions (Andreu-Perez et al., 2011; Rauch, Rukhlenko, Kolch, & Kholodenko, 2016; Ryu et al., 2015; Santos, Verveer, & Bastiaens, 2007). Three different quantitative measures could be utilized to assess ERK signaling: signal amplitude, duration (transient or sustained) and integral strength (derived from the other two measures) (Hornberg, Binder, et al., 2005; Hornberg, Bruggeman, et al., 2005). Prompted by these observations, the current thesis measured the ability of EGF^{low} and EGF^{high} to induce ERK1/2 activation in FaDu cells, monitoring pERK1/2 signal strength and duration. As shown in **Fig 33**, EGF^{low} resulted in a transient and weaker pERK1/2 dynamic, whereas EGF^{high} induced a sustained and stronger pERK1/2 activation. Thus, transient and weaker ERK activation in response to EGF^{low} led to proliferation (**Fig 38; left**), whereas more sustained and stronger ERK activation in response to EGF^{high} led to EMT (**Fig 38; right**). Consistent with the idea that different ERK activation dynamics govern cell fate decisions, several reports have described that transient and weak ERK signaling is typically associated with proliferation, whereas sustained and strong ERK responses tend to be linked with cell differentiation or EMT in several cancer cell types (Avraham & Yarden, 2011; Freed et al., 2017;

Ichikawa et al., 2015; Lemmon, Freed, Schlessinger, & Kiyatkin, 2016; Marshall, 1995; Murphy, Smith, Chen, Fingar, & Blenis, 2002; Ryu et al., 2015; Santos et al., 2007).

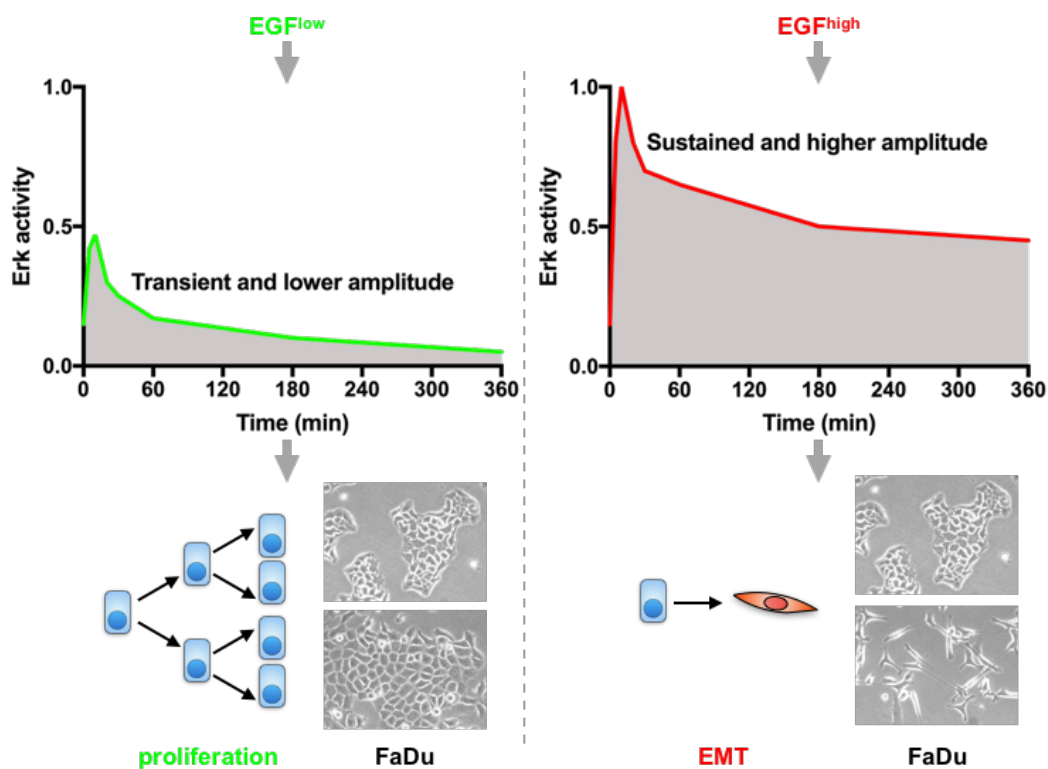


Fig 38. The duality of EGF-EGFR-ERK1/2 signaling.

Different ERK1/2 activation dynamics govern cell fate decisions, as seen in FaDu cells. EGF^{low} (left) induces transient and weak ERK1/2 activity, and associates with cell proliferation, whereas EGF^{high} (right) induces sustained and strong ERK responses, and links with EMT induction.

5.2 A novel cross-talk between EpCAM and EGFR

EpCAM was defined as an epithelial cell adhesion molecule and was also described as a signaling membrane glycoprotein involved in regulating differentiation and proliferation in cancer and stem cells (Chaves-Perez et al., 2013; Kuan et al., 2017; Litvinov, Bakker, Gourevitch, Velders, & Warnaar, 1994; Lu et al., 2010; Maetzel et al., 2009; Sankpal, Fleming, Sharma, Wiedner, & Gillanders, 2017; Sarrach et al., 2018;

Slanchev et al., 2009). More recently, EpCAM has been reported as surrogate marker for epithelial differentiation, with a contrary expression pattern to genes constituting a pEMT signature, including Slug and vimentin in HNSCCs (Puram et al., 2017). Reduction of EpCAM was observed during EMT (Driemel et al., 2014; Gorges et al., 2012; Hyun et al., 2016; Massoner et al., 2014; Vannier, Mock, Brabletz, & Driever, 2013; M. H. Wang et al., 2018), but the exact role of EpCAM in EMT is not fully understood.

Recently, a link between RIP of EpCAM and EGF-induced EMT was established. Hsu and colleagues reported that EGF treatment induces RIP of EpCAM in EGFR-dependent manner in endometrial carcinoma cell line RL95-2. EGF treatment resulted in shedding of the soluble extracellular domain of EpCAM (EpEX) and in the release of the intracellular domain (EpICD), which further functions as a nuclear transcriptional inducer of an EMT (Hsu et al., 2016). In the present thesis, however, RIP of EpCAM through EGF/EGFR activation could not be observed in a broad panel of carcinoma cell lines, independently of timescale and EGF concentrations used (**Fig 16-20**). Therefore, RIP of EpCAM is neither a common nor a frequent event in EGF-induced EMT in an array of carcinoma cell lines.

The contradicting role of EpCAM in EMT regulation has not been interpreted on a molecular basis yet. In accordance with such contradictory observations, high expression levels of EpCAM often, but not always, correlate with poor prognosis in breast cancer, esophagus, colorectal cancer, pancreatic cancer, ovarian cancer, as

well as in bladder cancer (Fong et al., 2008; Seeber et al., 2016; Spizzo et al., 2002; Spizzo et al., 2004; Stoecklein et al., 2006; van der Gun et al., 2010). However, high levels of EpCAM correlated with improved survival in renal, thyroid, colonic, gastric cancers (Ralhan et al., 2010; Seligson et al., 2004; Went et al., 2005; Went et al., 2006), and in HNSCCs, as shown in the present thesis and by Baumeister *et al.* (Baumeister et al., 2018).

Alternatively, the present study describes a novel functional cross-talk between EGFR signaling and EpCAM. Data described in the present thesis showed that endogenous EpCAM and EGFR interact, as evidenced by bi-directional co-immunoprecipitation and that the soluble ectodomain of EpCAM (EpEX), which is shed upon RIP of EpCAM in HNSCC cell lines (**Fig 22**), is a genuine novel ligand of EGFR that binds directly to the extracellular domain of EGFR, and induces classical ERK1/2 and AKT signaling pathway (**Fig 24, 25**). Furthermore, cross-linking experiments with purified recombinant extracellular domains of EGFR (EGFR_{ex}) and EpCAM (EpEX) suggested that EpEX competes with EGF binding to EGFR_{ex} (**Fig 24B**). EpEX-induced activation of EGFR downstream signaling was specific, as it required the expression of EGFR and was blocked by EGFR-specific inhibitors, Cetuximab, and TKIs (**Fig 25A, B, C**). EpEX induces EGFR and ERK1/2 less potently and more transiently in comparison with EGF (**Fig 25, 33**). The finding of interaction between EpEX and EGFR is consistent with recent reports on the activation of EGFR signaling by EpEX (Kuan et al., 2019; Liang et al., 2018). Liang *et al.* showed that EpEX can induce ERK and AKT signaling

through EGFR in colon carcinoma cells, which supported cell proliferation and enhanced RIP of EpCAM through the activation of ADAM17 and γ -secretase (Liang et al., 2018). Kuan *et al.* further published that EpEX stimulates EGFR signaling in mesenchymal stem cells and thereby promotes cell proliferation and multipotency (Kuan et al., 2019). However, experimental evidence for the actual binding of EpEX to EGFR was lacking in both of studies, and is provided in our own study (Pan et al., 2018).

5.3 Functional consequences of the crosstalk between EGFR and EpCAM

5.3.1 EpEX induces proliferation and exhibits an inhibitory effect on EGF-induced cell migration

The EGFR-ERK/MAPK signaling cascade is a central driver of cell proliferation (Albeck, Mills, & Brugge, 2013). EpEX-induced ERK1/2 activation resulted in enhanced proliferation of HNSCC cells (**Fig 27**), which is in line with aforementioned reports (Kuan et al., 2019; Liang et al., 2018). EpEX-induced proliferation in HNSCC cells was entirely blocked upon co-treatment with Cetuximab (**Fig 27A green line**), demonstrating that EpEX exerts proliferative effects specifically through EGFR. By contrast, EpEX induced less potent proliferation compared to EGF^{low} treatment (**Fig 27**), which can be reasoned to weaker and more transient ERK dynamics induced by EpEX in comparison to EGF^{low} (**Fig25, 33**). In contrary to previous report that EpEX enhanced migration of colon carcinoma cells (Liang et al., 2018), no increases in cell migration could be detected in EpEX-treated FaDu and Kyse30 HNSCC cells (**Fig 28**).

Oppositely, the increased cell migration in response to EGF^{high} was diminished significantly by co-treatment with EpEX-Fc (**Fig 28**), demonstrating an inhibitory effect of EpEX on EGF-induced cell migration.

5.3.2 EpEX impedes EGF-induced EMT by altering the integrated signal strength of ERK1/2 activation.

Morphological and molecular characterization of EGF and EpEX-Fc co-treated cells demonstrated that EpEX-Fc impedes EGF-induced EMT in HNSCC cells (**Fig 29, 31**). Co-treatment with EpEX-Fc and EGF resulted in reduced expression of the EMT-TFs Snail, Slug, and Zeb1 (**Fig 31**) and, most importantly, decline of the causal effector pERK1/2 activity (**Fig 33, 34**). The present thesis suggests that EpEX can compete with EGF for binding to the extracellular domain of EGFR, altering the integrated strength of EGFR-pERK-Slug signaling and consequentially impeding EMT in HNSCC cells (**Fig 39**).

It has been reported that full-length EpCAM has inhibitory effect on EGF-induced ERK activation in carcinoma cells. EpCAM down-regulation was associated with enhanced ERK activation and increased Slug expression following EGF treatment. Oppositely, forced expression of EpCAM resulted in reduced ERK activity and Slug expression (Sankpal et al., 2017). In accordance with these results, knockdown of EpCAM in Kyse30 cells also led to enhanced ERK1/2 activation induced by EGF *in vitro*. *A priori*, the findings of a promoting effect of EpEX on ERK1/2 activation reported in the present thesis are in contradiction to the report by Sankpal *et al.* (Sankpal et al., 2017). However, the findings in my thesis demonstrate that EpEX can compete with the strong

activation of ERK and Slug induced by EGF, and, consequently, represses EGF-induced EMT (**Fig 29, 31, 33, 34, 39**). Therefore, in addition to an inhibitory effect of EpEX on the EGF-induced strong activation of ERK1/2, EpEX exerts a weak activating effect on ERK1/2 activity in HNSCC cells that results in proliferation. The counteracting role of EpEX in EGF-induced EMT demonstrated in the present thesis, is contradictory to the reported role of EpCAM in the activation of pluripotency genes and EMT regulators in colon cancer cells (Lin et al., 2012). Notably, work by Lin and colleagues differed from the present thesis in the cellular systems utilized and especially the molecules addressed. Lin *et al.* focused on role of EpCAM in the regulation of transcription factors, whereas the present thesis determined the crosstalk between EGFR and the soluble extracellular domain of EpCAM, EpEX. From the cellular system in the present study, I conclude that EpEX binding to EGFR impedes EGF-induced EMT through repressing EMT-TFs, but neither induces EMT-TFs nor EMT. Thus, EpCAM and EGFR cross-regulate the integrated ERK activity and consequently, govern cellular fate.

5.3.3 EGFR and EpCAM define subpopulations of HNSCC with differing clinical outcome

In the present thesis, LMU HNSCCs patients were subclassified into four subgroups with $EGFR^{high}/EpCAM^{low}$, $EGFR^{low}/EpCAM^{high}$, $EGFR^{high}/EpCAM^{high}$, and $EGFR^{low}/EpCAM^{low}$ expression patterns based on IHC scoring and with distinct clinical outcome. Survival analysis utilizing a combination of EpCAM and EGFR as biomarker revealed significantly improved OS and DFS of $EGFR^{low}/EpCAM^{high}$ HNSCC patients

whereas disclosed strongly reduced OS and DFS of EGFR^{high}/EpCAM^{low} HNSCC patients (**Fig 11**). Even after accounting for HPV status and sub-localization of the tumors, statistical analyses confirmed a significantly improved OS and DFS of EGFR^{low}/EpCAM^{high} *in comparison with* EGFR^{high}/EpCAM^{low} tumors (**Fig 12, 13**). To my knowledge, this is the first demonstration that the combined EGFR and EpCAM expression profile predicts the clinical outcome of HNSCC patients, and particularly, that an EGFR^{low}/EpCAM^{high} expression profile correlates with outstandingly improved survival.

It can therefore be proposed that the cross-talk between EpCAM and EGFR, and an impeding effect of EpEX in EGF-induced EMT through altering integrated ERK dynamics, may provide a molecular basis for the observed disparity in clinical survival rates. In order to judge the potential relevance of the EpEX/EGFR crosstalk *in vivo* in tumors, it is important to consider whether naturally shed EpEX exists in the tumor microenvironment (TME). Naturally shed EpEX was demonstrated to be present in the supernatant of several HNSCC cell lines, in monomeric, dimeric, and multimeric forms (**Fig 22B**). Serum levels of EpEX were reported to be detectable at low concentration in tumor patients (Abe et al., 2002; Gebauer et al., 2014; Kimura et al., 2007; Petsch et al., 2011), but represent systemic levels, which hints towards considerably higher levels in the tumor microenvironment (TME) and at the interface of tumor cells, where EpEX is actively shed upon RIP of EpCAM (Denzel et al., 2009). Hence, shedding of EpEX by carcinoma cells could establish a functional crosstalk with EGFR locally, and

impact on the regulation of EGF/EGFR-dependent EMT, and thus can explain the improved clinical outcome observed in EGFR^{low}/EpCAM^{high} subgroup.

5.3.4 EGFR and EpCAM levels control EMT induction *in vitro* and mimic the *in vivo* situation

To further validate the hypothesis, recapitulation of the expression patterns of EGFR and EpCAM observed in four quadrants of clinical samples was utilized in a cellular system *in vitro* (**Fig 35**). By doing so, I could confirm a cross-regulatory mechanism of EGFR and EpCAM in ERK1/2 activity and EMT induction in HNSCC cells. Knockdown of EGFR expression strongly diminished ERK1/2 activation and Slug induction by EGF, and consequently abolished the EGF-induced EMT. Hence, these results confirmed the expected central role of EGFR in EGF-mediated EMT in HNSCC. Noteworthy, knockdown of EpCAM expression resulted in hyper-activation of ERK1/2 phosphorylation and enhanced Slug expression, and thus facilitated EGF-mediated EMT, with reduced levels of EGF required to do so. Overall, EGFR^{high}/EpCAM^{low} tumor cells have more potential to undergo EMT, while EGFR^{low}/EpCAM^{high} tumor cells were more refractory to the EMT-driving effect of EGF. It can therefore be proposed that EGFR and EpCAM levels *in vivo* exert regulatory effects on the integrated strength of ERK1/2 activity and Slug expression, and consequently control the induction of EMT, which is a central aspect of metastases formation and therapy resistance. Henceforward, EpCAM is not only instrumental as a surrogate marker to define the degree of epithelial differentiation of HNSCC (Puram et al., 2017), but represents a genuine mediator of epithelial differentiation with functional consequence in tumor cells

(Pan et al., 2018) and embryonic stem cells (Sarrach et al., 2018). High expression of EpCAM can be positive for cell fate and clinical outcome based on its role in cell-cell adhesion (Balzar et al., 1999; Litvinov et al., 1994), in endomesodermal differentiation (Sarrach et al., 2018), and, as first defined here, as a regulatory ligand of EGFR impeding EGF/EGFR-induced EMT through alteration of EGFR-dependent pERK1/2 activity.

5.3.5 pERK1/2 and Slug define HNSCC patients with poor outcome

The foregoing *in vivo*-mimicking cellular system data indicated that EGFR^{high}/EpCAM^{low} tumor cells were characterized by a stronger ERK phosphorylation and Slug induction following EGF stimuli, and thus have enhanced potential to undergo EMT. Oppositely, EGFR^{low}/EpCAM^{high} tumor cells exhibited substantially lower ERK activity and Slug transcription in response to EGF, and were accordingly more refractory to EMT induction (**see Fig 35**). In accordance with these *in vitro* data, expression patterns of pERK and Slug were positively correlated with EGFR/EpCAM levels in clinical samples of HNSCC, which indicated that ERK activity and Slug were controlled by EGFR/EpCAM levels in HNSCCs. Furthermore, a positive correlation of pERK1/2 with the EMT-TF Slug within clinical samples was identified and an association of high pERK1/2 and Slug with significantly decreased OS and DFS was demonstrated in the present thesis (**Fig 36, 37**). Hence, the elucidation of a novel EGFR/EpCAM crosstalk in HNSCC additionally identified pERK1/2 and Slug as valid biomarkers for the stratification of HNSCC patients. High integrated strength of ERK1/2 activity correlated

with increased Slug expression and enhanced cell migration, as shown in the present thesis (**Fig 35**) and reported in breast cancer (Chen et al., 2009). In turn, Slug was the only up-regulated EMT-TF in the pEMT-signature, as reported in single cell transcriptomic study of HNSCC (Puram et al., 2017), and appears as an early EMT-inducing factor compared to other EMT-TFs. These reports and our own results suggest a central role for ERK1/2 signaling and Slug in the regulation of EMT in HNSCC, which will be the focus of future research.

Intriguingly, pERK1/2 and Slug were frequently expressed concurrently in cells located to the edge of tumor areas in our cohort (**Fig 36A upper panel**), in conformity with the published intratumoral localization of pEMT-program cells at the leading edge of HNSCCs (Puram et al., 2017). Puram *et al.* reported that paracrine interactions between malignant cells and cancer-associated fibroblasts (CAFs) promote a pEMT program at the leading edge of HNSCC tumors. Accordingly, extracellular cues and signals encountered by HNSCC cells at the edges of tumors, which could originate from various cell types within the tumor microenvironment (TME), potentially regulate pEMT. Regulating cell types within the TME might include CAFs, myeloid-derived suppressor cells (Toh et al., 2011), and endothelial cells-secreted EGF in HNSCC (Z. Zhang et al., 2014). Therefore, modulation through EGF and EpEX might result in qualitative and quantitative differences of EGFR-ERK signaling, and could thus substantially impact on key processes of local invasion and therapy response, and thereby eventually on recurrence.

In summary, the present thesis describes a novel functional crosstalk between EGFR and EpCAM (**Fig 39**), which provides a molecular mechanism for substantially disparate clinical outcomes of HNSCC patients stratified based on EGFR/EpCAM expression. Molecularly, EGF/EGFR-ERK signaling has dual capacity to regulate cellular fate decision. Transient and weaker ERK activation in response to EGF^{low} leads to proliferation, whereas more sustained and stronger ERK activation in response to EGF^{high} leads to EMT induction. EpEX, as a novel ligand of EGFR, exerts a weak activating effect on ERK1/2 activity that supports proliferation, but impedes EGF/EGFR-mediated EMT through altering integrated strength of ERK1/2 activity and repressing EMT-TFs, and thus might be positively involved in the clinical outcome of HNSCC patients. In addition, pERK and Slug, regulated by EpCAM and EGFR expression, play a central role in EMT regulation, and are valid biomarkers associated with poor prognosis of HNSCC patients. Thus, the EpCAM/EGFR/pERK1/2/Slug axis comprises valid biomarkers with prognostic value to stratify HNSCCs patients, and represents a promising target to improve patient-specific adjuvant treatment of HNSCCs.

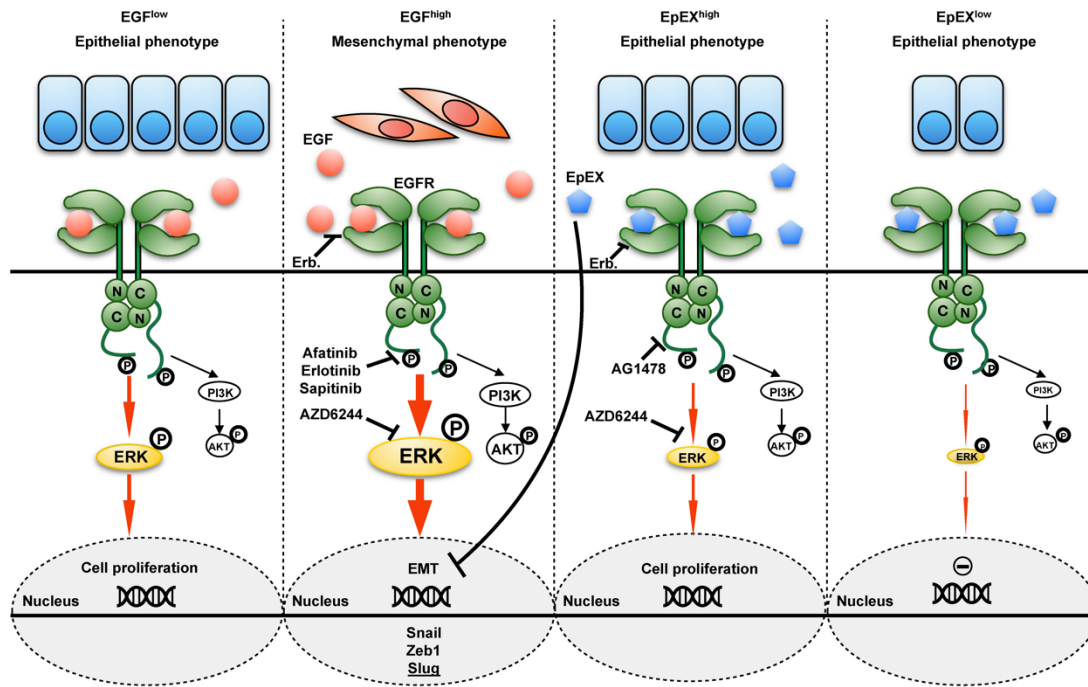


Fig 39. Schematic representation of EGF and EpEX cross-talk at the EGF receptor.

Transient and moderate ERK activity in response to EGFR activation by EGF^{low} leads to cell proliferation (left panel). Sustained and strong ERK activity in response to EGFR activation by EGF^{high} results in EMT induction, evidenced by mesenchymal phenotype and induction of EMT-TFs including Snail, Slug, Zeb1 (center-left panel). EpEX, identified as a novel ligand of EGFR, binds to extracellular domain of EGFR and activates downstream signaling pathway as ERK and AKT. High-dose EpEX exerts a weak activating effect on ERK1/2 activity that supports proliferation. EpEX can compete with EGF for binding to the extracellular domain of EGFR, altering the integrated strength of EGFR-pERK-Slug signaling and consequentially impeding EMT (center-right panel). Low-dose EpEX has no measurable effect on proliferation (right panel).

6. BIBLIOGRAPHY

- Abe, H., Kuroki, M., Imakiire, T., Yamauchi, Y., Yamada, H., Arakawa, F., & Kuroki, M. (2002). Preparation of recombinant MK-1/Ep-CAM and establishment of an ELISA system for determining soluble MK-1/Ep-CAM levels in sera of cancer patients. *J Immunol Methods*, 270(2), 227-233.
- Adamczyk, K. A., Klein-Scory, S., Tehrani, M. M., Warnken, U., Schmiegel, W., Schnolzer, M., & Schwarte-Waldhoff, I. (2011). Characterization of soluble and exosomal forms of the EGFR released from pancreatic cancer cells. *Life Sci*, 89(9-10), 304-312. doi:10.1016/j.lfs.2011.06.020
- Albanell, J., Codony-Servat, J., Rojo, F., Del Campo, J. M., Sauleda, S., Anido, J., . . . Baselga, J. (2001). Activated extracellular signal-regulated kinases: association with epidermal growth factor receptor/transforming growth factor alpha expression in head and neck squamous carcinoma and inhibition by anti-epidermal growth factor receptor treatments. *Cancer Res*, 61(17), 6500-6510.
- Albeck, J. G., Mills, G. B., & Brugge, J. S. (2013). Frequency-modulated pulses of ERK activity transmit quantitative proliferation signals. *Mol Cell*, 49(2), 249-261. doi:10.1016/j.molcel.2012.11.002
- Almendro, V., Marusyk, A., & Polyak, K. (2013). Cellular heterogeneity and molecular evolution in cancer. *Annu Rev Pathol*, 8, 277-302. doi:10.1146/annurev-pathol-020712-163923
- Amatangelo, M. D., Goodyear, S., Varma, D., & Stearns, M. E. (2012). c-Myc expression and MEK1-induced Erk2 nuclear localization are required for TGF-beta induced epithelial-mesenchymal transition and invasion in prostate cancer. *Carcinogenesis*, 33(10), 1965-1975. doi:10.1093/carcin/bgs227
- Andreu-Perez, P., Esteve-Puig, R., de Torre-Minguela, C., Lopez-Fauqued, M., Bech-Serra, J. J., Tenbaum, S., . . . Recio, J. A. (2011). Protein arginine methyltransferase 5 regulates ERK1/2 signal transduction amplitude and cell fate through CRAF. *Sci Signal*, 4(190), ra58. doi:10.1126/scisignal.2001936
- Ang, K. K., Harris, J., Wheeler, R., Weber, R., Rosenthal, D. I., Nguyen-Tan, P. F., . . . Gillison, M. L. (2010). Human papillomavirus and survival of patients with oropharyngeal cancer. *N Engl J Med*, 363(1), 24-35. doi:10.1056/NEJMoa0912217
- Arkipov, A., Shan, Y., Das, R., Endres, N. F., Eastwood, M. P., Wemmer, D. E., . . . Shaw, D. E. (2013). Architecture and membrane interactions of the EGF receptor. *Cell*, 152(3), 557-569. doi:10.1016/j.cell.2012.12.030
- Avraham, R., & Yarden, Y. (2011). Feedback regulation of EGFR signalling: decision making by early and delayed loops. *Nat Rev Mol Cell Biol*, 12(2), 104-117. doi:10.1038/nrm3048
- Baeuerle, P. A., & Gires, O. (2007). EpCAM (CD326) finding its role in cancer. *Br J Cancer*, 96(3), 417-423. doi:10.1038/sj.bjc.6603494

- Balzar, M., Briaire-de Bruijn, I. H., Rees-Bakker, H. A., Prins, F. A., Helfrich, W., de Leij, L., . . . Litvinov, S. V. (2001). Epidermal growth factor-like repeats mediate lateral and reciprocal interactions of Ep-CAM molecules in homophilic adhesions. *Mol Cell Biol*, *21*(7), 2570-2580. doi:10.1128/MCB.21.7.2570-2580.2001
- Balzar, M., Prins, F. A., Bakker, H. A., Fleuren, G. J., Warnaar, S. O., & Litvinov, S. V. (1999). The structural analysis of adhesions mediated by Ep-CAM. *Exp Cell Res*, *246*(1), 108-121. doi:10.1006/excr.1998.4263
- Baumeister, P., Hollmann, A., Kitz, J., Afthonidou, A., Simon, F., Shakhtour, J., . . . Gires, O. (2018). High Expression of EpCAM and Sox2 is a Positive Prognosticator of Clinical Outcome for Head and Neck Carcinoma. *Sci Rep*, *8*(1), 14582. doi:10.1038/s41598-018-32178-8
- Bedard, P. L., Hansen, A. R., Ratain, M. J., & Siu, L. L. (2013). Tumour heterogeneity in the clinic. *Nature*, *501*(7467), 355-364. doi:10.1038/nature12627
- Bei, R., Budillon, A., Masuelli, L., Cereda, V., Vitolo, D., Di Gennaro, E., . . . Muraro, R. (2004). Frequent overexpression of multiple ErbB receptors by head and neck squamous cell carcinoma contrasts with rare antibody immunity in patients. *J Pathol*, *204*(3), 317-325. doi:10.1002/path.1642
- Bertotti, A., & Sassi, F. (2015). Molecular Pathways: Sensitivity and Resistance to Anti-EGFR Antibodies. *Clin Cancer Res*, *21*(15), 3377-3383. doi:10.1158/1078-0432.CCR-14-0848
- Bierie, B., Pierce, S. E., Kroeger, C., Stover, D. G., Pattabiraman, D. R., Thiru, P., . . . Weinberg, R. A. (2017). Integrin-beta4 identifies cancer stem cell-enriched populations of partially mesenchymal carcinoma cells. *Proc Natl Acad Sci U S A*, *114*(12), E2337-E2346. doi:10.1073/pnas.1618298114
- Blaj, C., Schmidt, E. M., Lamprecht, S., Hermeking, H., Jung, A., Kirchner, T., & Horst, D. (2017). Oncogenic Effects of High MAPK Activity in Colorectal Cancer Mark Progenitor Cells and Persist Irrespective of RAS Mutations. *Cancer Res*, *77*(7), 1763-1774. doi:10.1158/0008-5472.CAN-16-2821
- Blobel, C. P. (2005). ADAMs: key components in EGFR signalling and development. *Nat Rev Mol Cell Biol*, *6*(1), 32-43. doi:10.1038/nrm1548
- Boerner, J. L., Demory, M. L., Silva, C., & Parsons, S. J. (2004). Phosphorylation of Y845 on the epidermal growth factor receptor mediates binding to the mitochondrial protein cytochrome c oxidase subunit II. *Mol Cell Biol*, *24*(16), 7059-7071. doi:10.1128/MCB.24.16.7059-7071.2004
- Bonner, J. A., Harari, P. M., Giralt, J., Azarnia, N., Shin, D. M., Cohen, R. B., . . . Ang, K. K. (2006). Radiotherapy plus cetuximab for squamous-cell carcinoma of the head and neck. *N Engl J Med*, *354*(6), 567-578. doi:10.1056/NEJMoa053422
- Brabletz, T., Kalluri, R., Nieto, M. A., & Weinberg, R. A. (2018). EMT in cancer. *Nat Rev Cancer*, *18*(2), 128-134. doi:10.1038/nrc.2017.118
- Braig, F., Kriegs, M., Voigtlaender, M., Habel, B., Grob, T., Biskup, K., . . . Binder, M. (2017). Cetuximab Resistance in Head and Neck Cancer Is Mediated by

- EGFR-K521 Polymorphism. *Cancer Res*, 77(5), 1188-1199. doi:10.1158/0008-5472.CAN-16-0754
- Brown, M. S., Ye, J., Rawson, R. B., & Goldstein, J. L. (2000). Regulated intramembrane proteolysis: a control mechanism conserved from bacteria to humans. *Cell*, 100(4), 391-398.
- Buonato, J. M., Lan, I. S., & Lazzara, M. J. (2015). EGF augments TGFbeta-induced epithelial-mesenchymal transition by promoting SHP2 binding to GAB1. *J Cell Sci*, 128(21), 3898-3909. doi:10.1242/jcs.169599
- Burrell, R. A., McGranahan, N., Bartek, J., & Swanton, C. (2013). The causes and consequences of genetic heterogeneity in cancer evolution. *Nature*, 501(7467), 338-345. doi:10.1038/nature12625
- Cancer Genome Atlas, N. (2015). Comprehensive genomic characterization of head and neck squamous cell carcinomas. *Nature*, 517(7536), 576-582. doi:10.1038/nature14129
- Chandra Mangalhar, K., Manvati, S., Saini, S. K., Ponnusamy, K., Agarwal, G., Abraham, S. K., & Bamezai, R. N. K. (2017). ERK2-ZEB1-miR-101-1 axis contributes to epithelial-mesenchymal transition and cell migration in cancer. *Cancer Lett*, 391, 59-73. doi:10.1016/j.canlet.2017.01.016
- Chaves-Perez, A., Mack, B., Maetzel, D., Kremling, H., Eggert, C., Harreus, U., & Gires, O. (2013). EpCAM regulates cell cycle progression via control of cyclin D1 expression. *Oncogene*, 32(5), 641-650. doi:10.1038/onc.2012.75
- Chen, H., Zhu, G., Li, Y., Padia, R. N., Dong, Z., Pan, Z. K., . . . Huang, S. (2009). Extracellular signal-regulated kinase signaling pathway regulates breast cancer cell migration by maintaining slug expression. *Cancer Res*, 69(24), 9228-9235. doi:10.1158/0008-5472.CAN-09-1950
- Chiu, L. Y., Hsin, I. L., Yang, T. Y., Sung, W. W., Chi, J. Y., Chang, J. T., . . . Sheu, G. T. (2017). The ERK-ZEB1 pathway mediates epithelial-mesenchymal transition in pemetrexed resistant lung cancer cells with suppression by vinca alkaloids. *Oncogene*, 36(2), 242-253. doi:10.1038/onc.2016.195
- Chong, J. M., & Speicher, D. W. (2001). Determination of disulfide bond assignments and N-glycosylation sites of the human gastrointestinal carcinoma antigen GA733-2 (CO17-1A, EGP, KS1-4, KSA, and Ep-CAM). *J Biol Chem*, 276(8), 5804-5813. doi:10.1074/jbc.M008839200
- Chung, C. H., Parker, J. S., Karaca, G., Wu, J., Funkhouser, W. K., Moore, D., . . . Perou, C. M. (2004). Molecular classification of head and neck squamous cell carcinomas using patterns of gene expression. *Cancer Cell*, 5(5), 489-500.
- Ciardello, F., & Tortora, G. (2008). EGFR antagonists in cancer treatment. *N Engl J Med*, 358(11), 1160-1174. doi:10.1056/NEJMra0707704
- Cui, L., Song, J., Wu, L., Cheng, L., Chen, A., Wang, Y., . . . Huang, L. (2017). Role of Annexin A2 in the EGF-induced epithelial-mesenchymal transition in human CaSki cells. *Oncol Lett*, 13(1), 377-383. doi:10.3892/ol.2016.5406

- De Craene, B., & Berx, G. (2013). Regulatory networks defining EMT during cancer initiation and progression. *Nat Rev Cancer*, 13(2), 97-110. doi:10.1038/nrc3447
- Demontis, F., Habermann, B., & Dahmann, C. (2006). PDZ-domain-binding sites are common among cadherins. *Dev Genes Evol*, 216(11), 737-741. doi:10.1007/s00427-006-0097-0
- Denzel, S., Maetzel, D., Mack, B., Eggert, C., Barr, G., & Gires, O. (2009). Initial activation of EpCAM cleavage via cell-to-cell contact. *BMC Cancer*, 9, 402. doi:10.1186/1471-2407-9-402
- Diaz-Lopez, A., Moreno-Bueno, G., & Cano, A. (2014). Role of microRNA in epithelial to mesenchymal transition and metastasis and clinical perspectives. *Cancer Manag Res*, 6, 205-216. doi:10.2147/CMAR.S38156
- Driemel, C., Kremling, H., Schumacher, S., Will, D., Wolters, J., Lindenlauf, N., . . . Gires, O. (2014). Context-dependent adaption of EpCAM expression in early systemic esophageal cancer. *Oncogene*, 33(41), 4904-4915. doi:10.1038/onc.2013.441
- Ferguson, K. M., Darling, P. J., Mohan, M. J., Macatee, T. L., & Lemmon, M. A. (2000). Extracellular domains drive homo- but not hetero-dimerization of erbB receptors. *EMBO J*, 19(17), 4632-4643. doi:10.1093/emboj/19.17.4632
- Ferris, R. L., Blumenschein, G., Jr., Fayette, J., Guigay, J., Colevas, A. D., Licitra, L., . . . Gillison, M. L. (2016). Nivolumab for Recurrent Squamous-Cell Carcinoma of the Head and Neck. *N Engl J Med*, 375(19), 1856-1867. doi:10.1056/NEJMoa1602252
- Fong, D., Steurer, M., Obrist, P., Barbieri, V., Margreiter, R., Amberger, A., . . . Spizzo, G. (2008). Ep-CAM expression in pancreatic and ampullary carcinomas: frequency and prognostic relevance. *J Clin Pathol*, 61(1), 31-35. doi:10.1136/jcp.2006.037333
- Forster, M. D., & Devlin, M. J. (2018). Immune Checkpoint Inhibition in Head and Neck Cancer. *Front Oncol*, 8, 310. doi:10.3389/fonc.2018.00310
- Freed, D. M., Bessman, N. J., Kiyatkin, A., Salazar-Cavazos, E., Byrne, P. O., Moore, J. O., . . . Lemmon, M. A. (2017). EGFR Ligands Differentially Stabilize Receptor Dimers to Specify Signaling Kinetics. *Cell*, 171(3), 683-695 e618. doi:10.1016/j.cell.2017.09.017
- Fu, H., He, Y., Qi, L., Chen, L., Luo, Y., Chen, L., . . . Guo, H. (2017). cPLA2alpha activates PI3K/AKT and inhibits Smad2/3 during epithelial-mesenchymal transition of hepatocellular carcinoma cells. *Cancer Lett*, 403, 260-270. doi:10.1016/j.canlet.2017.06.022
- Fukuda, S., Nishida-Fukuda, H., Nanba, D., Nakashiro, K., Nakayama, H., Kubota, H., & Higashiyama, S. (2016). Reversible interconversion and maintenance of mammary epithelial cell characteristics by the ligand-regulated EGFR system. *Sci Rep*, 6, 20209. doi:10.1038/srep20209

- Gan, Y., Shi, C., Inge, L., Hibner, M., Balducci, J., & Huang, Y. (2010). Differential roles of ERK and Akt pathways in regulation of EGFR-mediated signaling and motility in prostate cancer cells. *Oncogene*, 29(35), 4947-4958. doi:10.1038/onc.2010.240
- Gao, J., Yan, Q., Wang, J., Liu, S., & Yang, X. (2015). Epithelial-to-mesenchymal transition induced by TGF-beta1 is mediated by AP1-dependent EpCAM expression in MCF-7 cells. *J Cell Physiol*, 230(4), 775-782. doi:10.1002/jcp.24802
- Gebauer, F., Struck, L., Tachezy, M., Vashist, Y., Wicklein, D., Schumacher, U., . . . Bockhorn, M. (2014). Serum EpCAM expression in pancreatic cancer. *Anticancer Res*, 34(9), 4741-4746.
- George, J. T., Jolly, M. K., Xu, S., Somarelli, J. A., & Levine, H. (2017). Survival Outcomes in Cancer Patients Predicted by a Partial EMT Gene Expression Scoring Metric. *Cancer Res*, 77(22), 6415-6428. doi:10.1158/0008-5472.CAN-16-3521
- Gerashchenko, T. S., Denisov, E. V., Litviakov, N. V., Zavyalova, M. V., Vtorushin, S. V., Tsyganov, M. M., . . . Cherdynitseva, N. V. (2013). Intratumor heterogeneity: nature and biological significance. *Biochemistry (Mosc)*, 78(11), 1201-1215. doi:10.1134/S0006297913110011
- Gires, O. (2017). EGFR-Dependent Regulated Intramembrane Proteolysis of EpCAM-Letter. *Cancer Res*, 77(7), 1775-1776. doi:10.1158/0008-5472.CAN-16-2456
- Goldberg, R. M. (2005). Cetuximab. *Nat Rev Drug Discov, Suppl*, S10-11.
- Gorges, T. M., Tinhofner, I., Drosch, M., Rose, L., Zollner, T. M., Krahn, T., & von Ahsen, O. (2012). Circulating tumour cells escape from EpCAM-based detection due to epithelial-to-mesenchymal transition. *BMC Cancer*, 12, 178. doi:10.1186/1471-2407-12-178
- Grandis, J. R., & Tweardy, D. J. (1993). Elevated levels of transforming growth factor alpha and epidermal growth factor receptor messenger RNA are early markers of carcinogenesis in head and neck cancer. *Cancer Res*, 53(15), 3579-3584.
- Grassi, M. L., Palma, C. S., Thome, C. H., Lanfredi, G. P., Poersch, A., & Faca, V. M. (2017). Proteomic analysis of ovarian cancer cells during epithelial-mesenchymal transition (EMT) induced by epidermal growth factor (EGF) reveals mechanisms of cell cycle control. *J Proteomics*, 151, 2-11. doi:10.1016/j.jprot.2016.06.009
- Grosse-Wilde, A., Fouquier d'Herouel, A., McIntosh, E., Ertaylan, G., Skupin, A., Kuestner, R. E., . . . Huang, S. (2015). Stemness of the hybrid Epithelial/Mesenchymal State in Breast Cancer and Its Association with Poor Survival. *PLoS One*, 10(5), e0126522. doi:10.1371/journal.pone.0126522
- Gunawardana, D. (2016). PDZ Binding Domains, Structural Disorder and Phosphorylation: A Menage-a-trois Tailing Dcp2 mRNA Decapping Enzymes. *Protein Pept Lett*, 23(7), 612-618.

- Hachmeister, M., Bobowski, K. D., Hognl, S., Dislich, B., Fukumori, A., Eggert, C., . . . Gires, O. (2013). Regulated intramembrane proteolysis and degradation of murine epithelial cell adhesion molecule mEpCAM. *PLoS One*, *8*(8), e71836. doi:10.1371/journal.pone.0071836
- Han, W., & Lo, H. W. (2012). Landscape of EGFR signaling network in human cancers: biology and therapeutic response in relation to receptor subcellular locations. *Cancer Lett*, *318*(2), 124-134. doi:10.1016/j.canlet.2012.01.011
- Harris, R. C., Chung, E., & Coffey, R. J. (2003). EGF receptor ligands. *Exp Cell Res*, *284*(1), 2-13.
- Herr, R., Wohrle, F. U., Danke, C., Berens, C., & Brummer, T. (2011). A novel MCF-10A line allowing conditional oncogene expression in 3D culture. *Cell Commun Signal*, *9*, 17. doi:10.1186/1478-811X-9-17
- Hiley, C., de Bruin, E. C., McGranahan, N., & Swanton, C. (2014). Deciphering intratumor heterogeneity and temporal acquisition of driver events to refine precision medicine. *Genome Biol*, *15*(8), 453. doi:10.1186/s13059-014-0453-8
- Holz, C., Niehr, F., Boyko, M., Hristozova, T., Distel, L., Budach, V., & Tinhofer, I. (2011). Epithelial-mesenchymal-transition induced by EGFR activation interferes with cell migration and response to irradiation and cetuximab in head and neck cancer cells. *Radiother Oncol*, *101*(1), 158-164. doi:10.1016/j.radonc.2011.05.042
- Hong, T., Watanabe, K., Ta, C. H., Villarreal-Ponce, A., Nie, Q., & Dai, X. (2015). An Ovnl2-Zeb1 Mutual Inhibitory Circuit Governs Bidirectional and Multi-step Transition between Epithelial and Mesenchymal States. *PLoS Comput Biol*, *11*(11), e1004569. doi:10.1371/journal.pcbi.1004569
- Hornberg, J. J., Binder, B., Bruggeman, F. J., Schoeberl, B., Heinrich, R., & Westerhoff, H. V. (2005). Control of MAPK signalling: from complexity to what really matters. *Oncogene*, *24*(36), 5533-5542. doi:10.1038/sj.onc.1208817
- Hornberg, J. J., Bruggeman, F. J., Binder, B., Geest, C. R., de Vaate, A. J., Lankelma, J., . . . Westerhoff, H. V. (2005). Principles behind the multifarious control of signal transduction. ERK phosphorylation and kinase/phosphatase control. *FEBS J*, *272*(1), 244-258. doi:10.1111/j.1432-1033.2004.04404.x
- Hsu, Y. T., Osmulski, P., Wang, Y., Huang, Y. W., Liu, L., Ruan, J., . . . Huang, T. H. (2016). EpCAM-Regulated Transcription Exerts Influences on Nanomechanical Properties of Endometrial Cancer Cells That Promote Epithelial-to-Mesenchymal Transition. *Cancer Res*, *76*(21), 6171-6182. doi:10.1158/0008-5472.CAN-16-0752
- Huang, R. Y., Wong, M. K., Tan, T. Z., Kuay, K. T., Ng, A. H., Chung, V. Y., . . . Thiery, J. P. (2013). An EMT spectrum defines an anoikis-resistant and spheroidogenic intermediate mesenchymal state that is sensitive to e-cadherin restoration by a src-kinase inhibitor, saracatinib (AZD0530). *Cell Death Dis*, *4*, e915. doi:10.1038/cddis.2013.442

- Huang, Y., Chanou, A., Kranz, G., Pan, M., Kohlbauer, V., Ettinger, A., & Gires, O. (2019). Membrane-associated epithelial cell adhesion molecule is slowly cleaved by gamma-secretase prior to efficient proteasomal degradation of its intracellular domain. *J Biol Chem*, 294(9), 3051-3064. doi:10.1074/jbc.RA118.005874
- Hynes, N. E., & Lane, H. A. (2005). ERBB receptors and cancer: the complexity of targeted inhibitors. *Nat Rev Cancer*, 5(5), 341-354. doi:10.1038/nrc1609
- Hyun, K. A., Koo, G. B., Han, H., Sohn, J., Choi, W., Kim, S. I., . . . Kim, Y. S. (2016). Epithelial-to-mesenchymal transition leads to loss of EpCAM and different physical properties in circulating tumor cells from metastatic breast cancer. *Oncotarget*, 7(17), 24677-24687. doi:10.18632/oncotarget.8250
- Ichikawa, K., Kubota, Y., Nakamura, T., Weng, J. S., Tomida, T., Saito, H., & Takekawa, M. (2015). MCRIP1, an ERK substrate, mediates ERK-induced gene silencing during epithelial-mesenchymal transition by regulating the co-repressor CtBP. *Mol Cell*, 58(1), 35-46. doi:10.1016/j.molcel.2015.01.023
- Irwin, M. E., Mueller, K. L., Bohin, N., Ge, Y., & Boerner, J. L. (2011). Lipid raft localization of EGFR alters the response of cancer cells to the EGFR tyrosine kinase inhibitor gefitinib. *J Cell Physiol*, 226(9), 2316-2328. doi:10.1002/jcp.22570
- Janda, E., Lehmann, K., Killisch, I., Jechlinger, M., Herzig, M., Downward, J., . . . Grunert, S. (2002). Ras and TGF[beta] cooperatively regulate epithelial cell plasticity and metastasis: dissection of Ras signaling pathways. *J Cell Biol*, 156(2), 299-313. doi:10.1083/jcb.200109037
- Jolly, M. K., Tripathi, S. C., Jia, D., Mooney, S. M., Celiktas, M., Hanash, S. M., . . . Levine, H. (2016). Stability of the hybrid epithelial/mesenchymal phenotype. *Oncotarget*, 7(19), 27067-27084. doi:10.18632/oncotarget.8166
- Kalyankrishna, S., & Grandis, J. R. (2006). Epidermal growth factor receptor biology in head and neck cancer. *J Clin Oncol*, 24(17), 2666-2672. doi:10.1200/JCO.2005.04.8306
- Kimura, H., Kato, H., Faried, A., Sohda, M., Nakajima, M., Fukai, Y., . . . Kuwano, H. (2007). Prognostic significance of EpCAM expression in human esophageal cancer. *Int J Oncol*, 30(1), 171-179.
- Kovacs, E., Zorn, J. A., Huang, Y., Barros, T., & Kuriyan, J. (2015). A structural perspective on the regulation of the epidermal growth factor receptor. *Annu Rev Biochem*, 84, 739-764. doi:10.1146/annurev-biochem-060614-034402
- Kuan, II, Lee, C. C., Chen, C. H., Lu, J., Kuo, Y. S., & Wu, H. C. (2019). The extracellular domain of epithelial cell adhesion molecule (EPCAM) enhances multipotency of mesenchymal stem cells through EGFR-LIN28-LET7 signaling. *J Biol Chem*. doi:10.1074/jbc.RA119.007386
- Kuan, II, Liang, K. H., Wang, Y. P., Kuo, T. W., Meir, Y. J., Wu, S. C., . . . Wu, H. C. (2017). EpEX/EpCAM and Oct4 or Klf4 alone are sufficient to generate induced

- pluripotent stem cells through STAT3 and HIF2alpha. *Sci Rep*, 7, 41852. doi:10.1038/srep41852
- Lambert, A. W., Pattabiraman, D. R., & Weinberg, R. A. (2017). Emerging Biological Principles of Metastasis. *Cell*, 168(4), 670-691. doi:10.1016/j.cell.2016.11.037
- Lamouille, S., Xu, J., & Derynck, R. (2014). Molecular mechanisms of epithelial-mesenchymal transition. *Nat Rev Mol Cell Biol*, 15(3), 178-196. doi:10.1038/nrm3758
- Leemans, C. R., Braakhuis, B. J., & Brakenhoff, R. H. (2011). The molecular biology of head and neck cancer. *Nat Rev Cancer*, 11(1), 9-22. doi:10.1038/nrc2982
- Leemans, C. R., Snijders, P. J. F., & Brakenhoff, R. H. (2018). The molecular landscape of head and neck cancer. *Nat Rev Cancer*, 18(5), 269-282. doi:10.1038/nrc.2018.11
- Lemieux, E., Bergeron, S., Durand, V., Asselin, C., Saucier, C., & Rivard, N. (2009). Constitutively active MEK1 is sufficient to induce epithelial-to-mesenchymal transition in intestinal epithelial cells and to promote tumor invasion and metastasis. *Int J Cancer*, 125(7), 1575-1586. doi:10.1002/ijc.24485
- Lemmon, M. A., Freed, D. M., Schlessinger, J., & Kiyatkin, A. (2016). The Dark Side of Cell Signaling: Positive Roles for Negative Regulators. *Cell*, 164(6), 1172-1184. doi:10.1016/j.cell.2016.02.047
- Lemmon, M. A., Schlessinger, J., & Ferguson, K. M. (2014). The EGFR family: not so prototypical receptor tyrosine kinases. *Cold Spring Harb Perspect Biol*, 6(4), a020768. doi:10.1101/cshperspect.a020768
- Li, J., Shan, F., Xiong, G., Chen, X., Guan, X., Wang, J. M., . . . Bai, Y. (2014). EGF-induced C/EBPbeta participates in EMT by decreasing the expression of miR-203 in esophageal squamous cell carcinoma cells. *J Cell Sci*, 127(Pt 17), 3735-3744. doi:10.1242/jcs.148759
- Li, Y., Lin, Z., Chen, B., Chen, S., Jiang, Z., Zhou, T., . . . Wang, Y. (2017). Ezrin/NF-kB activation regulates epithelial- mesenchymal transition induced by EGF and promotes metastasis of colorectal cancer. *Biomed Pharmacother*, 92, 140-148. doi:10.1016/j.biopha.2017.05.058
- Liang, K. H., Tso, H. C., Hung, S. H., Kuan, I., Lai, J. K., Ke, F. Y., . . . Wu, H. C. (2018). Extracellular domain of EpCAM enhances tumor progression through EGFR signaling in colon cancer cells. *Cancer Lett*, 433, 165-175. doi:10.1016/j.canlet.2018.06.040
- Lin, C. W., Liao, M. Y., Lin, W. W., Wang, Y. P., Lu, T. Y., & Wu, H. C. (2012). Epithelial cell adhesion molecule regulates tumor initiation and tumorigenesis via activating reprogramming factors and epithelial-mesenchymal transition gene expression in colon cancer. *J Biol Chem*, 287(47), 39449-39459. doi:10.1074/jbc.M112.386235
- Litvinov, S. V., Bakker, H. A., Gourevitch, M. M., Velders, M. P., & Warnaar, S. O. (1994). Evidence for a role of the epithelial glycoprotein 40 (Ep-CAM) in epithelial cell-cell adhesion. *Cell Adhes Commun*, 2(5), 417-428.

- Liu, A., Garg, P., Yang, S., Gong, P., Pallero, M. A., Annis, D. S., . . . Goldblum, S. E. (2009). Epidermal growth factor-like repeats of thrombospondins activate phospholipase C γ and increase epithelial cell migration through indirect epidermal growth factor receptor activation. *J Biol Chem*, *284*(10), 6389-6402. doi:10.1074/jbc.M809198200
- Lu, T. Y., Lu, R. M., Liao, M. Y., Yu, J., Chung, C. H., Kao, C. F., & Wu, H. C. (2010). Epithelial cell adhesion molecule regulation is associated with the maintenance of the undifferentiated phenotype of human embryonic stem cells. *J Biol Chem*, *285*(12), 8719-8732. doi:10.1074/jbc.M109.077081
- Lydiatt, W. M., Patel, S. G., O'Sullivan, B., Brandwein, M. S., Ridge, J. A., Migliacci, J. C., . . . Shah, J. P. (2017). Head and Neck cancers-major changes in the American Joint Committee on cancer eighth edition cancer staging manual. *CA Cancer J Clin*, *67*(2), 122-137. doi:10.3322/caac.21389
- Mack, B., & Gires, O. (2008). CD44s and CD44v6 expression in head and neck epithelia. *PLoS One*, *3*(10), e3360. doi:10.1371/journal.pone.0003360
- Maetzel, D., Denzel, S., Mack, B., Canis, M., Went, P., Benk, M., . . . Gires, O. (2009). Nuclear signalling by tumour-associated antigen EpCAM. *Nat Cell Biol*, *11*(2), 162-171. doi:10.1038/ncb1824
- Makrodouli, E., Oikonomou, E., Koc, M., Andera, L., Sasazuki, T., Shirasawa, S., & Pintzas, A. (2011). BRAF and RAS oncogenes regulate Rho GTPase pathways to mediate migration and invasion properties in human colon cancer cells: a comparative study. *Mol Cancer*, *10*, 118. doi:10.1186/1476-4598-10-118
- Maramotti, S., Paci, M., Micciche, F., Ciarrocchi, A., Cavazza, A., De Bortoli, M., . . . Bongarzone, I. (2012). Soluble epidermal growth factor receptor isoforms in non-small cell lung cancer tissue and in blood. *Lung Cancer*, *76*(3), 332-338. doi:10.1016/j.lungcan.2011.11.018
- Marshall, C. J. (1995). Specificity of receptor tyrosine kinase signaling: transient versus sustained extracellular signal-regulated kinase activation. *Cell*, *80*(2), 179-185.
- Massoner, P., Thomm, T., Mack, B., Untergasser, G., Martowicz, A., Bobowski, K., . . . Puhr, M. (2014). EpCAM is overexpressed in local and metastatic prostate cancer, suppressed by chemotherapy and modulated by MET-associated miRNA-200c/205. *Br J Cancer*, *111*(5), 955-964. doi:10.1038/bjc.2014.366
- McCarthy, A. J., Coleman-Vaughan, C., & McCarthy, J. V. (2017). Regulated intramembrane proteolysis: emergent role in cell signalling pathways. *Biochem Soc Trans*, *45*(6), 1185-1202. doi:10.1042/BST20170002
- Molinolo, A. A., Amornphimoltham, P., Squarize, C. H., Castilho, R. M., Patel, V., & Gutkind, J. S. (2009). Dysregulated molecular networks in head and neck carcinogenesis. *Oral Oncol*, *45*(4-5), 324-334. doi:10.1016/j.oraloncology.2008.07.011
- Montal, R., Oliva, M., Taberna, M., De Avila, L., Rovira, A., Cos, M., . . . Mesia, R. (2016). Residual neck disease management in squamous-cell carcinoma of the

- head and neck treated with radiotherapy plus cetuximab. *Clin Transl Oncol*, 18(11), 1140-1146. doi:10.1007/s12094-016-1496-y
- Mroz, E. A., Tward, A. D., Hammon, R. J., Ren, Y., & Rocco, J. W. (2015). Intra-tumor genetic heterogeneity and mortality in head and neck cancer: analysis of data from the Cancer Genome Atlas. *PLoS Med*, 12(2), e1001786. doi:10.1371/journal.pmed.1001786
- Mroz, E. A., Tward, A. D., Pickering, C. R., Myers, J. N., Ferris, R. L., & Rocco, J. W. (2013). High intratumor genetic heterogeneity is related to worse outcome in patients with head and neck squamous cell carcinoma. *Cancer*, 119(16), 3034-3042. doi:10.1002/cncr.28150
- Munz, M., Fellingner, K., Hofmann, T., Schmitt, B., & Gires, O. (2008). Glycosylation is crucial for stability of tumour and cancer stem cell antigen EpCAM. *Front Biosci*, 13, 5195-5201.
- Munz, M., Murr, A., Kvesic, M., Rau, D., Mangold, S., Pflanz, S., . . . Raum, T. (2010). Side-by-side analysis of five clinically tested anti-EpCAM monoclonal antibodies. *Cancer Cell Int*, 10, 44. doi:10.1186/1475-2867-10-44
- Murphy, L. O., Smith, S., Chen, R. H., Fingar, D. C., & Blenis, J. (2002). Molecular interpretation of ERK signal duration by immediate early gene products. *Nat Cell Biol*, 4(8), 556-564. doi:10.1038/ncb822
- Murugaesu, N., Chew, S. K., & Swanton, C. (2013). Adapting clinical paradigms to the challenges of cancer clonal evolution. *Am J Pathol*, 182(6), 1962-1971. doi:10.1016/j.ajpath.2013.02.026
- Muthusami, S., Prabakaran, D. S., Yu, J. R., & Park, W. Y. (2014). EGF-induced expression of Fused Toes Homolog (FTS) facilitates epithelial-mesenchymal transition and promotes cell migration in ME180 cervical cancer cells. *Cancer Lett*, 351(2), 252-259. doi:10.1016/j.canlet.2014.06.007
- Nagai, T., Arai, T., Furuta, K., Sakai, K., Kudo, K., Kaneda, H., . . . Nishio, K. (2011). Sorafenib inhibits the hepatocyte growth factor-mediated epithelial mesenchymal transition in hepatocellular carcinoma. *Mol Cancer Ther*, 10(1), 169-177. doi:10.1158/1535-7163.MCT-10-0544
- Nieto, M. A., Huang, R. Y., Jackson, R. A., & Thiery, J. P. (2016). EMT: 2016. *Cell*, 166(1), 21-45. doi:10.1016/j.cell.2016.06.028
- Nubel, T., Preobraschenski, J., Tuncay, H., Weiss, T., Kuhn, S., Ladwein, M., . . . Zoller, M. (2009). Claudin-7 regulates EpCAM-mediated functions in tumor progression. *Mol Cancer Res*, 7(3), 285-299. doi:10.1158/1541-7786.MCR-08-0200
- O'Sullivan, B., Huang, S. H., Su, J., Garden, A. S., Sturgis, E. M., Dahlstrom, K., . . . Xu, W. (2016). Development and validation of a staging system for HPV-related oropharyngeal cancer by the International Collaboration on Oropharyngeal cancer Network for Staging (ICON-S): a multicentre cohort study. *Lancet Oncol*, 17(4), 440-451. doi:10.1016/S1470-2045(15)00560-4

- Ocana, O. H., Corcoles, R., Fabra, A., Moreno-Bueno, G., Acloque, H., Vega, S., . . . Nieto, M. A. (2012). Metastatic colonization requires the repression of the epithelial-mesenchymal transition inducer Prrx1. *Cancer Cell*, 22(6), 709-724. doi:10.1016/j.ccr.2012.10.012
- Ongkeko, W. M., Altuna, X., Weisman, R. A., & Wang-Rodriguez, J. (2005). Expression of protein tyrosine kinases in head and neck squamous cell carcinomas. *Am J Clin Pathol*, 124(1), 71-76. doi:10.1309/BTLN5WTMJ3PCNRRC
- Pan, M., Schinke, H., Luxenburger, E., Kranz, G., Shakhtour, J., Libl, D., . . . Gires, O. (2018). EpCAM ectodomain EpEX is a ligand of EGFR that counteracts EGF-mediated epithelial-mesenchymal transition through modulation of phospho-ERK1/2 in head and neck cancers. *PLoS Biol*, 16(9), e2006624. doi:10.1371/journal.pbio.2006624
- Parkin, D. M., Bray, F., Ferlay, J., & Pisani, P. (2005). Global cancer statistics, 2002. *CA Cancer J Clin*, 55(2), 74-108.
- Pastushenko, I., Brisebarre, A., Sifrim, A., Fioramonti, M., Revenco, T., Boumahdi, S., . . . Blanpain, C. (2018). Identification of the tumour transition states occurring during EMT. *Nature*, 556(7702), 463-468. doi:10.1038/s41586-018-0040-3
- Patriarca, C., Macchi, R. M., Marschner, A. K., & Mellstedt, H. (2012). Epithelial cell adhesion molecule expression (CD326) in cancer: a short review. *Cancer Treat Rev*, 38(1), 68-75. doi:10.1016/j.ctrv.2011.04.002
- Pauli, C., Munz, M., Kieu, C., Mack, B., Breinl, P., Wollenberg, B., . . . Gires, O. (2003). Tumor-specific glycosylation of the carcinoma-associated epithelial cell adhesion molecule EpCAM in head and neck carcinomas. *Cancer Lett*, 193(1), 25-32.
- Pavsic, M., Guncar, G., Djinic-Carugo, K., & Lenarcic, B. (2014). Crystal structure and its bearing towards an understanding of key biological functions of EpCAM. *Nat Commun*, 5, 4764. doi:10.1038/ncomms5764
- Pei, D., Shu, X., Gassama-Diagne, A., & Thiery, J. P. (2019). Mesenchymal-epithelial transition in development and reprogramming. *Nat Cell Biol*, 21(1), 44-53. doi:10.1038/s41556-018-0195-z
- Perez-Torres, M., Valle, B. L., Maihle, N. J., Negron-Vega, L., Nieves-Alicea, R., & Cora, E. M. (2008). Shedding of epidermal growth factor receptor is a regulated process that occurs with overexpression in malignant cells. *Exp Cell Res*, 314(16), 2907-2918. doi:10.1016/j.yexcr.2008.07.013
- Petsch, S., Gires, O., Ruttinger, D., Denzel, S., Lippold, S., Baeuerle, P. A., & Wolf, A. (2011). Concentrations of EpCAM ectodomain as found in sera of cancer patients do not significantly impact redirected lysis and T-cell activation by EpCAM/CD3-bispecific BiTE antibody MT110. *MAbs*, 3(1), 31-37.

- Price, K. A., & Cohen, E. E. (2012). Current treatment options for metastatic head and neck cancer. *Curr Treat Options Oncol*, *13*(1), 35-46. doi:10.1007/s11864-011-0176-y
- Psyrrri, A., Yu, Z., Weinberger, P. M., Sasaki, C., Haffty, B., Camp, R., . . . Burtneess, B. A. (2005). Quantitative determination of nuclear and cytoplasmic epidermal growth factor receptor expression in oropharyngeal squamous cell cancer by using automated quantitative analysis. *Clin Cancer Res*, *11*(16), 5856-5862. doi:10.1158/1078-0432.CCR-05-0420
- Puisieux, A., Brabletz, T., & Caramel, J. (2014). Oncogenic roles of EMT-inducing transcription factors. *Nat Cell Biol*, *16*(6), 488-494. doi:10.1038/ncb2976
- Puram, S. V., Tirosh, I., Parikh, A. S., Patel, A. P., Yizhak, K., Gillespie, S., . . . Bernstein, B. E. (2017). Single-Cell Transcriptomic Analysis of Primary and Metastatic Tumor Ecosystems in Head and Neck Cancer. *Cell*, *171*(7), 1611-1624 e1624. doi:10.1016/j.cell.2017.10.044
- Ralhan, R., Cao, J., Lim, T., Macmillan, C., Freeman, J. L., & Walfish, P. G. (2010). EpCAM nuclear localization identifies aggressive thyroid cancer and is a marker for poor prognosis. *BMC Cancer*, *10*, 331. doi:10.1186/1471-2407-10-331
- Rauch, N., Rukhlenko, O. S., Kolch, W., & Kholodenko, B. N. (2016). MAPK kinase signalling dynamics regulate cell fate decisions and drug resistance. *Curr Opin Struct Biol*, *41*, 151-158. doi:10.1016/j.sbi.2016.07.019
- Riesenberg, R., Buchner, A., Pohla, H., & Lindhofer, H. (2001). Lysis of prostate carcinoma cells by trifunctional bispecific antibodies (alpha EpCAM x alpha CD3). *J Histochem Cytochem*, *49*(7), 911-917. doi:10.1177/002215540104900711
- Ronan, T., Macdonald-Obermann, J. L., Huelsmann, L., Bessman, N. J., Naegle, K. M., & Pike, L. J. (2016). Different Epidermal Growth Factor Receptor (EGFR) Agonists Produce Unique Signatures for the Recruitment of Downstream Signaling Proteins. *J Biol Chem*, *291*(11), 5528-5540. doi:10.1074/jbc.M115.710087
- Ryu, H., Chung, M., Dobrzynski, M., Fey, D., Blum, Y., Lee, S. S., . . . Pertz, O. (2015). Frequency modulation of ERK activation dynamics rewires cell fate. *Mol Syst Biol*, *11*(11), 838. doi:10.15252/msb.20156458
- Saada-Bouazid, E., Peyrade, F., & Guigay, J. (2019). Immunotherapy in recurrent and or metastatic squamous cell carcinoma of the head and neck. *Curr Opin Oncol*. doi:10.1097/CCO.0000000000000522
- Said, N. A., & Williams, E. D. (2011). Growth factors in induction of epithelial-mesenchymal transition and metastasis. *Cells Tissues Organs*, *193*(1-2), 85-97. doi:10.1159/000320360
- Saito, N., Mine, N., Kufe, D. W., Von Hoff, D. D., & Kawabe, T. (2017). CBP501 inhibits EGF-dependent cell migration, invasion and epithelial-to-mesenchymal

- transition of non-small cell lung cancer cells by blocking KRas to calmodulin binding. *Oncotarget*, 8(43), 74006-74018. doi:10.18632/oncotarget.18598
- Sankpal, N. V., Fleming, T. P., Sharma, P. K., Wiedner, H. J., & Gillanders, W. E. (2017). A double-negative feedback loop between EpCAM and ERK contributes to the regulation of epithelial-mesenchymal transition in cancer. *Oncogene*, 36(26), 3706-3717. doi:10.1038/onc.2016.504
- Santos, S. D., Verveer, P. J., & Bastiaens, P. I. (2007). Growth factor-induced MAPK network topology shapes Erk response determining PC-12 cell fate. *Nat Cell Biol*, 9(3), 324-330. doi:10.1038/ncb1543
- Sarrach, S., Huang, Y., Niedermeyer, S., Hachmeister, M., Fischer, L., Gille, S., . . . Gires, O. (2018). Spatiotemporal patterning of EpCAM is important for murine embryonic endo- and mesodermal differentiation. *Sci Rep*, 8(1), 1801. doi:10.1038/s41598-018-20131-8
- Schilling, C., Stoeckli, S. J., Haerle, S. K., Broglie, M. A., Huber, G. F., Sorensen, J. A., . . . McGurk, M. (2015). Sentinel European Node Trial (SENT): 3-year results of sentinel node biopsy in oral cancer. *Eur J Cancer*, 51(18), 2777-2784. doi:10.1016/j.ejca.2015.08.023
- Schnell, U., Cirulli, V., & Giepmans, B. N. (2013). EpCAM: structure and function in health and disease. *Biochim Biophys Acta*, 1828(8), 1989-2001. doi:10.1016/j.bbamem.2013.04.018
- Seeber, A., Untergasser, G., Spizzo, G., Terracciano, L., Lugli, A., Kasal, A., . . . Fong, D. (2016). Predominant expression of truncated EpCAM is associated with a more aggressive phenotype and predicts poor overall survival in colorectal cancer. *Int J Cancer*, 139(3), 657-663. doi:10.1002/ijc.30099
- Seiwert, T. Y., Burtness, B., Mehra, R., Weiss, J., Berger, R., Eder, J. P., . . . Chow, L. Q. (2016). Safety and clinical activity of pembrolizumab for treatment of recurrent or metastatic squamous cell carcinoma of the head and neck (KEYNOTE-012): an open-label, multicentre, phase 1b trial. *Lancet Oncol*, 17(7), 956-965. doi:10.1016/S1470-2045(16)30066-3
- Seligson, D. B., Pantuck, A. J., Liu, X., Huang, Y., Horvath, S., Bui, M. H., . . . Figlin, R. A. (2004). Epithelial cell adhesion molecule (KSA) expression: pathobiology and its role as an independent predictor of survival in renal cell carcinoma. *Clin Cancer Res*, 10(8), 2659-2669.
- Sheng, W., Chen, C., Dong, M., Wang, G., Zhou, J., Song, H., . . . Ding, S. (2017). Calreticulin promotes EGF-induced EMT in pancreatic cancer cells via Integrin/EGFR-ERK/MAPK signaling pathway. *Cell Death Dis*, 8(10), e3147. doi:10.1038/cddis.2017.547
- Shin, D. M., Ro, J. Y., Hong, W. K., & Hittelman, W. N. (1994). Dysregulation of epidermal growth factor receptor expression in premalignant lesions during head and neck tumorigenesis. *Cancer Res*, 54(12), 3153-3159.
- Shin, S., Dimitri, C. A., Yoon, S. O., Dowdle, W., & Blenis, J. (2010). ERK2 but not ERK1 induces epithelial-to-mesenchymal transformation via DEF motif-

- dependent signaling events. *Mol Cell*, 38(1), 114-127. doi:10.1016/j.molcel.2010.02.020
- Shirakihara, T., Horiguchi, K., Miyazawa, K., Ehata, S., Shibata, T., Morita, I., . . . Saitoh, M. (2011). TGF-beta regulates isoform switching of FGF receptors and epithelial-mesenchymal transition. *EMBO J*, 30(4), 783-795. doi:10.1038/emboj.2010.351
- Slanchev, K., Carney, T. J., Stemmler, M. P., Koschorz, B., Amsterdam, A., Schwarz, H., & Hammerschmidt, M. (2009). The epithelial cell adhesion molecule EpCAM is required for epithelial morphogenesis and integrity during zebrafish epiboly and skin development. *PLoS Genet*, 5(7), e1000563. doi:10.1371/journal.pgen.1000563
- Spizzo, G., Obrist, P., Ensinger, C., Theurl, I., Dunser, M., Ramoni, A., . . . Gastl, G. (2002). Prognostic significance of Ep-CAM AND Her-2/neu overexpression in invasive breast cancer. *Int J Cancer*, 98(6), 883-888.
- Spizzo, G., Went, P., Dirnhofer, S., Obrist, P., Moch, H., Baeuerle, P. A., . . . Zeimet, A. G. (2006). Overexpression of epithelial cell adhesion molecule (Ep-CAM) is an independent prognostic marker for reduced survival of patients with epithelial ovarian cancer. *Gynecol Oncol*, 103(2), 483-488. doi:10.1016/j.ygyno.2006.03.035
- Spizzo, G., Went, P., Dirnhofer, S., Obrist, P., Simon, R., Spichtin, H., . . . Gastl, G. (2004). High Ep-CAM expression is associated with poor prognosis in node-positive breast cancer. *Breast Cancer Res Treat*, 86(3), 207-213. doi:10.1023/B:BREA.0000036787.59816.01
- Stoecklein, N. H., Siegmund, A., Scheunemann, P., Luebke, A. M., Erbersdobler, A., Verde, P. E., . . . Hosch, S. B. (2006). Ep-CAM expression in squamous cell carcinoma of the esophagus: a potential therapeutic target and prognostic marker. *BMC Cancer*, 6, 165. doi:10.1186/1471-2407-6-165
- Stransky, N., Egloff, A. M., Tward, A. D., Kostic, A. D., Cibulskis, K., Sivachenko, A., . . . Grandis, J. R. (2011). The mutational landscape of head and neck squamous cell carcinoma. *Science*, 333(6046), 1157-1160. doi:10.1126/science.1208130
- Swindle, C. S., Tran, K. T., Johnson, T. D., Banerjee, P., Mayes, A. M., Griffith, L., & Wells, A. (2001). Epidermal growth factor (EGF)-like repeats of human tenascin-C as ligands for EGF receptor. *J Cell Biol*, 154(2), 459-468.
- Tam, W. L., & Weinberg, R. A. (2013). The epigenetics of epithelial-mesenchymal plasticity in cancer. *Nat Med*, 19(11), 1438-1449. doi:10.1038/nm.3336
- Tashiro, E., Henmi, S., Otake, H., Ino, S., & Imoto, M. (2016). Involvement of the MEK/ERK pathway in EGF-induced E-cadherin down-regulation. *Biochem Biophys Res Commun*, 477(4), 801-806. doi:10.1016/j.bbrc.2016.06.138
- Thiery, J. P., Acloque, H., Huang, R. Y., & Nieto, M. A. (2009). Epithelial-mesenchymal transitions in development and disease. *Cell*, 139(5), 871-890. doi:10.1016/j.cell.2009.11.007

- Toh, B., Wang, X., Keeble, J., Sim, W. J., Khoo, K., Wong, W. C., . . . Abastado, J. P. (2011). Mesenchymal transition and dissemination of cancer cells is driven by myeloid-derived suppressor cells infiltrating the primary tumor. *PLoS Biol*, *9*(9), e1001162. doi:10.1371/journal.pbio.1001162
- Trebak, M., Begg, G. E., Chong, J. M., Kanazireva, E. V., Herlyn, D., & Speicher, D. W. (2001). Oligomeric state of the colon carcinoma-associated glycoprotein GA733-2 (Ep-CAM/EGP40) and its role in GA733-mediated homotypic cell-cell adhesion. *J Biol Chem*, *276*(3), 2299-2309. doi:10.1074/jbc.M004770200
- Trivedi, S., Rosen, C. A., & Ferris, R. L. (2016). Current understanding of the tumor microenvironment of laryngeal dysplasia and progression to invasive cancer. *Curr Opin Otolaryngol Head Neck Surg*, *24*(2), 121-127. doi:10.1097/MOO.0000000000000245
- Tsaktanis, T., Kremling, H., Pavsic, M., von Stackelberg, R., Mack, B., Fukumori, A., . . . Gires, O. (2015). Cleavage and cell adhesion properties of human epithelial cell adhesion molecule (HEPCAM). *J Biol Chem*, *290*(40), 24574-24591. doi:10.1074/jbc.M115.662700
- van der Gun, B. T., Melchers, L. J., Ruiters, M. H., de Leij, L. F., McLaughlin, P. M., & Rots, M. G. (2010). EpCAM in carcinogenesis: the good, the bad or the ugly. *Carcinogenesis*, *31*(11), 1913-1921. doi:10.1093/carcin/bgq187
- Vannier, C., Mock, K., Brabletz, T., & Driever, W. (2013). Zeb1 regulates E-cadherin and Epcam (epithelial cell adhesion molecule) expression to control cell behavior in early zebrafish development. *J Biol Chem*, *288*(26), 18643-18659. doi:10.1074/jbc.M113.467787
- Varga, M., Obrist, P., Schneeberger, S., Muhlmann, G., Felgel-Farnholz, C., Fong, D., . . . Spizzo, G. (2004). Overexpression of epithelial cell adhesion molecule antigen in gallbladder carcinoma is an independent marker for poor survival. *Clin Cancer Res*, *10*(9), 3131-3136.
- Vergara, D., Valente, C. M., Tinelli, A., Siciliano, C., Lorusso, V., Acierno, R., . . . Maffia, M. (2011). Resveratrol inhibits the epidermal growth factor-induced epithelial mesenchymal transition in MCF-7 cells. *Cancer Lett*, *310*(1), 1-8. doi:10.1016/j.canlet.2011.04.009
- Voisin, L., Julien, C., Duhamel, S., Gopalbhai, K., Claveau, I., Saba-EI-Leil, M. K., . . . Meloche, S. (2008). Activation of MEK1 or MEK2 isoform is sufficient to fully transform intestinal epithelial cells and induce the formation of metastatic tumors. *BMC Cancer*, *8*, 337. doi:10.1186/1471-2407-8-337
- Wang, M. H., Sun, R., Zhou, X. M., Zhang, M. Y., Lu, J. B., Yang, Y., . . . Mai, S. J. (2018). Epithelial cell adhesion molecule overexpression regulates epithelial-mesenchymal transition, stemness and metastasis of nasopharyngeal carcinoma cells via the PTEN/AKT/mTOR pathway. *Cell Death Dis*, *9*(1), 2. doi:10.1038/s41419-017-0013-8

- Wang, P., Ma, M., & Zhang, S. (2017). EGF-induced urokinase plasminogen activator receptor promotes epithelial to mesenchymal transition in human gastric cancer cells. *Oncol Rep*, 38(4), 2325-2334. doi:10.3892/or.2017.5920
- Wang, Y. N., Lee, H. H., Lee, H. J., Du, Y., Yamaguchi, H., & Hung, M. C. (2012). Membrane-bound trafficking regulates nuclear transport of integral epidermal growth factor receptor (EGFR) and ErbB-2. *J Biol Chem*, 287(20), 16869-16879. doi:10.1074/jbc.M111.314799
- Warzecha, C. C., & Carstens, R. P. (2012). Complex changes in alternative pre-mRNA splicing play a central role in the epithelial-to-mesenchymal transition (EMT). *Semin Cancer Biol*, 22(5-6), 417-427. doi:10.1016/j.semcancer.2012.04.003
- Went, P., Dirnhofer, S., Salvisberg, T., Amin, M. B., Lim, S. D., Diener, P. A., & Moch, H. (2005). Expression of epithelial cell adhesion molecule (EpCam) in renal epithelial tumors. *Am J Surg Pathol*, 29(1), 83-88.
- Went, P., Vasei, M., Bubendorf, L., Terracciano, L., Tornillo, L., Riede, U., . . . Baeuerle, P. A. (2006). Frequent high-level expression of the immunotherapeutic target Ep-CAM in colon, stomach, prostate and lung cancers. *Br J Cancer*, 94(1), 128-135. doi:10.1038/sj.bjc.6602924
- Wilken, J. A., Perez-Torres, M., Nieves-Alicea, R., Cora, E. M., Christensen, T. A., Baron, A. T., & Maihle, N. J. (2013). Shedding of soluble epidermal growth factor receptor (sEGFR) is mediated by a metalloprotease/fibronectin/integrin axis and inhibited by cetuximab. *Biochemistry*, 52(26), 4531-4540. doi:10.1021/bi400437d
- Xie, L., Law, B. K., Chytil, A. M., Brown, K. A., Aakre, M. E., & Moses, H. L. (2004). Activation of the Erk pathway is required for TGF-beta1-induced EMT in vitro. *Neoplasia*, 6(5), 603-610. doi:10.1593/neo.04241
- Xu, Q., Zhang, Q., Ishida, Y., Hajjar, S., Tang, X., Shi, H., . . . Le, A. D. (2017). EGF induces epithelial-mesenchymal transition and cancer stem-like cell properties in human oral cancer cells via promoting Warburg effect. *Oncotarget*, 8(6), 9557-9571. doi:10.18632/oncotarget.13771
- Xue, L., Su, D., Li, D., Gao, W., Yuan, R., & Pang, W. (2015). MiR-200 Regulates Epithelial-Mesenchymal Transition in Anaplastic Thyroid Cancer via EGF/EGFR Signaling. *Cell Biochem Biophys*, 72(1), 185-190. doi:10.1007/s12013-014-0435-1
- Yamashita, N., Tokunaga, E., Iimori, M., Inoue, Y., Tanaka, K., Kitao, H., . . . Maehara, Y. (2018). Epithelial Paradox: Clinical Significance of Coexpression of E-cadherin and Vimentin With Regard to Invasion and Metastasis of Breast Cancer. *Clin Breast Cancer*, 18(5), e1003-e1009. doi:10.1016/j.clbc.2018.02.002
- Yarden, Y., & Sliwkowski, M. X. (2001). Untangling the ErbB signalling network. *Nat Rev Mol Cell Biol*, 2(2), 127-137. doi:10.1038/35052073

- Ye, X., Tam, W. L., Shibue, T., Kaygusuz, Y., Reinhardt, F., Ng Eaton, E., & Weinberg, R. A. (2015). Distinct EMT programs control normal mammary stem cells and tumour-initiating cells. *Nature*, *525*(7568), 256-260. doi:10.1038/nature14897
- Yu, M., Bardia, A., Wittner, B. S., Stott, S. L., Smas, M. E., Ting, D. T., . . . Maheswaran, S. (2013). Circulating breast tumor cells exhibit dynamic changes in epithelial and mesenchymal composition. *Science*, *339*(6119), 580-584. doi:10.1126/science.1228522
- Zhang, J., Tian, X. J., Zhang, H., Teng, Y., Li, R., Bai, F., . . . Xing, J. (2014). TGF-beta-induced epithelial-to-mesenchymal transition proceeds through stepwise activation of multiple feedback loops. *Sci Signal*, *7*(345), ra91. doi:10.1126/scisignal.2005304
- Zhang, Y., Du, J., Zheng, J., Liu, J., Xu, R., Shen, T., . . . Gu, L. (2015). EGF-reduced Wnt5a transcription induces epithelial-mesenchymal transition via Arf6-ERK signaling in gastric cancer cells. *Oncotarget*, *6*(9), 7244-7261. doi:10.18632/oncotarget.3133
- Zhang, Z., Dong, Z., Lauxen, I. S., Filho, M. S., & Nor, J. E. (2014). Endothelial cell-secreted EGF induces epithelial to mesenchymal transition and endows head and neck cancer cells with stem-like phenotype. *Cancer Res*, *74*(10), 2869-2881. doi:10.1158/0008-5472.CAN-13-2032
- Zhu, H., Cao, X., Ali-Osman, F., Keir, S., & Lo, H. W. (2010). EGFR and EGFRvIII interact with PUMA to inhibit mitochondrial translocation of PUMA and PUMA-mediated apoptosis independent of EGFR kinase activity. *Cancer Lett*, *294*(1), 101-110. doi:10.1016/j.canlet.2010.01.028
- Zimmermann, M., Zouhair, A., Azria, D., & Ozsahin, M. (2006). The epidermal growth factor receptor (EGFR) in head and neck cancer: its role and treatment implications. *Radiat Oncol*, *1*, 11. doi:10.1186/1748-717X-1-11
- Zuo, J. H., Zhu, W., Li, M. Y., Li, X. H., Yi, H., Zeng, G. Q., . . . Xiao, Z. Q. (2011). Activation of EGFR promotes squamous carcinoma SCC10A cell migration and invasion via inducing EMT-like phenotype change and MMP-9-mediated degradation of E-cadherin. *J Cell Biochem*, *112*(9), 2508-2517. doi:10.1002/jcb.23175

7. Contribution statement

Immunohistochemistry staining of serial cryosections of primary HNSCC tumors was performed by **Gisela Kranz** (Department of Otorhinolaryngology, Head and Neck Surgery, Grosshadern Medical Center, Ludwig-Maximilians-University, Munich, Germany).

Kaplan-Meier survival analysis were performed by **Henrik Schinke** (Department of Otorhinolaryngology, Head and Neck Surgery, Grosshadern Medical Center, Ludwig-Maximilians-University, Munich, Germany), and in collaboration with **Dr. Kristian Unger** (Clinical Cooperation Group “Personalized Radiotherapy in Head and Neck Cancer“, Helmholtz Zentrum München).

Cross-linking assays were performed in collaboration with **Aljaž Gaber, Miha Pavšič, Brigita Lenarčič** at the Department of Chemistry and Biochemistry, Faculty of Chemistry and Chemical Technology, University of Ljubljana, Slovenia.

8. PUBLICATIONS

Parts of the results presented in this doctoral thesis have been published in:

EpCAM ectodomain EpEX is a ligand of EGFR that counteracts EGF-mediated epithelial-mesenchymal transition through modulation of phospho-ERK1/2 in head and neck cancers.

Pan M, Schinke H, Luxenburger E, Kranz G, Shakhtour J, Libl D, Huang Y, Garber A, Pavsic M, Lenarcic B, Kitz J, Jakob M, Schwenk-Zieger S, Canis M, Hess J, Unger K, Baumeister P, Gires O.

PLoS Biology. 2018;16(9): e2006624.

Additional work during my work as doctoral student warranted authorships in:

Spatiotemporal patterning of EpCAM is important for murine embryonic endo- and mesodermal differentiation.

Sarrach S, Huang Y, Niedermeyer S, Hachmeister M, Fischer L, Gille S, **Pan M**, Mack B, Kranz G, Libl D, Merl-Pham J, Hauck SM, Paoluzzi Tomada E, Kieslinger M, Jeremias I, Scialdone A, Gires O.

Scientific Reports. 2018;8(1):1801.

Membrane-associated epithelial cell adhesion molecule is slowly cleaved by γ -secretase prior to efficient proteasomal degradation of its intracellular domain.

Huang Y, Chanou A, Kranz G, **Pan M**, Kohlbauer V, Ettinger A, Gires O.

Journal of Biological Chemistry. 2019;294(9):3051-3064.

Systemic Breast Carcinoma Cells with a Restricted Mesenchymal Shift are a Major Source of Metastasis.

Xiao Liu, Junjian Li, Markota A, Voigt C, Huang Z, Peter P. Lin, Daisy D. Wang, Gisela Kranz, Anna Krandick, Darko Libl, Horst Zitzelsberger, Isabella Zagorski, Herbert Braselman, **Min Pan**, Sibozhu, Yuanchi Huang, Sebastian Niedermeyer, Christoph A. Reichel, Bernd Uhl, Daria Briukhovetska, Javier Suárez Gosálvez, Sebastian Kobold, Olivier Gires, Hongxia Wang.

Science Advances. 2019 (accepted)

9. AFFIDAVIT/ EIDESSTATTLICHE VERSICHERUNG

Hiermit versichere ich an Eides statt, dass ich die vorliegende Dissertation „The role of a novel cross-talk between EpCAM and EGFR in the regulation of epithelial-to-mesenchymal transition (EMT) in head and neck carcinomas“ selbstständig angefertigt habe, mich außer der angegebenen keiner weiteren Hilfsmittel bedient und alle Erkenntnisse, die aus dem Schrifttum ganz oder annähernd übernommen sind, als solche kenntlich gemacht und nach ihrer Herkunft unter Bezeichnung der Fundstelle einzeln nachgewiesen habe.

I hereby confirm that the dissertation „ The role of a novel cross-talk between EpCAM and EGFR in the regulation of epithelial-to-mesenchymal transition (EMT) in head and neck carcinomas “ is the result of my own work and that I have only used sources or materials listed and specified in the dissertation.

Munich, 28.11.2019

Place, date

Min Pan

Name

10. ACKNOWLEDGMENT

This thesis has been greatly influenced by the guidance and support of a number of people. First of all, none of this work would have been possible without Prof. Olivier Gires, who provided me with unyielding scientific and professional support and mentorship over the last three years. Looking back, I am amazed at all I have learned from his advising throughout my doctorate study which supports my development as an independent scientist.

The process of finishing my doctorate study involved a great deal of time spent in lab with some wonderful colleagues on the same journey. I am very appreciative of the friendship, partnership and generous support that were always there from Master Henrik Schinke. I am very grateful for the unconditional support and help from Elke, Gisela, Yuanchi in the 'early' years and from Vera, Julius and Sabina more recently.

I want to express my gratitude to Dr. Philipp Baumeister for his wonderful job in clinical cohort study and valuable practical and theoretical advices. I would also like to thank our collaborators from other laboratories for their most valuable help in this project.

My family have always provided a grounded base for me, and I am forever grateful for their love, support and encouragement over the last three years. Finally, and most importantly, I thank Yang, my deeply loved girl. Her love has always been a truly invaluable component to this work and my life.